Stability analysis and stabilization of linear aperiodic sampled-data systems subject to input constraints

Daniel Denardi Huff

▶ **To cite this version:**

Daniel Denardi Huff. Stability analysis and stabilization of linear aperiodic sampled-data systems subject to input constraints. Automatic. Université Grenoble Alpes [2020-..]; Universidade Federal do Rio Grande do Sul (Porto Alegre, Brésil), 2022. English. NNT : 2022GRALT101 . tel-04032111

HAL Id: tel-04032111

https://theses.hal.science/tel-04032111v1

Submitted on 16 Mar 2023

HAL is a multi-disciplinary open access archive for the deposit and dissemination of scientific research documents, whether they are published or not. The documents may come from teaching and research institutions in France or abroad, or from public or private research centers.

L'archive ouverte pluridisciplinaire **HAL**, est destinée au dépôt et à la diffusion de documents scientifiques de niveau recherche, publiés ou non, émanant des établissements d'enseignement et de recherche français ou étrangers, des laboratoires publics ou privés.

THÈSE

Pour obtenir le grade de

DOCTEUR DE LA COMMUNAUTÉ UNIVERSITÉ GRENOBLE ALPES ET DE L'UNIVERSIDADE FEDERAL DO RIO GRANDE DO SUL

École doctorale : **Électronique Électrotechnique Automatique et Traitement du Signal (EEATS)**
Spécialité : **Automatique - Productique**
Unité de recherche : **Laboratoire Grenoble Images Parole Signal Automatique (GIPSA-Lab)**

Analyse de Stabilité et Stabilisation de Systèmes Linéaires Echantillonnés Apériodiquement soumis à des Contraintes d'Entrée

Stability Analysis and Stabilization of Linear Aperiodic Sampled-Data Systems subject to Input Constraints

Présentée par :

Daniel DENARDI HUFF

Thèse dirigée par **Mirko FIACCHINI** et par **João Manoel GOMES DA SILVA JR.**

Thèse soutenue publiquement le **14/12/2022** devant le jury composé de :

Lucíola CAMPESTRINI Professeure, Universidade Federal do Rio Grande do Sul	Présidente
Laurentiu HETEL Directeur de Recherche, CNRS	Rapporteur
Carlos Eduardo TRABUCO DÓREA Professeur, Universidade Federal do Rio Grande do Norte	Rapporteur
Sophie TARBOURIECH Directrice de Recherche, CNRS	Examinatrice
Giórgio VALMÓRBIDA Professeur, CentraleSupélec	Examinateur
John-Jairo MARTINEZ-MOLINA Professeur, Grenoble INP	Examinateur
Mirko FIACCHINI Directeur de Recherche, CNRS	Directeur de thèse
João Manoel GOMES DA SILVA JR. Professeur, Universidade Federal do Rio Grande do Sul	Directeur de thèse

ACKNOWLEDGMENTS

I would like to thank my family for all the support during the production of this work.

I would like to thank my advisors João and Mirko for all the help, new ideas, patience and careful revisions, without which this work would not have been possible. I also thank them for the good conversations and touristic suggestions at Grenoble.

I would like to thank my friends, among them Emerson, Arthur, Guillermo, Félix, Eduardo, Felipe, Pablo, Alexandre, Taia, Lucas, Mariana, Esteban, Maxime, Sohaib, Ana, Asma, for all the good times.

At last, I would like to thank the PPGEE and CAPES for the financial support in Brazil and the ANR for the financial support in France.

RÉSUMÉ

Motivé par l'utilisation croissante de contrôleurs embarqués dans différentes applications, où un protocole de communication est responsable par la transmission de données entre les algorithmes numériques, les actionneurs et les capteurs, l'analyse et la conception de contrôle pour les systèmes de contrôle échantillonnées ont été abordées dans de nombreux travaux. Dans ce contexte, l'échantillonnage apériodique peut être considéré comme une abstraction mathématique employée pour représenter, dans un cadre théorique, l'effet des imperfections sur le canal de communication telles que la gigue d'échantillonnage, les fluctuations et, dans certains cas, les pertes de paquets. De plus, en raison des limitations physiques des actionneurs, les contraintes d'entrée et, en particulier, la saturation des entrées sont omniprésentes dans les problèmes de contrôle réels. Ces contraintes sont une source de comportements non-linéaires et de dégradation de la performance. Dans de nombreux cas, seule la stabilité locale (ou régionale) du système en boucle fermée peut être assurée en présence de contraintes et de non-linéarités des actionneurs, même pour les systèmes linéaires.

Ce travail traite des systèmes linéaires échantillonnées apériodiquement où l'entrée de commande, soumise à des contraintes (par exemple la saturation), est calculée sur la base d'un retour d'état du système. Il se concentre sur deux problèmes principaux. Le premier consiste en l'analyse de stabilité de l'origine de tels systèmes avec la détermination d'estimations de la région d'attraction de l'origine (RAO). Le deuxième, à son tour, correspond à la conception de la commande, où une loi de commande à retour d'état est calculée afin d'agrandir une estimation de la RAO du système en boucle fermée résultant. Les méthodes proposées sont basées sur la programmation semi-définie ou linéaire et peuvent donc être facilement appliquées dans la pratique.

L'une des méthodes proposées considère un retour d'état linéaire soumis à la saturation et des fonctions de Lyapunov quadratiques, conduisant à des estimations ellipsoïdales de la RAO du système. Deux autres méthodes traitent de l'analyse de stabilité du système échantillonné soumis à la saturation des entrées fournissant des estimations polyédriques de la RAO. En raison de leur flexibilité, l'adoption de polyèdres au lieu d'ellipsoïdes permet une réduction du conservatisme mais est très exigeante en termes de complexité de calcul. Motivée par ce fait, cette thèse propose également une méthode de conception de contrôle basée sur une stratégie alternative, où la complexité des polyèdres est fixée *a priori*. Cette idée se traduit par un problème d'optimisation avec des contraintes bilinéaires, où une loi de commande linéaire par morceaux stabilisante de complexité relativement faible est trouvée pour le système échantillonné.

Les méthodes mentionnées ci-dessus considèrent un cadre non stochastique, où des limites inférieure et supérieure sont imposées pour l'intervalle d'échantillonnage inconnu et variable dans le temps du système. Comme contribution supplémentaire, cette thèse considère également un cadre stochastique. Une méthode de conception de contrôle est proposée pour la stabilisation globale dans le sens quadratique moyen du système échantillonné, où la loi de contrôle linéaire de retour d'état est soumise à des non-linéarités délimitées par secteur et les intervalles d'échantillonnage sont supposés être des variables aléatoires avec la distribution d'Erlang. La possibilité de pertes de paquets est aussi explicitement prise en compte via la distribution de Bernoulli. De plus, l'approche proposée, qui est basée sur le cadre des processus de Markov déterministes par morceaux, conduit à des conditions de stabilisation non conservatrices dans le cas linéaire sans contraintes.

Mots-clés: Commande échantillonnée, échantillonnage apériodique, échantillonnage aléatoire, invariance des ensembles, ensembles ellipsoïdales, ensembles polyédriques, region d'attraction de l'origine.

ABSTRACT

Motivated by the growing use of embedded controllers in different applications, where a communication protocol is responsible for the transmission of data between computer algorithms, actuators and sensors, the analysis and control design for sampled-data control systems have been addressed in many works. In this context, aperiodic sampling can be seen as a modeling abstraction employed to represent, in a theoretical framework, the effect of imperfections on the communication channel such as sampling jitters, fluctuations and, in some cases, packet dropouts. Moreover, due to physical limitations of actuators, input constraints and, in particular, input saturation are ubiquitous in real control problems. These constraints are source of nonlinear behaviors and performance degradation. In many cases, only local (or regional) stability of the closed-loop system can be ensured in the presence of actuators constraints and nonlinearities, even for linear plants.

This work deals with linear aperiodic sampled-data systems where the control input, subject to constraints (e.g. saturation), is computed based on a feedback of the system state. It focuses on two main problems. The first one regards the stability analysis of the origin of such systems, with the determination of estimates of the region of attraction of the origin (RAO). The second one, in turn, corresponds to the control design, where a state-feedback control law is computed in order to enlarge an estimate of the RAO of the resulting closed-loop system. The proposed methods are based on the use of semidefinite or linear programming and can therefore be easily applied in practice.

One of the proposed methods considers a linear saturating feedback of the system state and quadratic Lyapunov functions, leading to ellipsoidal estimates of the RAO of the system. Two other methods deal with the stability analysis of the sampled-data system subject to input saturation providing polyhedral estimates of the RAO. Because of their flexibility, adopting polyhedrons instead of ellipsoids allows a reduction of conservatism, but is very demanding in terms of computational complexity. Motivated by this fact, this thesis also proposes a control design method based on an alternative strategy, where the complexity of the polytopes is fixed *a priori*. This idea results in an optimization problem with bilinear constraints, where a stabilizing piecewise linear control law of relatively low complexity is found for the sampled-data system.

The aforementioned methods consider a non-stochastic framework, where lower and upper bounds are imposed for the unknown, time-varying sampling interval of the system. As an additional contribution, this thesis also considers a stochastic setting. A control design method is proposed for the global stabilization in the mean square sense of the sampled-data system, where the linear feedback control law is subject to sector bounded nonlinearities and the sampling intervals are assumed to be random variables with the Erlang distribution. The possibility of packet dropouts is also explicitly taken into account through the Bernoulli distribution. Moreover, the proposed approach, which is based on the framework of Piecewise Deterministic Markov Processes, leads to non-conservative stabilization conditions in the unconstrained linear case.

Keywords: Sampled-data control, aperiodic sampling, random sampling, set invariance, ellipsoidal sets, polyhedral sets, region of attraction of the origin.

LIST OF FIGURES

1 Closed-loop sampled-data system. 25
2 Closed-loop trajectories of Example 2.1 with $\delta_k = 0.18,\ \forall k \in \mathbb{N}$. 26
3 Closed-loop trajectories of Example 2.1 with $\delta_k = 0.54,\ \forall k \in \mathbb{N}$. 26
4 Closed-loop trajectories of Example 2.1 under aperiodic sampling with $\{\delta_k\}_{k\in\mathbb{N}} = \{0.18,0.54,0.18,0.54,\ldots\}$. 27
5 Behavior of $V(x(t))$. 40
6 Estimates of the RAO obtained with the proposed method (blue-dashed for $K = [2.6\ 1.4\ 0]$ and black-continuous for $K = [1.13\ 0.94\ 0.008]$) and with the methods proposed in [SG12] (black-dotted for $K = [2.6\ 1.4\ 0]$) and [FG18] (red-dotted for $K = [2.6\ 1.4\ 0]$). 47
7 Trajectories starting at the boundary of $\mathscr{E}(W_{11}^{-1})$ considering (67). 48
8 Sketch of property (73) for $m = 2$. 51
9 Estimates of the RAO of (1),(3),(5),(96) given by the proposed approach (black-continuous) and by the methods proposed in [SG12] (black-dotted), [FG18] (red-dotted) and Chapter 3 (blue-dashed). 59
10 Trajectories of (1),(3),(5),(96), where the initial conditions are depicted by the symbol *. 60
11 Estimate of the RAO of (1),(3),(5) given by the proposed approach. 61
12 Geometrical interpretation of Theorems 5.2 and 5.3 and Lemma 5.5. 69
13 Estimates of the RAO of (96) obtained with the proposed approach (black-continuous) and with the methods of Chapter 3 (blue-dashed), Chapter 4 (black-dashed), [FG18] (red-dotted) and [SG12] (black-dotted). 73
14 Sequence $\{\Omega_{i,x_p}\}_{i=0}^{9}$, where Ω_{5,x_p} is in red. 74
15 Estimates of the RAO of (123) obtained with the proposed approach (filled in green) and with the methods of Chapter 3 (blue-dashed line) and [FG18] (red-dotted line). A numerically evaluated approximation of the RAO is depicted by black circles. 74
16 Trajectories starting at the boundary of $\Omega_{\bar{i},x_p}$. 75
17 Partitions of $\Omega = \bigcup_{l=1}^{6} \Omega^l$ and of $\mathbb{R}^2 = \bigcup_{l=1}^{6} C^l$. 80
18 Estimates of the RAO of the closed-loop system considering (136) and the proposed method (black-continuous) and considering the linear saturated control (3) and the method of Chapter 3 (blue-dashed for $K_p = [2.6\ 1.4]$ and blue-continuous for $K_p = [1.13\ 0.94]$). 83
19 Partition of Ω into simplices for Example I. 83
20 Trajectories starting at the vertices of Ω for Example I. 84

21 Estimates of the RAO of the closed-loop system considering (136) and the proposed method (black-continuous for $n_v = 10$ and black-dashed for $n_v = 20$) and considering the linear saturated control (3) and the method of Chapter 3 (blue-dashed for $K_p = [-10.70\ 4.38]$). Outer approximations of the maximal controlled λ-contractive C-set for (126) in blue-continuous. 85
22 Partition of Ω into simplices for Example II. 86
23 Trajectories starting at the vertices of Ω for Example II. 86
24 Probability density function (144) of the Erlang distribution for different values of the parameters ν and λ. 91
25 Graphical representation of the SHS (149). 92
26 Cart–spring–pendulum system. Adapted from [TGGQ11, Example 8.3]. . . . 97
27 Trajectories of the closed-loop system composed by (140)-(141), (169) and (171) in the subspace of $[p(t)\ \beta(t)]^T$, where the initial conditions are depicted by blue circles and the state at the sampling instants t_k by black ones. 98
28 Trajectories of the closed-loop system composed by (140), (165), (172) and (173) in the x_p-subspace, where the initial conditions $x_p(0)$ are depicted by blue circles and the state at the sampling instants t_k by black ones. 99

LIST OF TABLES

1 Feedback gains of the piecewise linear control law (136) for Example I. 84
2 Feedback gains of the piecewise linear control law (136) for Example II. . . . 87

LIST OF ABBREVIATIONS

C-set	A compact and convex set containing the origin in its interior
i.i.d.	Independent, identically distributed
LMI	Linear Matrix Inequality
MES	Mean exponentially stable
P-set	A polyhedral C-set
PDMP	Piecewise Deterministic Markov Process
PWL	Piecewise linear
RAO	Region of attraction of the origin
SHS	Stochastic Hybrid System

LIST OF SYMBOLS

$\mathbb{R}_+$	$\triangleq \{x \in \mathbb{R} : \ x > 0\}$ and similarly for $\mathbb{N}_+, \mathbb{Z}_+$
$>, \geq, \lvert\cdot\rvert$	must be interpreted element-wise when applied to vectors or matrices
$\lceil x \rceil$	smallest integer greater than or equal to $x \in \mathbb{R}$
$\succ$ ($\succeq$)	characterizes positive (semi)-definiteness of symmetric matrices
$\star$	denotes a symmetric block when applied as an entry of a matrix
$\mathrm{Co}(\Omega)$	convex hull of the set Ω
Ω°	interior of the set Ω
$\overline{\Omega}$	closure of the set Ω
$\partial\Omega$	boundary of the set Ω
$\lambda\Omega$	$\triangleq \{\lambda x : x \in \Omega\}, \Omega \subseteq \mathbb{R}^n, \lambda \in \mathbb{R}$, and similarly for $\Lambda\Omega$ if $\Lambda \in \mathbb{R}^{m\times n}$
$\Omega \pm \Theta$	$\triangleq \bigcup_{\omega\in\Omega, \theta\in\Theta} \omega \pm \theta$, for sets Ω, Θ
$\Omega \setminus \Theta$	$\triangleq \{x : \ x \in \Omega, x \notin \Theta\}$, for sets Ω, Θ
$\mathbb{N}_m$	$\triangleq \{i \in \mathbb{N} : \ 1 \leq i \leq m\}$
$2^{\mathbb{N}_m}$	the set of all subsets of $\mathbb{N}_m$ (example: $2^{\mathbb{N}_2} = \{\emptyset, \{1\}, \{2\}, \{1,2\}\}$)
$f(t^-)$	for $f : \mathbb{R} \to \mathbb{R}^n$, $f(t^-) \triangleq \lim_{\tau\mapsto t, \tau<t} f(\tau)$ if the limit exists and similarly for $f(t^+)$
$M_{(i)}$	i-th row of matrix (or vector) M
$M^{(i)}$	i-th column of matrix M
$M_{(i,j)}$	(i,j)-entry of matrix M
M^T	transpose of matrix M
$\mathrm{Diag}(M,N)$	block diagonal matrix formed by matrices M and N
e_k	k-th canonical base vector of the Euclidean space
$\mathbf{1}$	$\triangleq [1 \ldots 1]^T$
$\lVert\cdot\rVert_p$	p-norm of a vector or induced p-norm of a matrix, $1 \leq p \leq \infty$
$\lVert\cdot\rVert$	Euclidean norm of a vector or induced 2-norm of a matrix
$\mathscr{B}_r$	$\triangleq \{x \in \mathbb{R}^n : \ \lVert x\rVert \leq r\}$ (n will be clear from the context)
$\mathscr{B}$	$\triangleq \mathscr{B}_1$

$\sigma_{max}(M)$	largest singular value of matrix M
$\sigma_{min}(M)$	smallest singular value of matrix M
$\sigma_{max}(\mathscr{M})$	$\triangleq \max_{M\in\mathscr{M}} \sigma_{max}(M)$ for a compact set $\mathscr{M} \subset \mathbb{R}^{m\times n}$ and similarly for $\sigma_{min}(\cdot)$
$\lambda_{max}(M)$	maximal real part of the eigenvalues of a square matrix M
$\lambda_{min}(M)$	minimal real part of the eigenvalues of a square matrix M
$\mathrm{sat}(\cdot)$	standard saturation function $\mathrm{sat} : \mathbb{R}^m \to \mathbb{R}^m$, whose elements $\mathrm{sat}_{(r)}(v)$ are given by $\mathrm{sat}_{(r)}(v) \triangleq \mathrm{sign}(v_{(r)})\min\{\lvert v_{(r)}\rvert, 1\}$, $\forall r = 1,\ldots,m$
I_n	identity matrix of dimension $n \times n$
0	scalar, vector or matrix of appropriate dimensions
$\mathscr{P}(H,h)$	$\triangleq \{x \in \mathbb{R}^n :\ Hx \leq h\}, H \in \mathbb{R}^{n_h\times n}, h \in \mathbb{R}^{n_h}$, hyperplane representation of a polyhedron
$\mathscr{V}(V)$	$\triangleq \left\{x = V\alpha \in \mathbb{R}^n :\ \alpha \geq 0, \mathbf{1}^T\alpha = 1, \alpha \in \mathbb{R}^{n_v}\right\}, V \in \mathbb{R}^{n\times n_v}$, vertex representation of a polytope (bounded polyhedron)
$\mathscr{V}_0(V)$	$\triangleq \left\{x = V\alpha \in \mathbb{R}^n :\ \alpha \geq 0, \mathbf{1}^T\alpha \leq 1, \alpha \in \mathbb{R}^{n_v}\right\}, V \in \mathbb{R}^{n\times n_v}$, vertex representation if the polytope contains the origin
$\mathscr{H}(M)$	$\triangleq \{x \in \mathbb{R}^n :\ \lVert Mx\rVert_\infty \leq 1\}, M \in \mathbb{R}^{m\times n}$
$\mathscr{E}(M)$	$\triangleq \{x \in \mathbb{R}^n :\ x^TMx \leq 1\}, M \in \mathbb{R}^{n\times n}$
$P[\cdot]$	probability of the argument
$\mathbb{E}[\cdot]$	expectation of the argument
$\mathtt{E}(\nu,\lambda)$	Erlang distribution of degree $\nu \in \mathbb{N}_+$ and rate (or intensity) $\lambda \in \mathbb{R}_+$
$\mathtt{E}(1,\lambda)$	exponential distribution of rate (or intensity) $\lambda \in \mathbb{R}_+$
$\mathrm{sec}[m,M]$	for $f : \mathbb{R} \to \mathbb{R}$, $f \in \mathrm{sec}[m,M]$ means that the graph of $f(\cdot)$ lies inside the sector formed by the lines $g_1(x) = mx$ and $g_2(x) = Mx$, with $M \geq m$

CONTENTS

1 INTRODUCTION 19
1.1 Scope 20
1.2 Main contributions 21

2 PRELIMINARIES 25
2.1 Linear aperiodic sampled-data systems subject to input constraints . . . 25
2.1.1 Impulsive models for sampled-data systems 28
2.1.2 Equivalent discrete-time uncertain system 28
2.2 Set invariance theory 30
2.2.1 Discrete-time case 32
2.2.2 Continuous-time case 34
2.3 Concluding remarks 36

3 STABILITY ANALYSIS AND STABILIZATION: QUADRATIC APPROACH 37
3.1 Equivalent discrete-time uncertain system 38
3.2 Stability analysis 39
3.2.1 Lyapunov setup 39
3.2.2 Convex conditions 41
3.2.3 Optimization problems 43
3.3 Stabilization 45
3.4 Numerical example 46
3.5 Concluding remarks 48

4 STABILITY ANALYSIS: POLYHEDRAL APPROACH I 49
4.1 The SNS Model 49
4.2 Stability analysis 52
4.2.1 Computation of a contractive set for $x_{p,k+1} \in F_{SNS}(x_{p,k}, \Delta_J, \mathscr{S})$ 52
4.2.2 Testing contractivity for system $x_{p,k+1} \in F_{SNS}(x_{p,k}, \Delta, \mathscr{S})$ 54
4.3 Numerical algorithm 58
4.4 Numerical examples 59
4.4.1 Example I 59
4.4.2 Example II 60
4.5 Concluding remarks 61

5 STABILITY ANALYSIS: POLYHEDRAL APPROACH II 63
5.1 Closed-loop system representation 63
5.2 SNS invariant and contractive sets 64
5.2.1 Computation of estimates of the RAO 67

5.2.2 Convergence properties . . . 72
5.3 Numerical examples . . . 72
5.3.1 Example I . . . 73
5.3.2 Example II . . . 73
5.4 Concluding remarks . . . 76

6 STABILIZATION: POLYHEDRAL APPROACH . . . 77
6.1 Computation of a controlled contractive set for system (126) . . . 78
6.1.1 Design of the control law . . . 79
6.2 Testing contractivity . . . 80
6.3 Stability of the closed-loop system . . . 82
6.4 Numerical examples . . . 82
6.4.1 Example I . . . 82
6.4.2 Example II . . . 84
6.5 Concluding remarks . . . 87

7 STABILIZATION IN A STOCHASTIC FRAMEWORK . . . 89
7.1 Problem Formulation . . . 89
7.1.1 Equivalent SHS representation . . . 91
7.2 Mean Square Exponential Stabilization . . . 93
7.2.1 The general case . . . 93
7.2.2 The linear case . . . 94
7.3 Numerical Examples . . . 97
7.3.1 Example I . . . 97
7.3.2 Example II . . . 99
7.4 Concluding remarks . . . 100

8 CONCLUSIONS . . . 101
8.1 Future works and perspectives . . . 102

BIBLIOGRAPHY . . . 105

APPENDIX A PROOFS OF SOME RESULTS . . . 113
A.1 Proof of Lemma 2.4 . . . 113
A.2 Proof of Lemma 2.6 . . . 113
A.3 Proof of Lemma 5.2 . . . 114
A.4 Proof of Lemma 5.3 . . . 115
A.5 Proof of Lemma 5.5 . . . 116
A.6 Proof of Lemma 5.6 . . . 116
A.7 Proof of Theorem 7.2 . . . 117
A.8 Proof of Theorem 7.3 . . . 119

1 INTRODUCTION

In many real-world applications, continuous-time plants are controlled by digital devices in a sampled-data fashion, where the control input is computed based on the value of the state/output of the plant at the sampling instants [AW84]. These sampled-data systems are often implemented through a network, where communication protocols are responsible for the transmission of data between computers, actuators and sensors [ZBP01]. The use of a shared network for different purposes has several advantages, including flexibility and simplicity of maintenance [ZBP01]. On the other hand, due to imperfections on the communication channels, such as sampling jitters, fluctuations and packet dropouts, the control loop is commonly subject to time-varying, uncertain, sampling intervals, i.e. *aperiodic sampling* [HNX07, ZBP01].

The case of *periodic sampling*, when the sampling interval is a known constant value, has been dealt with through several approaches (see [AW84, CF95] for an overview in the linear case or [NT01, MNC01] for the nonlinear case). *Aperiodic sampling*, in turn, has been the focus of many recent works. In this context, different methods exist to study the stability of linear sampled-data systems subject to a time-varying sampling interval. In [FSR04, Fri10, LF12] the system is considered as affected by time-varying delay acting on the control input and its stability analysis is based on Lyapunov-Krasovskii functionals. Following similar ideas, in [Seu12] an approach using the looped-functionals is presented. In [NHT08, Bri13, HDTP13] a hybrid system approach is explored. In [HDRJ11, FM16] the system is studied based on an uncertain discrete-time model that describes the evolution of the state at the sampling instants. The exponential dependence of the transition matrix of the resulting difference inclusion can be dealt with in different ways in order to obtain numerical tractable criteria for this approach. For instance, polytopic embeddings of this matrix are considered in [CVHN09, CHV$^+$10, LONH12]. Alternatively, norm-bounded approximations of it can be employed [Fuj09, FO11, KF13]. For a general overview of those methods and other references, the reader can refer to the survey [HFO$^+$17].

Moreover, due to physical limitations of actuators, input constraints and, more specifically, input saturation are ubiquitous in real control problems. These constraints are source of performance degradation and, in many cases, only local (or regional) stability of the closed-loop system can be ensured, even for linear plants, as in the case of exponentially unstable open-loop systems [SSY94, Ma91]. It is then useful to characterize and compute estimates of the region of attraction of the origin (RAO) of the closed-loop system. Moreover, even if the open-loop system is exponentially stable, to satisfy performance criteria around the origin, it may be interesting to use a control law that ensures only local stability of the origin and to compute the corresponding estimate of the RAO [TGGQ11]. In the *periodic sampling* case, an exact discretization is possible and the

problem can be treated in a discrete-time framework (see [TGGQ11] and the references therein). Nevertheless, for the *aperiodic sampling* case, the problem is more involved and requires a careful analysis of the behavior of the system. Regarding this case, we can cite, for instance, [SG12] and [FG18], which provide techniques based on LMIs (Linear Matrix Inequalities) to compute ellipsoidal estimates of the RAO of the closed-loop system with a linear saturating state-feedback control law, or [GQST16], which considers a dynamic output feedback.

Furthermore, the use of methods based on polyhedral sets to address the stability analysis and stabilization of dynamical systems is quite appealing [BM15, DH99, BCM10, FM16]. Because of their flexibility, adopting polyhedrons instead of ellipsoids allows a reduction of conservatism [BM15, Pg. 188]. In particular, it is known that a linear uncertain system is robustly stabilizable if and only if there exists a polyhedral control Lyapunov function for it or, equivalently, a polyhedral controlled invariant set [BM15]. Moreover, polyhedrons form a class of sets particularly suitable for the application of iterative procedures like the one in [Bla94], that converges to the maximal controlled invariant/contractive set for the system. However, the sets obtained by such algorithms become more complex at each iteration, making the obtained solutions intractable in many important cases [BM15]. In order to circumvent this problem, many approaches exist in the literature for linear systems subject to constraints, as, for instance, [AT19, FA18, BCM10, TJ15, BPC$^+$18, OJD20]. In [AT19] a procedure that does not rely on iterative computations is presented while in [FA18] an algorithm based on linear programming that allows to overcome the complexity inherent to the Minkowski set addition is exploited. In turn, [BCM10, TJ15, BPC$^+$18, OJD20] develop methods to compute polyhedrons of low complexity in order to get conservative but computationally affordable results.

1.1 Scope

Motivated by the exposed in the previous paragraphs, this thesis deals with linear aperiodic sampled-data systems where the control input, subject to saturation (or more general constraints in Chapters 6 and 7), is computed based on a feedback of the system state. It focuses on two main problems:

1. Stability analysis of the origin of the closed-loop system along with the determination of estimates of the region of attraction of the origin;

2. Control design, where a stabilizing state-feedback control law is computed based on some criterion, which in most cases corresponds to the size of an estimate of the RAO of the resulting closed-loop system.

Both quadratic and polyhedral Lyapunov functions are considered, leading to ellipsoidal and polyhedral estimates of the RAO, respectively. The developed methods consider either a *stochastic* or a *non-stochastic* framework, as follows:

- *Non-stochastic case* (all chapters with the exception of Chapter 7): lower and upper bounds are imposed for the unknown, time-varying interval between two successive sampling instants. The methods in this case rely on uncertain discrete-time systems, i.e. difference inclusions, that model the behavior of the system state at the sampling instants. In particular, it is shown that the asymptotic stability of the origin of the discrete-time system is sufficient to guarantee the asymptotic stability of the origin of the continuous-time one.

- *Stochastic case* (Chapter 7): the sampling interval of the system is assumed to be a random variable with the Erlang or exponential distribution and the stabilization problem is treated in a probabilistic sense. In this case, tools from the literature of stochastic systems are employed;

It should also be mentioned that, unlike the preceding chapters, Chapter 7 focuses on the global stabilization problem. Local stabilization in the *stochastic case* can be considered as an idea of future work.

1.2 Main contributions

Below the structure of the work and the main contributions are described in more detail.

In **Chapter 3**, a new method, which can be seen as an evolution of the approach in [FG18], is presented in order to analyze the stability of aperiodic sampled-data systems subject to control saturation. The method allows not only the stability analysis of the nonlinear closed-loop system but also provides a constructive way for designing a control law aiming at indirectly maximizing the RAO. Quadratic Lyapunov functions are used, leading to stability and stabilization conditions in LMI form and to ellipsoidal estimates of the RAO. Unlike [FG18], which considers the static linear feedback of the system state, a more general control law is employed: the control input can also depend linearly on its past value, resulting in a dynamic controller.

To derive our results, an impulsive system representation is employed, with a linear flow and a nonlinear (due to the saturation term) jump dynamics. It is shown that the evolution of the system at the sampling instants can be modeled by a difference inclusion defined by two set-valued maps. From this setup, we show that to ensure the asymptotic stability it is sufficient to verify that the candidate Lyapunov function decreases by a certain amount only at a grid of possible values for the sampling interval, as long as the increase of the function in continuous-time is conveniently bounded. The difference inclusion proposed is different from the one in [FG18]. In particular, this new formulation allows to tackle the stabilization problem through convex optimization, which was not possible with the one in [FG18]. Moreover, it is worth highlighting that this approach is different from the one in [CVHN09, CHV$^+$10, LONH12], for instance, where the decrease of the Lyapunov function between successive sampling instants is directly ensured for all possible sampling intervals through the use of polytopic embeddings of the system transition matrix.

Chapter 4, in turn, addresses the stability analysis problem focusing on the determination of polyhedral estimates of the RAO. As already explained, adopting polyhedrons instead of ellipsoids allows a reduction of conservatism [BM15, Pg. 188]. The proposed approach, inspired by [Bla94, FM16], relies on a difference inclusion obtained from the use of the saturated and nonsaturated (SNS) embedding for the saturation term [ACLC06]. It is shown that contractive sets for this difference inclusion remain contractive when scaled down and can therefore be associated to a Lyapunov function which is strictly decreasing at the sampling instants. It is also shown that the obtained contractive sets can be used as estimates of the RAO of the continuous-time closed-loop system. In order to obtain these estimates, a numerical algorithm based on linear programming is proposed. This algorithm generates a decreasing sequence of nested polytopes that converges to a contractive set for the considered difference inclusion in a finite number of steps under mild assumptions.

The main drawback of the method of Chapter 4 concerns the numerical execution of the proposed algorithm, which can become prohibitively complex before its stopping criterion is reached. The execution becomes slower at each new iteration of the algorithm because the numerical complexity of the polytopes generated by it tends to increase. Moreover, the polytopes generated at each intermediate iteration cannot be considered as invariant estimates of the RAO, i.e. regions of safe behavior for the closed-loop system. Thus, in practice, the method may fail to provide a valid estimate of the RAO of the system in an acceptable amount of time, even if in theory the stopping criterion of the algorithm is satisfied in a finite number of steps. This fact is not surprising: in general, algorithms which involve polyhedrons computations are very demanding in terms of computational complexity [BM15, Pg. 110].

In order to overcome the aforementioned problem, an alternative method is developed in **Chapter 5**, which also relies on the use of a difference inclusion and on the SNS embedding of the saturation function. The main difference is that an increasing sequence of nested polytopes is generated, where at each step a new invariant polyhedral estimate of the RAO of the system (larger than the previous one) is obtained. Therefore, the successful execution of the resulting algorithm does not depend on some stopping criterion, and the trade-off between number of iterations and complexity of the resulting polytope can be managed.

In **Chapter 6**, we propose a method to design a piecewise linear (PWL) state-feedback control law that guarantees the asymptotic stability of the origin of the sampled-data system and leads to a polyhedral estimate of the RAO. The method deals with a generic polyhedral set of input constraints, which includes the saturation function considered in Chapters 3–5 as a particular case. Following the ideas of [BPC+18, FEC20, OJD20], the complexity – given by the number of vertices – of the estimate of the RAO is fixed *a priori*. Thus, the resulting control law is of low complexity and suitable for practical use. Moreover, as shown by the numerical examples, the estimates of the RAO associated with the proposed feedback control law can be larger than the ones obtained with the approach of Chapter 3, which designs a linear feedback control law. The proposed method relies on an optimization problem with bilinear constraints that is used in order to obtain a controlled contractive polytope for the difference inclusion on which the method is based.

A common feature of the aforementioned chapters is that they consider a *non-stochastic framework*, where hard bounds are given for the time-varying sampling interval of the system. However, taking into account that this assumption may not be realistic, some recent works have addressed the stability analysis and stabilization of linear sampled-data systems subject to a random sampling interval, where the corresponding distribution function has possibly unbounded support [TCL18, SWH16, STWH17, HRDL22, SSC21, AHS13]. In particular, the works in [SWH16, STWH17, HRDL22, SSC21] address the stabilization problem (in a stochastic sense) of the discrete-time model that describes the evolution of the system state at the sampling instants. However, unlike the *non-stochastic case*, in the *stochastic case* the exponential stability of this discrete-time model is *not* equivalent to the exponential stability of the corresponding (continuous-time) sampled-data system, as remarked, for instance, in [TCL18, Pg. 222] and [AHS12, Pg. 610].

Thus, the aim of **Chapter 7** is to propose a control design method which guarantees the global stabilization (in the mean square sense) of the *continuous-time* system, as it is done for instance in [TCL18]. As in [STWH17], it is assumed that the random sampling intervals have the Erlang distribution, which includes the exponential distribution (considered, for instance, in [TCL18, TN08]) as a special case. Moreover, the possibil-

ity of packet dropouts is explicitly considered and modeled, as in [HRDL22], through a Bernoulli distribution. The proposed method also considers that the sampled-data linear system is subject to actuator nonlinearities which satisfy a sector condition. This includes, for instance, saturation, deadzone and quantization.

As in [AHS13], to derive the results, we use the framework of Piecewise Deterministic Markov Processes (PDMPs) [Dav93], which can be viewed as a subclass of stochastic hybrid systems (SHSs) [TSS14]. The proposed Lyapunov-based stabilization conditions are posed in terms of LMIs and can, therefore, be easily solved in practice using off-the-shelf semidefinite programming solvers. Moreover, the proposed approach leads to non-conservative stabilization conditions in the linear case, i.e. without actuator nonlinearities, unlike the one of [TCL18]. A detailed comparison between the proposed method and the one of [TCL18] is provided for the case of a Poisson sampling process, i.e. exponentially distributed sampling intervals.

In view of the above, a quick summary of the organization of the work is presented below with the corresponding journal/conference publications:

- **Chapter 2**: basic definitions and concepts;
- **Chapter 3**: stability analysis and control design considering a *non-stochastic framework* and a quadratic approach, where the linear feedback control law is subject to saturation and can depend not only on the system state but also on its last value, resulting in a dynamic controller (see also [HFG22e]);
- **Chapter 4**: stability analysis considering a *non-stochastic framework* and a polyhedral approach, where the linear feedback control law is subject to saturation (see also [HFG22d]);
- **Chapter 5**: same goal of Chapter 4, but with an alternative approach which is more convenient from a computational point of view (see also [HFG22c]);
- **Chapter 6**: design of a piecewise linear state-feedback control law considering a *non-stochastic framework* and a polyhedral approach, where the input constraints are represented by a polyhedral set $\mathscr{U}$, i.e. $u(t) \in \mathscr{U}$ (see also [HFG21]);
- **Chapter 7**: mean square exponential stabilization of the closed-loop system considering a *stochastic framework* and a linear dynamic controller as in Chapter 3, where the input is subject to sector-bounded nonlinearities (see also [HFG22b] and [HFG22a]).

2 PRELIMINARIES

In this chapter we will introduce basic concepts that will be used in Chapters 3–6. The stochastic framework of Chapter 7 is considerably different and will be directly presented in Chapter 7. Section 2.1 presents the system under study and Section 2.2 focuses on some definitions and results on set invariance theory.

2.1 Linear aperiodic sampled-data systems subject to input constraints

Consider the continuous-time plant described by the following linear model:

$$\dot{x}_p(t) = A_p x_p(t) + B_p u(t) \tag{1}$$

where $x_p \in \mathbb{R}^{n_p}$ and $u \in \mathbb{R}^m$ represent the state and the input of the plant, respectively. Matrices A_p and B_p have appropriate dimensions and are supposed to be constant, and B_p has full column rank. As shown in Figure 1, it is assumed that the control input is computed based on the sampled value of the state at the *sampling instants* t_k and kept constant (by means of a zero-order-hold) for all $t \in [t_k, t_{k+1})$, i.e.

$$u(t) = f(x_p(t_k)), \quad \forall t \in [t_k, t_{k+1}),\ \forall k \in \mathbb{N}, \tag{2}$$

where $f : \mathbb{R}^{n_p} \to \mathscr{U} \subset \mathbb{R}^m, f(0) = 0$ and $\mathscr{U}$ is a polyhedral C-set[1] that represents control signal constraints.

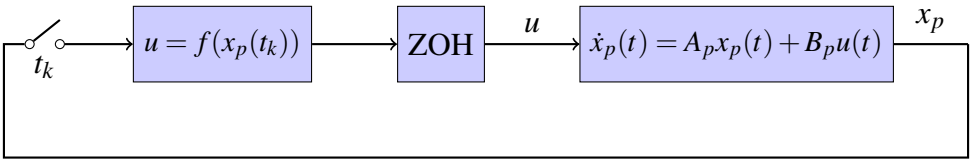

Figure 1: Closed-loop sampled-data system.

A particular case of (2) that will be the focus of Chapters 3-5 corresponds to the linear saturated state feedback:

$$u(t) = \text{sat}(K_p x_p(t_k)), \quad \forall t \in [t_k, t_{k+1}),\ \forall k \in \mathbb{N}, \tag{3}$$

where K_p is a matrix of appropriate dimensions, $\mathscr{U} = \{u \in \mathbb{R}^m : \|u\|_\infty \leq 1\}$ and $\text{sat} : \mathbb{R}^m \to \mathbb{R}^m$ is the standard saturation function, whose elements are given by

$$\text{sat}_{(r)}(v) \triangleq \text{sign}(v_{(r)}) \min\{|v_{(r)}|, 1\}, \quad \forall r = 1, \ldots, m. \tag{4}$$

[1] A C-set is defined as a compact and convex set containing the origin in its interior (see Section 2.2).

In some cases, the control law will also depend on the last input value applied to the plant on the time interval $[t_{k-1}, t_k)$ and (2) is then replaced by a more general expression:

$$u(t) = f(x_p(t_k), u(t_k^-)), \quad \forall t \in [t_k, t_{k+1}), \ \forall k \in \mathbb{N}.$$

However, for the moment let us consider just the control law (2) to simplify the exposition of the key ideas.

By definition, the system starts to operate at $t_0 = 0$ (without loss of generality). The *intersampling time* (or *sampling interval*) is the difference $\delta_k \triangleq t_{k+1} - t_k$ between two successive sampling instants. We consider that the sampling interval is time-varying, which allows to model an aperiodic sampling strategy. The following motivating example, taken from [HFO+17], illustrates the rich complexity of phenomena that may occur under aperiodic sampling.

Example 2.1. *Consider a sampled-data system given by* (1)-(2) *with*

$$A_p = \begin{bmatrix} 1 & 3 \\ 2 & 1 \end{bmatrix}, \ B_p = \begin{bmatrix} 1 \\ 0.6 \end{bmatrix}, \ f(x_p(t_k)) = K_p x_p(t_k), \ K_p = -\begin{bmatrix} 1 & 6 \end{bmatrix}.$$

Under periodic sampling with either $\delta_k = 0.18, \ \forall k \in \mathbb{N}$, *or* $\delta_k = 0.54, \ \forall k \in \mathbb{N}$, *the resulting closed-loop system is stable, as it is shown in Figs. 2 and 3, respectively. However, this does not imply stability under aperiodic sampling with* $\delta_k \in \{0.18, 0.54\}, \ \forall k \in \mathbb{N}$. *Consider for instance the sequence*

$$\delta_0 = 0.18, \ \delta_1 = 0.54, \ \delta_2 = 0.18, \ \delta_3 = 0.54, \ldots$$

In this case, the resulting closed loop is unstable, cf. Figure 4.

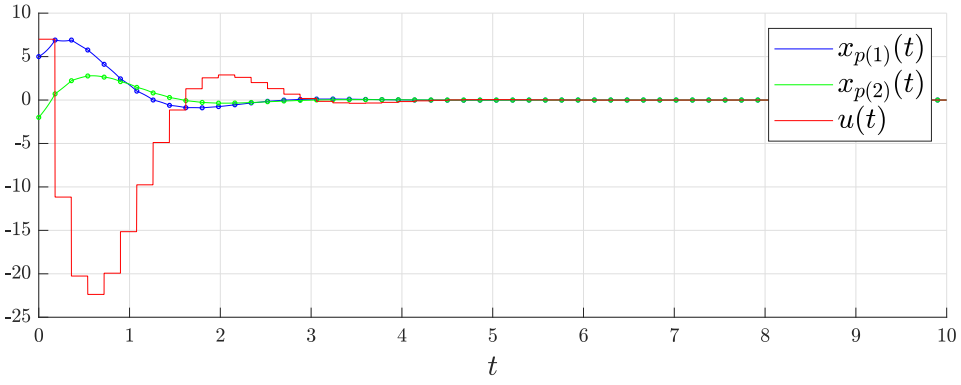

Figure 2: Closed-loop trajectories of Example 2.1 with $\delta_k = 0.18, \ \forall k \in \mathbb{N}$.

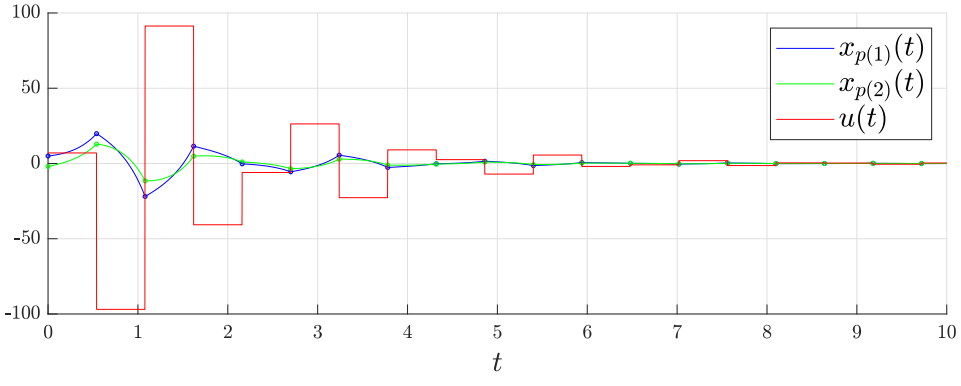

Figure 3: Closed-loop trajectories of Example 2.1 with $\delta_k = 0.54, \ \forall k \in \mathbb{N}$.

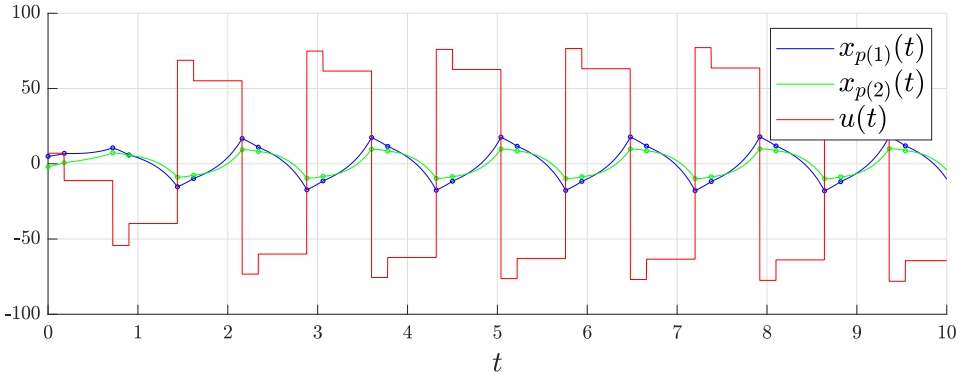

Figure 4: Closed-loop trajectories of Example 2.1 under aperiodic sampling with $\{\delta_k\}_{k\in\mathbb{N}} = \{0.18, 0.54, 0.18, 0.54, \ldots\}$.

We conclude from the example above that, unlike periodic sampling, aperiodic sampling requires a nontrivial analysis even in the linear case. From now on, δ_k is considered to be lower and upper bounded as follows:

$$0 < \tau_m \leq \delta_k \leq \tau_M, \qquad \forall k \in \mathbb{N}. \tag{5}$$

Thus, given the interval $\Delta \triangleq [\tau_m, \tau_M]$, the set of sequences of admissible sampling instants is defined as follows:

$$\Theta(\Delta) \triangleq \Big\{ \{t_k\}_{k\in\mathbb{N}} : \; t_{k+1} = t_k + \delta_k, \delta_k \in \Delta, \forall k \in \mathbb{N}, t_0 = 0 \Big\}. \tag{6}$$

Since $\tau_m > 0$, $\mathscr{T} \in \Theta(\Delta)$ is an unbounded strictly increasing sequence of positive scalars.

The following definitions are adapted from [Kha02].

Definition 2.1. *The equilibrium point $x_p = 0$ of (1),(2),(5) is*

- *stable if, for each $\varepsilon > 0$, there is $\beta = \beta(\varepsilon) > 0$ such that*

$$\|x_p(0)\| \leq \beta \Rightarrow \|x_p(t)\| \leq \varepsilon, \; \forall t \geq 0 \tag{7}$$

- *asymptotically stable if it is stable and $\beta > 0$ can be chosen such that*

$$\|x_p(0)\| \leq \beta \Rightarrow \lim_{t\to\infty} x_p(t) = 0 \tag{8}$$

  where the choice $\beta = \beta(\varepsilon) > 0$ must hold uniformly for all possible realizations of $\{\delta_k\}_{k\in\mathbb{N}}$ satisfying (5).

Definition 2.2. *The region of attraction of the origin (RAO) Γ of system (1),(2),(5) (assuming the origin is asymptotically stable) is the set of all $x_p \in \mathbb{R}^{n_p}$ such that for $x_p(0) = x_p$ it follows that $\lim_{t\to\infty} x_p(t) = 0$ for all possible realizations of $\{\delta_k\}_{k\in\mathbb{N}}$ satisfying (5).*

This study (with the exception of Chapter 7) focuses on two main problems related to the closed-loop system described above.

Problem 2.1 (Stability Analysis)**.** *Given the bounds τ_m and τ_M on the intersampling time, provide conditions that allow to asses the asymptotic stability of the origin of the closed-loop system and to characterize estimates of the RAO.*

Problem 2.2 (Control Design)**.** *Given the bounds τ_m and τ_M on the intersampling time, design a control law in order to asymptotically stabilize the origin and enlarge an estimate of the RAO of the resulting closed-loop system.*

It should be noticed that, due to the input constraints, the global stability of the origin cannot be *a priori* guaranteed. As $\mathscr{U}$ is assumed to be bounded, if matrix A_p is unstable, the global stabilization is actually impossible [SSY94]. In this case, since the analytical characterization of the RAO is in general not possible, the idea is to estimate it through well-defined sets.

2.1.1 Impulsive models for sampled-data systems

For every $\mathscr{T} \in \Theta(\Delta)$, the sampled-data model (1),(2) can be represented as follows:

$$\begin{cases} \dot{x}_p(t) = A_p x_p(t) + B_p u(t), & \forall t \in \mathbb{R}_+ \setminus \mathscr{T}, \\ \dot{u}(t) = 0, & \\ x_p(t) = x_p(t^-) = x_p(t^+), & \forall t \in \mathscr{T}. \\ u(t) = u(t^+) = f(x_p(t^-)), & \end{cases}$$

Equivalently, defining the extended system state $x \triangleq [x_p^T \ u^T]^T \in \mathbb{R}^n, n \triangleq n_p + m$, one has the following impulsive system [HDTP13]:

$$\begin{cases} \dot{x}(t) = A_c x(t), & \forall t \in \mathbb{R}_+ \setminus \mathscr{T}, \\ x(t) = x(t^+) = \bar{f}(x(t^-)), & \forall t \in \mathscr{T}, \end{cases} \tag{9}$$

where

$$A_c \triangleq \begin{bmatrix} A_p & B_p \\ 0 & 0 \end{bmatrix} \in \mathbb{R}^{n \times n} \tag{10}$$

and $\bar{f} : \mathbb{R}^{n_p} \times \mathbb{R}^m \to \mathbb{R}^{n_p} \times \mathscr{U}$ is defined as $\bar{f}(x) = \bar{f}(x_p, u) \triangleq [x_p^T \ f^T(x_p)]^T$.

Notice that $x_p(t)$ is a continuous function while both $u(t)$ and $x(t)$ are right-continuous by convention.

2.1.2 Equivalent discrete-time uncertain system

In order to tackle Problems 2.1 and 2.2, it will be useful to consider difference inclusions that model the behavior of the state of the system at the sampling instants. In particular, notice that the evolution of the state $x_p(t)$ in the intersampling interval satisfies (1) and is given by

$$x_p(t) = e^{A_p(t-t_k)} x_p(t_k) + \int_0^{t-t_k} e^{A_p s} \mathrm{d}s B_p f(x_p(t_k)), \ \forall t \in [t_k, t_{k+1}], \ \forall k \in \mathbb{N}. \tag{11}$$

Thus, denoting $x_{p,k} \triangleq x_p(t_k)$, it follows that the dynamics between two successive sampling instants can be described by the following difference inclusion:

$$x_{p,k+1} \in \left\{ A(\delta) x_{p,k} + B(\delta) f(x_{p,k}) : \ \delta \in \Delta \right\} \tag{12}$$

where $A(\delta) \triangleq e^{A_p \delta}$ and $B(\delta) \triangleq \int_0^\delta e^{A_p s} \mathrm{d}s B_p$. Notice that, even if we fix the initial condition $x_{p,0}$, (12) represents a family of possible trajectories $\{x_{p,k}\}_{k=0}^\infty$ rather than a single one due to the uncertainty δ_k.

Definitions 2.1 and 2.2 also apply for discrete-time systems such as (12), as shown below.

Definition 2.3. *The equilibrium point $x_p = 0$ of (12) is*

- *stable if, for each $\varepsilon > 0$, there is $\beta = \beta(\varepsilon) > 0$ such that*

$$\|x_{p,0}\| \leq \beta \Rightarrow \|x_{p,k}\| \leq \varepsilon, \ \forall k \in \mathbb{N}$$

- *asymptotically stable if it is stable and $\beta > 0$ can be chosen such that*

$$\|x_{p,0}\| \leq \beta \Rightarrow \lim_{k\to\infty} x_{p,k} = 0$$

where the choice $\beta = \beta(\varepsilon) > 0$ must hold uniformly for all possible trajectories $\{x_{p,k}\}_{k\in\mathbb{N}}$ satisfying (12).

Definition 2.4. *The RAO of (12) is the set of all x_p such that for $x_{p,0} = x_p$ it follows that $\lim_{k\to\infty} x_{p,k} = 0$ for all possible trajectories $\{x_{p,k}\}_{k\in\mathbb{N}}$ satisfying (12).*

A key property which will be used in this work is the fact that the stability analysis of the aperiodic sampled-data system (1),(2),(5) can be done considering the discrete-time model (12). Moreover, an estimate of the RAO of (12) is also a valid estimate of the RAO of (1),(2),(5). These statements are formalized in the next lemma.

Lemma 2.1. *Assume that $f : \mathbb{R}^{n_p} \to \mathscr{U} \subset \mathbb{R}^m$ is locally Lipschitz at the origin.*

a) If the origin of the discrete-time system (12) is stable, then the origin of the continuous-time system (1),(2),(5) is also stable;

b) If the origin of the discrete-time system (12) is asymptotically stable, then the origin of the continuous-time system (1),(2),(5) is also asymptotically stable;

c) The RAO of the discrete-time system (12) is included in the RAO of the continuous-time system (1),(2),(5).

Proof:

a) Since $f(\cdot)$ is locally Lipschitz at the origin and $f(0) = 0$, there exist $r, L > 0$ such that

$$\|f(x_p)\| \leq L\|x_p\|, \ \forall x_p \in \mathscr{B}_r, \tag{13}$$

where

$$\mathscr{B}_r \triangleq \{x_p \in \mathbb{R}^{n_p} : \ \|x_p\| \leq r\}. \tag{14}$$

Define

$$C_\delta \triangleq \sup_{\delta\in[0,\tau_M]} \big(\|A(\delta)\| + \|B(\delta)\|L\big).$$

Consider now $\varepsilon > 0$ as in Definition 2.1 and $\bar{\varepsilon} \triangleq \min\{\varepsilon/C_\delta, r\}$. From the stability assumption of the discrete-time system (12) and Definition 2.3, there exists $\beta = \beta(\bar{\varepsilon}) > 0$ such that

$$x_{p,0} \in \mathscr{B}_\beta \ \Rightarrow \ x_{p,k} \in \mathscr{B}_{\bar{\varepsilon}}, \ \forall k \geq 0 \tag{15}$$

for all possible realizations of $\{\delta_k\}_{k=0}^{\infty}$. Notice now that the corresponding continuous-time trajectory $x_p(t)$ of (1),(2),(5) is bounded as follows for $x_p(0) = x_{p,0} \in \mathscr{B}_\beta$:

$$\begin{aligned}\|x_p(t)\| &\leq \|A(t-t_k)\|\|x_p(t_k)\| + \|B(t-t_k)\|\|f(x_p(t_k))\| \\ &\leq \big(\|A(t-t_k)\| + \|B(t-t_k)\|L\big)\|x_{p,k}\| \\ &\leq C_\delta \|x_{p,k}\| \\ &\leq C_\delta(\varepsilon/C_\delta) = \varepsilon, \quad \forall t \in [t_k, t_{k+1}],\ \forall k \in \mathbb{N}\end{aligned}$$

where the first inequality follows from (11), the second one from $x_p(t_k) = x_{p,k} \in \mathscr{B}_{\bar{\varepsilon}} \subseteq \mathscr{B}_r$ and (13) and the last one from $x_{p,k} \in \mathscr{B}_{\bar{\varepsilon}} \subseteq \mathscr{B}_{\varepsilon/C_\delta}$. That is, $\beta > 0$ satisfies property (7) of Definition 2.1. In other words, if $x_p(0) = x_{p,0} \in \mathscr{B}_\beta$ then the discrete-time trajectory remains in $\mathscr{B}_{\bar{\varepsilon}}$ and the continuous-time one in $\mathscr{B}_\varepsilon$.

b), c) These statements will follow directly from the considerations above if we show that

$$x_{p,k} \overset{k\to\infty}{\to} 0 \ \Rightarrow\ x_p(t) \overset{t\to\infty}{\to} 0.$$

The property above is indeed true because

$$\|x_p(t)\| \leq C_\delta \|x_{p,k}\|, \quad \forall t \in [t_k, t_{k+1}], \tag{16}$$

for $x_{p,k} \in \mathscr{B}_r$, where r and C_δ are defined in the proof of item a).

■

The result of Lemma 2.1 also holds in the opposite direction, that is, if the origin of the continuous-time system (1),(2),(5) is (asymptotically) stable, then the origin of the discrete-time system (12) is also (asymptotically) stable. The proof is somewhat simpler and will be omitted. Moreover, the RAO of the discrete-time system is actually *equal* to the one of the continuous-time system.

2.2 Set invariance theory

Besides the well-known Lyapunov theorem and its variants, there are some additional concepts related to the invariance of sets that will be useful in this work, specially when dealing with polyhedral sets. By invariance in this work we always mean positive invariance, that is, considering the behavior of the system for $t \geq 0$.

Given a function $Q : \mathbb{R}^n \to \mathbb{R}$, its sublevel sets are defined below:

$$\Omega_c \triangleq \{x \in \mathbb{R}^n :\ Q(x) \leq c\}, \quad c \in \mathbb{R}. \tag{17}$$

One of the classes of sets that we will consider in this study (in Chapter 3, in particular) is that of ellipsoids, which corresponds to sublevel sets of quadratic functions

$$Q(x) = (x - x_c)^T P (x - x_c),$$

where x_c denotes the center of the set and $P = P^T$ is a positive definite matrix of appropriate dimensions.

Another class of sets of interest is that of polyhedrons. Although there are different definitions in the literature, we define a (convex) *polyhedron* as the intersection of finitely many closed half-spaces (in any dimension). In turn, a (convex) *polytope* is a bounded polyhedron.

Considering the definition above, a polyhedron can be described by its *hyperplane-representation (H-representation)* as follows:

$$\mathscr{P}(H,h) \triangleq \{x \in \mathbb{R}^n : \ Hx \leq h\}, \quad H \in \mathbb{R}^{n_h \times n}, \ h \in \mathbb{R}^{n_h}. \tag{18}$$

If it is bounded, it turns out that it can be equivalently described by the *vertex-representation (V-representation)* of a polytope [Zie95]:

$$\mathscr{V}(V) \triangleq \left\{x = V\alpha \in \mathbb{R}^n : \ \alpha \geq 0, \mathbf{1}^T\alpha = 1, \alpha \in \mathbb{R}^{n_v}\right\}, \quad V \in \mathbb{R}^{n \times n_v}, \tag{19}$$

where $\mathbf{1} \triangleq [1 \dots 1]^T$, that is, any point in the polytope can be obtained as a convex combination of its vertices, given by the columns of V.

If the polytope contains the origin, then it can be represented in a slightly different way:

$$\mathscr{V}_0(V) \triangleq \left\{x = V\alpha \in \mathbb{R}^n : \ \alpha \geq 0, \mathbf{1}^T\alpha \leq 1, \alpha \in \mathbb{R}^{n_v}\right\}, \quad V \in \mathbb{R}^{n \times n_v}. \tag{20}$$

Notice that both the H-representation and the V-representation may or may not be redundant, i.e. it may be possible to discard some of the lines of matrix H or columns of matrix V without changing the resulting set. We can check whether or not a line/column is redundant through the solution of a linear programming problem [Zie95]. Moreover, in order to convert one of the representations into the other one, it is possible to use, for instance, the Fourier-Motzkin elimination method [Zie95, Chapter 1] or the reverse search enumeration method [AF92]. In this study we use the MPT toolbox [HKJM13] to perform these and other operations with polyhedrons.

A convex and compact set containing the origin in its interior is called a *C-set* while a polyhedral C-set (i.e. a polytope that contains the origin in its interior) will sometimes be referred to as a *P-set*. Given a C-set $\Omega \subset \mathbb{R}^n$, its Minkowski function $\Psi_\Omega : \mathbb{R}^n \to \mathbb{R}$ is defined as follows:

$$\Psi_\Omega(x) \triangleq \min\{\alpha \geq 0 : \ x \in \alpha\Omega\}. \tag{21}$$

This function satisfies the following properties:

Lemma 2.2. [Lue97] *(Minkowski function properties)*

- *It is positive definite, continuous and convex;*
- *It is positively homogeneous of order* 1*:*

$$\Psi_\Omega(\lambda x) = \lambda\Psi_\Omega(x) \ \textit{for} \ \lambda \geq 0;$$

- *It is sub-additive:* $\Psi_\Omega(x_1 + x_2) \leq \Psi_\Omega(x_1) + \Psi_\Omega(x_2)$*;*
- *Its unitary level set corresponds to the set* Ω*;*
- *If* Ω *is symmetric, then* $\Psi_\Omega(x)$ *is a vector norm;*
- *It is lower and upper bounded as follows:*

$$\exists m, M > 0 : \quad m\|x\| \leq \Psi_\Omega(x) \leq M\|x\|. \tag{22}$$

Equivalently,

$$\mathscr{B}_{1/M} \subseteq \Omega \subseteq \mathscr{B}_{1/m},$$

where $\mathscr{B}_r \triangleq \{x \in \mathbb{R}^n : \ \|x\| \leq r\}$.

The concept of Minkowski function can be extended to sets: given a C-set $\Omega \subset \mathbb{R}^n$, we define the Minkowski function of a compact set $S \subset \mathbb{R}^n$ as

$$\Psi_\Omega(S) \triangleq \max_{x \in S} \Psi_\Omega(x).$$

Next we will define invariance and contractivity of sets, considering discrete-time and continuous-time dynamics.

2.2.1 Discrete-time case

Consider a generic difference inclusion of the form

$$x_{k+1} \in \mathscr{F}(x_k) \tag{23}$$

where $\mathscr{F}(\cdot)$ is a set-valued map, $F(0) = \{0\}$ and $\mathscr{F}(x_k)$ denotes all the possible successors x_{k+1} of x_k. Models of this type are useful to describe, for instance, systems subject to bounded uncertainties as the sampled-data one introduced in Section 2.1 (see (12)). Definitions 2.3 and 2.4 also apply for (23) *mutatis mutandis*.

We define invariance and contractivity with respect to (23) as follows.

Definition 2.5. *Given $\lambda \in [0,1)$, the set $\Omega \subseteq \mathbb{R}^n$ is said to be λ-contractive for (23) if $\mathscr{F}(x_k) \subseteq \lambda\Omega$ for all $x_k \in \Omega$. If $\lambda = 1$, Ω is an invariant set for (23).*

The notion above can be extended to systems with constrained inputs of the form

$$x_{k+1} \in \mathscr{G}(x_k, u_k), \tag{24}$$

where $u_k \in \mathscr{U}$ and $\mathscr{G}(\cdot,\cdot)$ is a set-valued map, as shown next.

Definition 2.6. *Given $\lambda \in [0,1)$, the set $\Omega \subseteq \mathbb{R}^n$ is said to be controlled λ-contractive for (24) if there exists a feedback control $f : \Omega \to \mathscr{U}$ such that*

$$\mathscr{G}(x_k, f(x_k)) \subseteq \lambda\Omega, \quad \forall x_k \in \Omega. \tag{25}$$

If $\lambda = 1$, Ω is a controlled invariant set for (24).

In other words, for each $x_k \in \Omega$ there exists a control value $u_k \in \mathscr{U}$ such that all the possible successors $x_{k+1} \in \mathscr{G}(x_k, u_k)$ of x_k belong to $\lambda\Omega$.

Consider now the case where Ω and $\mathscr{U}$ are C-sets and system (24) satisfies

$$\mathscr{G}(cx, cu) = c\mathscr{G}(x,u), \quad \forall (x,u,c) \in \Omega \times \mathscr{U} \times [0,1]. \tag{26}$$

The difference inclusions considered in this study will indeed have the homogeneity property above, which holds for the particular case of linear systems, for instance.

The following result, which can be seen as an adaptation of [BM15, Theorem 4.24], guarantees that a controlled contractive set remains controlled contractive when scaled down.

Lemma 2.3. *If the C-set Ω is controlled λ-contractive for (24), $\mathscr{U}$ is a C-set and (26) holds, then $\varepsilon\Omega$ is also controlled λ-contractive for (24) for all $\varepsilon \in [0,1]$.*

Proof: Consider the nontrivial case $\varepsilon \neq 0$. Given $x \in \varepsilon\Omega$, we have to prove that $\mathscr{G}(x,u) \subseteq \lambda\varepsilon\Omega$ for some $u(x) \in \mathscr{U}$. Define $\bar{x} \triangleq x/\varepsilon \in \Omega$. From the contractivity assumption of Ω, there exists $\bar{u} \in \mathscr{U}$ such that

$$\mathscr{G}(\bar{x},\bar{u}) \subseteq \lambda\Omega. \tag{27}$$

Define now $u \triangleq \varepsilon\bar{u}$ and notice that $u \in \mathscr{U}$ since $\mathscr{U}$ is a C-set and $0 < \varepsilon \leq 1$. It follows that

$$\mathscr{G}(x,u) = \mathscr{G}(\varepsilon\bar{x},\varepsilon\bar{u}) \underbrace{=}_{(26)} \varepsilon\mathscr{G}(\bar{x},\bar{u}) \underbrace{\subseteq}_{(27)} \lambda(\varepsilon\Omega),$$

as we wanted to show. ■

The lemma above has the following corollary for the uncontrolled case.

Corollary 2.1. *If the C-set Ω is λ-contractive for (23) and*

$$\mathscr{F}(cx) = c\mathscr{F}(x), \quad \forall (x,c) \in \Omega \times [0,1],$$

then:

a) $\varepsilon\Omega$ is also λ-contractive for (23) for all $\varepsilon \in [0,1]$;

b) All trajectories $\{x_k\}_{k\in\mathbb{N}}$ satisfying (23) have the following property:

$$x_k \in \varepsilon\Omega \;\Rightarrow\; x_{k+p} \in \lambda^p\varepsilon\Omega, \quad \forall \varepsilon \in [0,1],\ \forall p \in \mathbb{N}. \tag{28}$$

Proof:

a) The proof is analogous to the one of Lemma 2.3;

b) Follows from the recursive application of a).

■

Property (28) implies that $x_k \overset{k\to\infty}{\to} 0$ if $x_0 \in \Omega$ since Ω is a C-set and, hence, bounded by definition. Moreover, the origin of (23) is asymptotic stable and Ω belongs to its RAO. Notice that we arrived at these conclusions without making direct use of the Lyapunov theorem, even if there is a natural way to define a Lyapunov function associated to the set Ω, as shown next.

From the definition of the Minkowski function of Ω, (28) is equivalent to

$$\Psi_\Omega(x_k) \leq \varepsilon \;\Rightarrow\; \Psi_\Omega(x_{k+p}) \leq \lambda^p\varepsilon, \quad \forall \varepsilon \in [0,1],\ \forall p \in \mathbb{N}. \tag{29}$$

That is, $\Psi_\Omega(\cdot)$ is a Lyapunov function for (23) inside Ω.

Moreover, if Ω is a C-set, the relation (25) in Definition 2.6 is equivalent to:

$$\begin{aligned}\mathscr{G}(x_k,f(x_k)) \subseteq \lambda\Omega,\ \forall x_k \in \Omega \;&\Leftrightarrow \Psi_\Omega(x_{k+1}) \leq \lambda,\ \forall x_{k+1} \in \mathscr{G}(x_k,f(x_k)),\ \forall x_k \in \Omega \\ &\Leftrightarrow \Psi_\Omega(\mathscr{G}(x_k,f(x_k))) \leq \lambda,\ \forall x_k \in \Omega.\end{aligned}$$

In order to obtain (controlled) contractive/invariant sets for discrete-time systems, many methods in the literature use the concept of *one-step set* (or *preimage set*), as defined next.

Definition 2.7. *The one-step set of $\Omega \subseteq \mathbb{R}^n$ for system (24) is given by:*

$$\mathrm{Pre}(\Omega) \triangleq \{x \in \mathbb{R}^n : \ \exists u \in \mathscr{U} \ s.t. \ \mathscr{G}(x,u) \subseteq \Omega\}. \tag{30}$$

That is, $\mathrm{Pre}(\Omega)$ corresponds to the set of all states $x_k \in \mathbb{R}^n$ that can be driven into Ω for an appropriate choice of the input, which must be simultaneously valid for all possible successors $x_{k+1} \in \mathscr{G}(x_k, u_k)$ of x_k. From this definition it follows that a set Ω is controlled λ-contractive for (24) if and only if $\Omega \subseteq \mathrm{Pre}(\lambda\Omega)$. The uncontrolled version of Definition 2.7 is analogous:

Definition 2.8. *The one-step set of $\Omega \subseteq \mathbb{R}^n$ for system (23) is given by:*

$$\mathrm{Pre}(\Omega) \triangleq \{x \in \mathbb{R}^n : \ \mathscr{F}(x) \subseteq \Omega\}.$$

The definition below presents the concept of maximal (controlled) λ-contractive C-set included in a given C-set Ω_0.

Definition 2.9. *Given a C-set Ω_0, a (controlled) λ-contractive C-set $\Omega \subseteq \Omega_0$ is maximal in Ω_0 if every (controlled) λ-contractive C-set Ω' included in Ω_0 is also included in Ω.*

2.2.2 Continuous-time case

For simplicity, in this section we will present the concept of invariance directly to the case of interest (the linear one), even if the notions can be generalized. We will assume that Ω is a C-set and consider the dynamics

$$\dot{x}(t) = A_c x(t). \tag{31}$$

Before defining invariance in the continuous-time case, notice that functions such as $\Psi_\Omega(x)$ are not differentiable everywhere, so it is convenient to work with an alternative definition of derivative [BM15]:

Definition 2.10. *(Directional derivative) Given a locally Lipschitz function $\Psi : \mathbb{R}^n \to \mathbb{R}$ and the linear time-invariant system (31), the (upper right) directional derivative of $\Psi(x)$ with respect to this system is defined as follows:*

$$D^+\Psi(x) \triangleq \limsup_{h \to 0^+} \frac{\Psi(x + hA_c x) - \Psi(x)}{h}. \tag{32}$$

Remark 2.1. *If $\Psi(x)$ is continuously differentiable, then we retrieve the usual expression [BM15]:*

$$D^+\Psi(x) = \nabla\Psi^T(x) A_c x$$

where $\nabla\Psi(x)$ is the gradient of $\Psi(x)$.

Given a locally Lipschitz function $\Psi : \mathbb{R}^n \to \mathbb{R}$, we want to characterize its behavior along the trajectories of (31). Consider then the composite function

$$\psi(t) \triangleq \Psi(x(t)). \tag{33}$$

This function is usually not differentiable. However, it is locally Lipschitz (as the composition of locally Lipschitz functions). Thus, the limit taken in the definition below is well defined. This definition introduces an alternative notion of derivative which coincides with the standard one when the latter exists.

Definition 2.11. *(Dini derivative) The (upper right) Dini derivative $D^+\psi(t)$ of ψ at t is*

$$D^+\psi(t) \triangleq \limsup_{h\to 0^+} \frac{\psi(t+h)-\psi(t)}{h}. \tag{34}$$

Now we are ready to state the following theorem, which makes a connection between the two definitions of derivative presented above.

Theorem 2.1. [RHL77, Appendix 1, Th. 4.3] *Let $x(t)$ be a solution of (31) and $\Psi:\mathbb{R}^n\to\mathbb{R}$ be a locally Lipschitz function. Then the composite function $\psi(t)=\Psi(x(t))$ satisfies*

$$D^+\psi(t) = D^+\Psi(x(t)) \quad \textit{for almost all } t. \tag{35}$$

Since $\psi(t)$ is locally Lipschitz, it is absolutely continuous in any compact interval [RF10, Ch. 6, Prop. 7]. Thus, it is differentiable almost everywhere [RF10, Ch. 6, Th. 10] and (35) implies

$$\dot\psi(t) = D^+\Psi(x(t)) \quad \text{for almost all } t \tag{36}$$

(recall that $D^+\psi(t)$ coincides with $\dot\psi(t)$ when the latter exists, as it can be verified from the definition of $D^+\psi(t)$).

From now on we will consider $\Psi:\mathbb{R}^n\to\mathbb{R}$ to be the Minkowski function Ψ_Ω of a C-set Ω and define invariance of Ω for (31) using this function. Notice that Ψ_Ω is indeed Lipschitz, so the previously stated results hold. We define β-invariance in the continuous-time case as follows:

Definition 2.12. [BM15] *Given $\beta\in\mathbb{R}$, the C-set $\Omega\subset\mathbb{R}^n$ is said to be β-invariant for system (31) if the following condition holds:*

$$D^+\Psi_\Omega(x) \le \beta, \quad \forall x\in\partial\Omega. \tag{37}$$

Strictly speaking, the set is invariant in the usual sense only if $\beta\le 0$, but it will be convenient for the development of the results to consider also the case $\beta>0$. Condition (37) is rather technical. The lemma below, proved in Appendix A.1, presents a concrete consequence of it.

Lemma 2.4. *If the C-set Ω is β-invariant for system (31), then the trajectories of (31) satisfy*

$$\Psi_\Omega(x(t)) \le e^{\beta t}\Psi_\Omega(x(0)), \quad \forall t\ge 0. \tag{38}$$

The result above has the following corollary.

Corollary 2.2. [FM16, Proposition 21] *If the C-set Ω is β-invariant for system (31), then*

$$e^{A_c\tau}\Omega \subseteq \alpha\Omega, \quad \forall\tau\in[0,\bar\tau], \tag{39}$$

where $\alpha\triangleq\max\{1,e^{\beta\bar\tau}\}$, $\bar\tau>0$.

Proof: Given $(z,\tau)\in\Omega\times[0,\bar\tau]$, we have to show that $e^{A_c\tau}z\in\alpha\Omega$. Consider the solution $x(t)$ of (31) with the initial condition $x(0)=z$, which is given by $x(t)=e^{A_ct}z$. Substituting it in (38) with $t=\tau$ and using the fact that $\Psi_\Omega(z)\le 1$ one obtains

$$\Psi_\Omega(e^{A_c\tau}z) \le e^{\beta\tau}\Psi_\Omega(z) \le e^{\beta\tau} \le \left\{\begin{array}{ll} 1 & \text{if } \beta<0 \\ e^{\beta\bar\tau} & \text{if } \beta\ge 0 \end{array}\right\} \le \max\{1,e^{\beta\bar\tau}\} = \alpha.$$

This relation is equivalent to $e^{A_c\tau}z\in\alpha\Omega$, as we wanted to show. ■

An important feature of the concept of β-invariance is that it can be characterized in terms of a linear programming problem when the system is linear and time-invariant and the C-set Ω is polyhedral, as shown below [Bit91, CH93, BM15].

Lemma 2.5. *Consider the polyhedral C-set $\Omega = \mathscr{P}(H, \mathbf{1})$, where $H \in \mathbb{R}^{n_h \times n}$. The following statements are equivalent.*

a) Ω is β-invariant for system (31);

b) There exists $T \in \mathbb{R}^{n_h \times n_h}$ such that

$$\begin{cases} HA_c = TH \\ T\mathbf{1} \leq \beta \mathbf{1} \\ T_{(i,j)} \geq 0, \qquad \forall i \neq j. \end{cases} \tag{40}$$

Moreover, the following technical result, which will be useful later, holds.

Lemma 2.6. *Given a family of C-sets $\{\Omega_i\}_{i \in I}$ included in $\mathbb{R}^n$, where I is the corresponding index set, such that*

$$\mathscr{B}_{r_1} \subseteq \Omega_i \subseteq \mathscr{B}_{r_2}, \quad \forall i \in I, \tag{41}$$

where $r_1, r_2 > 0$, there exists $\beta \in \mathbb{R}$ such that Ω_i is β-invariant for (31) for all $i \in I$.

Proof: See Appendix A.2. ■

2.3 Concluding remarks

As already explained, the concepts introduced in this chapter will be used in Chapters 3–6. The stochastic framework of Chapter 7 will be directly presented in Chapter 7.

Chapter 3 focuses on the computation of ellipsoidal estimates of the RAO of the sampled-data system and is directly based on the Lyapunov theorem. Chapters 4–6, on the other hand, apply the definitions and results of set invariance theory in order to compute polyhedral estimates of the RAO.

3 STABILITY ANALYSIS AND STABILIZATION: QUADRATIC APPROACH

In this chapter we will consider a generalization of the linear saturated state feedback (3), as follows:

$$u(t) = \text{sat}(K_p x_p(t_k^-) + K_u u(t_k^-)), \quad \forall t \in [t_k, t_{k+1}), \tag{42}$$

where matrix K_u has appropriate dimensions. That is, the control input to be applied in the interval $[t_k, t_{k+1})$ depends both on the sampled value of the state and the value of the control signal applied in the previous sampling interval $[t_{k-1}, t_k)$. This kind of control law is also considered in [Bri18], for instance. Notice that (3) is a particular case of (42) with $K_u = 0$. Considering $K_u \neq 0$ will allow to solve the control design problem through LMI conditions without imposing any structural constraint on the Lyapunov matrix $P = P^T \succ 0$. In fact, if we assume $K_u = 0$ then P must be block diagonal in order to obtain convex conditions. On the other hand, in the stability analysis case, it is possible to obtain an optimization problem in LMI form with a generic matrix $P = P^T \succ 0$ with or without the constraint $K_u = 0$.

Denoting $x = [x_p^T \ u^T]^T \in \mathbb{R}^n, n = n_p + m$, as in Section 2.1.1, the dynamics (1),(42) can be represented by the following impulsive system for every $\mathscr{T} \in \Theta(\Delta)$:

$$\begin{cases} \dot{x}(t) = A_c x(t), & \forall t \in \mathbb{R}_+ \setminus \mathscr{T}, \\ x(t) = x(t^+) = A_r x(t^-) + B_r \text{sat}(Kx(t^-)), & \forall t \in \mathscr{T}, \\ x(0) = [x_{p,0}^T \ \ \text{sat}^T(K_p x_{p,0} + K_u u(0^-))]^T \in \mathbb{R}^n, & \end{cases} \tag{43}$$

where A_c is defined in (10) and

$$A_r \triangleq \begin{bmatrix} I_{n_p} & 0 \\ 0 & 0 \end{bmatrix} \in \mathbb{R}^{n \times n}, \quad B_r \triangleq \begin{bmatrix} 0 \\ I_m \end{bmatrix} \in \mathbb{R}^{n \times m}, \quad K \triangleq \begin{bmatrix} K_p & K_u \end{bmatrix} \in \mathbb{R}^{m \times n}. \tag{44}$$

The objective of this chapter is to solve Problems 2.1 and 2.2 presented in Chapter 2 for system (43) considering quadratic Lyapunov functions and semidefinite programming problems. In other words, regarding Problem 2.1, we aim at certifying the asymptotic stability of the origin and obtaining ellipsoidal estimates of the RAO of the system using some size criterion in order to enlarge them. When the value of the feedback gain K is free, then it will be conveniently chosen in order to enlarge even more the size of these ellipsoids, according to Problem 2.2.

The chapter is organized as follows. Section 3.1 introduces the difference inclusions that model the evolution of the system state at the sampling instants. Section 3.2 presents the stability analysis of the system. Section 3.3 shows how to derive stabilization conditions from the previous results. A numerical example is provided in Section 3.4. Some concluding remarks end the chapter.

3.1 Equivalent discrete-time uncertain system

For a given initial condition and $\mathscr{T} \in \Theta(\Delta)$, the evolution of the state x between two successive sampling instants, i.e. for $t \in [t_k, t_{k+1})$, is continuous. Thus, since the dynamics in this interval is linear, it follows that:

$$x(t) = e^{A_c(t-t_k)}x(t_k), \qquad \forall t \in [t_k, t_{k+1}). \tag{45}$$

Hence, taking into account (45) and the fact that $x(t_k^-) \neq x(t_k)$ (due to the impulsive control update, in fact, there is a discontinuity between $x(t_k^-)$ and $x(t_k)$, see (43)), the dynamics between two successive sampling instants is given by the following discrete-time equation

$$\begin{aligned} x(t_{k+1}^-) &= e^{A_c(t_{k+1}-t_k)}x(t_k) \\ &= e^{A_c(t_{k+1}-t_k)}\left(A_r x(t_k^-) + B_r \mathrm{sat}(Kx(t_k^-))\right) \\ &= e^{A_c\delta_k}A_r x(t_k^-) + e^{A_c\delta_k}B_r \mathrm{sat}(Kx(t_k^-)) \end{aligned}$$

where δ_k was defined in (5). Thus, denoting $A_z(\delta) \triangleq e^{A_c\delta}A_r$, $B_z(\delta) \triangleq e^{A_c\delta}B_r$ and $z_k \triangleq x(t_k^-)$, we obtain the following difference inclusion:

$$z_{k+1} \in \{A_z(\delta)z_k + B_z(\delta)\mathrm{sat}(Kz_k) : \ \delta \in \Delta\}. \tag{46}$$

Following a similar argument to the one of Lemma 2.1, the problems of stability analysis and stabilization of the sampled-data system (43) can be addressed by considering the discrete-time nonlinear parametric uncertain system (46). In particular, since the system dynamics obeys (45), it follows that

$$z_{k+1} = x(t_{k+1}^-) = e^{A_c(t_{k+1}-t)}x(t), \quad \forall t \in [t_k, t_{k+1})$$

and, equivalently, we have

$$x(t) = e^{A_c(t-t_{k+1})}z_{k+1}, \quad \forall t \in [t_k, t_{k+1}).$$

Consequently, the state $x(t)$ of (43) is bounded by z_k as follows:

$$\|x(t)\| \leq \sup_{\delta\in[0,\tau_M]} \|e^{-A_c\delta}\|\|z_{k+1}\|, \quad \forall t \in [t_k, t_{k+1}), \ \forall k \in \mathbb{N}. \tag{47}$$

The bound above will be used in the proof of Theorem 3.1. In particular, it guarantees that the origin of (43) is asymptotically stable if the origin of (46) is asymptotically stable and that $x(t) \overset{t\to\infty}{\to} 0$ if $z_k = x(t_k^-) \overset{k\to\infty}{\to} 0$.

Consider now the partition of the interval $\Delta = [\tau_m, \tau_M]$ in $J \in \mathbb{N}_+$ sub-intervals and define the set:

$$\Delta_J \triangleq \{d_j \triangleq \tau_m + (j-1)\tau_J : \ j \in \mathbb{N}_J\}, \quad \tau_J \triangleq \frac{\tau_M - \tau_m}{J}, \quad \mathbb{N}_J \triangleq \{i \in \mathbb{N} : \ 1 \leq i \leq J\}. \tag{48}$$

From (48), we have that for every $\delta \in \Delta$ there exist $d \in \Delta_J$ and $\tau \in [0, \tau_J]$ such that $\delta = d + \tau$ and it follows that:

$$\begin{aligned} A_z(\delta) = A_z(d+\tau) = e^{A_c(d+\tau)}A_r = e^{A_c\tau}A_z(d), \\ B_z(\delta) = B_z(d+\tau) = e^{A_c(d+\tau)}B_r = e^{A_c\tau}B_z(d). \end{aligned}$$

Thus, from (46), we can write that:

$$z_{k+1} = e^{A_c\tau}A_z(d)z_k + e^{A_c\tau}B_z(d)\text{sat}(Kz_k),$$

with $d \in \Delta_J$ and $\tau \in [0, \tau_J]$. Then, given the value $x(t_k^-) = z_k$, the possible successors $x(t_{k+1}^-) = z_{k+1}$ are given by the difference inclusion

$$z_{k+1} \in \left\{ e^{A_c\tau}\left(A_z(d)z_k + B_z(d)\text{sat}(Kz_k)\right) : \ d \in \Delta_J, \tau \in [0, \tau_J] \right\}.$$

Hence, defining the following set-valued maps

$$\begin{array}{l} \mathscr{F}_J(\mathscr{Z}) = \left\{A_z(d_j)z + B_z(d_j)\text{sat}(Kz) : \ j \in \mathbb{N}_J, z \in \mathscr{Z}\right\} \subseteq \mathbb{R}^n, \\ \mathscr{G}_J(\mathscr{Y}) = \left\{e^{A_c\tau}y : \ \tau \in [0, \tau_J], y \in \mathscr{Y}\right\} \subseteq \mathbb{R}^n, \end{array} \tag{49}$$

where $\mathscr{Y}, \mathscr{Z} \subseteq \mathbb{R}^n$,[1] then for some $y_k \in \mathscr{F}_J(z_k)$ we have that $z_{k+1} \in \mathscr{G}_J(y_k)$, i.e. the dynamics in (46) is equivalently given by the difference inclusions

$$z_{k+1} \in \mathscr{G}_J(\mathscr{F}_J(z_k)). \tag{50}$$

Thus, the difference inclusion system (50) permits to analyze the stability of the sampled-data system (43) under aperiodic sampling with intersampling time bounded by τ_m and τ_M. The next section will use (50) to present sufficient conditions under which the origin of (46) is asymptotically stable and its state converges to zero and then, as already discussed, these properties will be inherited by system (43).

3.2 Stability analysis

3.2.1 Lyapunov setup

Considering a Lyapunov function $V(x)$ and the difference inclusion in (50), a sufficient condition for the asymptotic stability of the origin of system (43) and the characterization of estimates of the RAO are given in the following theorem, where the sublevel sets Ω_c of $V(x)$ are defined in (17).

Theorem 3.1. *Let $V(x) : \mathbb{R}^n \to \mathbb{R}$ be a differentiable positive definite Lyapunov candidate function. Let $\mathscr{D} \subseteq \mathbb{R}^n$ be a neighborhood of the origin. Suppose that there exists $c > 0$ such that Ω_c is bounded and $\Omega_c \subseteq \mathscr{D}$. Assume also that there exist $\lambda \in (0,1)$ and $J \in \mathbb{N}_+$ such that the following conditions hold:*

a) $V(y_k) \leq \lambda V(z_k)$ for all $z_k \in \mathscr{D}$ and $y_k \in \mathscr{F}_J(z_k)$, with $\mathscr{F}_J(\cdot)$ as defined in (49);

b) $\dot{V}(x) < \alpha V(x)$ along the (nonzero) trajectories belonging to $\mathscr{D}$ of

$$\dot{x}(t) = A_c x(t), \tag{51}$$

with $\alpha = -ln(\lambda)/\tau_J$. Then, the origin of the aperiodic sampled-data saturated control system (43) is asymptotically stable. Moreover the set Ω_c is contained in the RAO.

[1] When $\mathscr{Z} \subseteq \mathbb{R}^n$ is a singleton, i.e. $\mathscr{Z} = \{z\}, z \in \mathbb{R}^n$, we simply write $\mathscr{F}_J(z)$ instead of $\mathscr{F}_J(\{z\})$ and similarly for $\mathscr{G}_J(\cdot)$.

Proof: Given $z_k = x(t_k^-) \in \Omega_c$, $z_k \neq 0$, we prove first that $V(z_{k+1}) < V(z_k)$ for all $z_{k+1} = x(t_{k+1}^-)$ satisfying (50) (equivalently, (46)).

For each $z_{k+1} \in \mathscr{G}_J(\mathscr{F}_J(z_k))$, there exist $d_j \in \Delta_J$, $y_k \in \mathscr{F}_J(z_k)$ and $\tau \in [0, \tau_J]$ such that $z_{k+1} = e^{A_c \tau} y_k$, where

$$y_k = A_z(d_j) z_k + B_z(d_j) \text{sat}(K z_k). \tag{52}$$

From condition a) we have that $V(y_k) \leq \lambda V(z_k)$. Moreover, notice that $z_{k+1} = e^{A_c \tau} y_k$ corresponds to the solution of (51) at time $t + \tau$ with initial condition $x(t) = y_k$. Then from condition b) and since $\alpha = -\ln(\lambda)/\tau_J > 0$ one obtains:

$$\begin{array}{ll} V(z_{k+1}) = V(y_k) < e^{\alpha \tau_J} V(y_k) = \frac{1}{\lambda} V(y_k) \leq V(z_k), & \text{if } \tau = 0 \\ V(z_{k+1}) < e^{\alpha \tau} V(y_k) \leq e^{\alpha \tau_J} V(y_k) \leq V(z_k), & \text{if } \tau > 0. \end{array}$$

That is, $V(z_{k+1}) < V(z_k)$, for all $z_{k+1} \in \mathscr{G}_J(\mathscr{F}_J(z_k))$. It follows from standard Lyapunov theory arguments that the state $z_k = x(t_k^-)$ of the discrete-time system (46) remains in Ω_c and converges to zero as $k \to \infty$, provided that $z_0 \in \Omega_c$. Hence, from (47) we conclude that $x(t) \to 0$ as $t \to \infty$ and that the origin of the aperiodic sampled-data saturated control system (43) is asymptotically stable. Moreover, the set $\Omega_c \subseteq \mathscr{D}$ is contained in the RAO. ■

Fig. 5 gives a graphical interpretation of the reasoning implied by conditions a) and b) in terms of the behavior of the function $V(x)$. More precisely, the Lyapunov function decreases at least by a factor of λ after a time interval $d_j \in \Delta_J$, i.e. $V(y_k) \leq \lambda V(z_k)$, according to condition a). Moreover, even if $V(x)$ may increase in continuous-time, as also sketched, its increase is conveniently bounded by condition b). Thus, it is possible to guarantee that $V(z_{k+1}) < V(z_k)$.

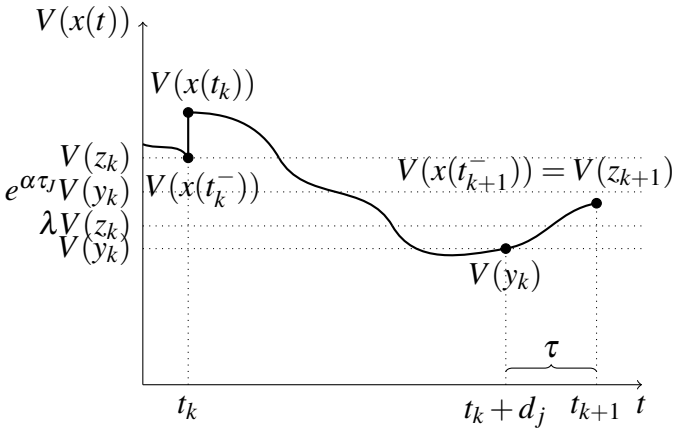

Figure 5: Behavior of $V(x(t))$.

Remark 3.1. *The estimate Ω_c of the RAO is related to $z_0 = x(0^-) = [x_p^T(0),\ u^T(0^-)]^T$ where $x_p(0) = x_p(0^-)$ is the initial plant state and $u(0^-)$ is a free value that can be conveniently chosen to initialize the control such that $z_0 \in \Omega_c$.*

Remark 3.2. *Since α is a positive scalar, condition b) in Theorem 3.1 does not impose a decreasing of the function $V(\cdot)$ in continuous-time. Actually, it ensures a bound on its potential increasing, which means that A_c is not required to be Hurwitz. In fact, note that A_c will never be Hurwitz because of its particular structure including null eigenvalues. So the verification of condition b) will require a sufficiently large $\alpha > 0$. See also Remark 3.5 in this regard.*

In the next theorem we show that Theorem 3.1 is not conservative in the sense that, if there exists an exponentially decreasing Lyapunov function for the system (50) which satisfies (53) and (54), then the conditions in Theorem 3.1 will also hold for this function.

Theorem 3.2. *Let $\mathscr{D} \subset \mathbb{R}^n$ be a bounded neighborhood of the origin. Suppose that there exists a continuously differentiable and positive definite function $V(x) : \mathbb{R}^n \to \mathbb{R}$ satisfying*

$$V(z_{k+1}) \leq \bar{\lambda} V(z_k) \tag{53}$$

for all $z_k \in \mathscr{D}$ and for all z_{k+1} given by (50), with $\bar{\lambda} \in (0,1)$. Assume that $V(\cdot)$ also satisfies

$$\dot{V}(x) < \beta_1 V(x), \qquad \forall x \in \mathscr{N} \setminus \{0\} \tag{54}$$

along the trajectories of (51), with $\mathscr{N}$ an arbitrary neighborhood of the origin and an arbitrary $\beta_1 \in \mathbb{R}$. Then there exists $J \in \mathbb{N}$, $\lambda \in (0,1)$ such that items a) and b) of Theorem 3.1 hold.

Proof: Since $\mathscr{F}_J(z_k) \subseteq \mathscr{G}_J(\mathscr{F}_J(z_k))$ for all $J \in \mathbb{N}$, it follows that

$$V(y_k) \leq \bar{\lambda} V(z_k), \quad \forall z_k \in \mathscr{D},\ \forall y_k \in \mathscr{F}_J(z_k).$$

Thus condition a) is satisfied with $\lambda = \bar{\lambda}$.

Since $V(\cdot)$ and its derivative are continuous and $\overline{\mathscr{D} \setminus \mathscr{N}}$ is compact (it is closed by definition and bounded since $\mathscr{D}$ is bounded) and does not contain the origin, there exists $\beta_2 > 0$ such that

$$\frac{|\nabla V(x)^T A_c x|}{V(x)} < \beta_2, \qquad \forall x \in \overline{\mathscr{D} \setminus \mathscr{N}}.$$

It follows that

$$\dot{V}(x) < \beta_2 V(x), \qquad \forall x \in \overline{\mathscr{D} \setminus \mathscr{N}} \tag{55}$$

along the trajectories of (51). From (54) and (55), and for $J \in \mathbb{N}$ big enough, then $\max\{\beta_1, \beta_2\} \leq -\ln(\lambda)/\tau_J = \alpha$, which implies satisfaction of b). ■

3.2.2 Convex conditions

In order to obtain testable conditions, in this section we apply Theorem 3.1 considering $V(x)$ as a quadratic function. This will allow to express conditions a) and b) as linear matrix inequalities (LMIs) and therefore to formulate convex optimization problems to determine estimates of the RAO of the closed-loop system.

To deal with the saturation term present in (52), we consider the generalized sector condition proposed in [GT05]. For this, consider a deadzone nonlinearity defined as follows:

$$\phi(Kx) \triangleq \text{sat}(Kx) - Kx \tag{56}$$

Lemma 3.1. [GT05] *Let a matrix $G \in \mathbb{R}^{m \times n}$. The relation*

$$\phi^T(Kx) T \left(\phi(Kx) + Gx\right) \leq 0$$

is verified for any diagonal positive definite matrix $T \in \mathbb{R}^{m \times m}$, provided that x belongs to the set

$$\mathscr{H}(K-G) \triangleq \{x \in \mathbb{R}^n :\ \|(K-G)x\|_\infty \leq 1\}.$$

Using the deadzone function defined in (56) it follows that (52) can be re-written as

$$y_k = \left(A_z(d_j) + B_z(d_j)K\right) z_k + B_z(d_j)\phi(Kz_k). \tag{57}$$

Based on (57) and the conditions in Theorem 3.1 with a quadratic function $V(x) = x^T Px,\ P = P^T \succ 0$, we can now state the following result, where $\lambda_{max}(A_c)$ denotes the maximal real part of the eigenvalues of matrix A_c.

Theorem 3.3. *If there exist a matrix $W = W^T \succ 0$, $W \in \mathbb{R}^{n\times n}$, matrices $R_j \in \mathbb{R}^{m\times n}$ and diagonal positive definite matrices $S_j \in \mathbb{R}^{m\times m}\ \forall j \in \mathbb{N}_J$, and scalars $\lambda \in (0,1)$ and $\alpha = -ln(\lambda)/\tau_J > \max\{2\lambda_{max}(A_c),0\}$ satisfying the following LMIs*

$$\begin{bmatrix} \lambda W & R_j^T & WA_z^T(d_j) + WK^T B_z^T(d_j) \\ \star & 2S_j & S_j B_z^T(d_j) \\ \star & \star & W \end{bmatrix} \succeq 0,\ \forall j \in \mathbb{N}_J \tag{58}$$

$$\begin{bmatrix} W & WK_{(i)}^T - R_{j(i)}^T \\ \star & 1 \end{bmatrix} \succeq 0,\ \forall j \in \mathbb{N}_J,\ \forall i \in \mathbb{N}_m \tag{59}$$

$$WA_c^T + A_c W - \alpha W \prec 0 \tag{60}$$

then, for all $x(0^-) = z_0 \in \mathscr{E}(W^{-1}) \triangleq \{x \in \mathbb{R}^n :\ x^T W^{-1} x \leq 1\}$, it follows that the corresponding trajectory of the sampled-data system (43), with δ_k satisfying (5), converges asymptotically to the origin.

Proof: Consider $V(x) = x^T Px$ with $P = W^{-1}$. By using the change of variables $G_j = R_j P$ and by left and right multiplying (58) by $\mathrm{Diag}(P, T_j, I_n)$, denoting $T_j = S_j^{-1}$, one has

$$\begin{bmatrix} \lambda P & G_j^T T_j & A_z^T(d_j) + K^T B_z^T(d_j) \\ \star & 2T_j & B_z^T(d_j) \\ \star & \star & W \end{bmatrix} \succeq 0,\ \forall j \in \mathbb{N}_J.$$

Using Schur's complement we then get

$$\begin{bmatrix} \lambda P & G_j^T T_j \\ \star & 2T_j \end{bmatrix} - \begin{bmatrix} \left(A_z(d_j) + B_z(d_j)K\right)^T \\ B_z^T(d_j) \end{bmatrix} P \begin{bmatrix} A_z(d_j) + B_z(d_j)K & B_z(d_j) \end{bmatrix} \succeq 0,\ \forall j \in \mathbb{N}_J.$$

Left and right multiplying the resulting inequality respectively by $[z_k^T\ \ \phi^T(Kz_k)]$ and its transpose, one can conclude that:

$$y_k^T P y_k \leq \lambda z_k^T P z_k + 2\phi^T(Kz_k)T_j\left(\phi(Kz_k) + G_j z_k\right),$$

for all $j \in \mathbb{N}_J$ and all $z_k \in \mathbb{R}^n$, with y_k given by (57). Thus, from Lemma 3.1, it follows that $V(y_k) \leq \lambda V(z_k)$ for all $y_k \in \mathscr{F}_J(z_k)$, provided that $z_k \in \bigcap_{j\in\mathbb{N}_J} \mathscr{H}(K - G_j)$. That is, condition a) of Theorem 3.1 is satisfied with

$$\mathscr{D} = \bigcap_{j\in\mathbb{N}_J} \mathscr{H}(K - G_j).$$

Moreover, from (60) it follows that item b) of Theorem 3.1 is verified with $V(x) = x^T Px$. At this point note that (60) can be verified if and only if the eigenvalues of A_c have

real part strictly smaller than $\alpha/2$. Thus, it is necessary to consider $\alpha > \max\{2\lambda_{max}(A_c),0\}$ in order to ensure the feasibility of inequality (60).

Hence, from Theorem 3.1, the sublevel set $\Omega_1 = \mathscr{E}(W^{-1})$ associated to function V is included in the RAO of system (43) provided that $\mathscr{E}(W^{-1}) \subseteq \mathscr{D}$, which is guaranteed by (59), as shown next.

Applying Schur's complement to (59) and left and right multiplying the resulting inequality by $z_k^T P$ and Pz_k respectively, it follows that

$$|(K - G_j)_{(i)} z_k|^2 \leq z_k^T P z_k, \;\; \forall j \in \mathbb{N}_J, \; \forall i \in \mathbb{N}_m, \; \forall z_k \in \mathbb{R}^n,$$

which ensures that $\mathscr{E}(W^{-1}) \subseteq \mathscr{D}$ and concludes the proof. ■

Remark 3.3. *Notice that the periodic sampling case (i.e. when $\tau_m = \tau_M$) is obtained as a particular case with the set Δ_J as $\Delta_J = \{\tau_m\} = \{\tau_M\}$. In this case condition (60) can be neglected and the LMIs (58) and (59) turn out to be the classical LMIs used for linear discrete-time systems subject to input saturations when the generalized sector condition is used to deal with the saturation term (see [TGGQ11, Section 3.6]).*

Remark 3.4. *It is possible to adapt the conditions of Theorem 3.3 for the global stabilization case using the sector condition*

$$\phi^T(Kx)T\left(\phi(Kx) + Kx\right) \leq 0,$$

which is globally satisfied by the deadzone nonlinearity for any diagonal positive definite matrix $T \in \mathbb{R}^{m\times m}$. In this case, LMI (59) is discarded and R_j in (58) must be replaced by KW for all $j \in \mathbb{N}_J$.

3.2.3 Optimization problems

Given the bounds τ_m and τ_M on δ_k, we can use the conditions of Theorem 3.3 to compute regions of guaranteed stability for the sampled-data closed-loop system, i.e. estimates of the region of attraction of the origin. Actually, provided $z_0 \in \mathscr{E}(P)$ (with $P = W^{-1}$), conditions of Theorem 3.1 guarantee that the corresponding trajectory converges asymptotically to the origin.

As pointed out in Remark 3.1, the region $\mathscr{E}(P)$ is defined in the space of $x = [x_p^T \; u^T]^T$ but we want to define the estimate of the RAO in the x_p-subspace, considering the initial value of $u(0^-)$ as a free parameter to be determined. In fact, if the extended state $z_0 = [x_{p,0}^T \; u^T(0^-)]^T$ is in $\mathscr{E}(W^{-1})$, with W satisfying the LMI conditions given in Theorem 3.3, then $z_k \in \mathscr{E}(W^{-1})$ for all $k \in \mathbb{N}$ and converges asymptotically to the origin. Thus, the set of states $x_{p,0}$ for which an input $u(0^-)$ can be defined such that the resulting $z_0 = [x_{p,0}^T \; u^T(0^-)]^T$ belongs to $\mathscr{E}(W^{-1})$ is an estimate of the RAO.

Defining the following partitions of P and $W = P^{-1}$:

$$P = \begin{bmatrix} P_{11} & P_{12} \\ P_{12}^T & P_{22} \end{bmatrix}, \quad W = \begin{bmatrix} W_{11} & W_{12} \\ W_{12}^T & W_{22} \end{bmatrix} \tag{61}$$

where $P_{11}, W_{11} \in \mathbb{R}^{n_p \times n_p}, P_{22}, W_{22} \in \mathbb{R}^{m\times m}$ and

$$u(0^-) = -P_{22}^{-1} P_{12}^T x_{p,0}, \tag{62}$$

the set $\mathscr{E}(P_{11}-P_{12}P_{22}^{-1}P_{12}^T)\subseteq\mathbb{R}^{n_p}$ results to be an estimate of the RAO. In fact, if $x_{p,0}\in\mathscr{E}(P_{11}-P_{12}P_{22}^{-1}P_{12}^T)$ and $u(0^-)$ is as in (62) then

$$\begin{aligned} z_0^T P z_0 &= x_{p,0}^T P_{11} x_{p,0} + 2x_{p,0}^T P_{12} u(0^-) + u^T(0^-) P_{22} u(0^-) \\ &= x_{p,0}^T P_{11} x_{p,0} - x_{p,0}^T P_{12} P_{22}^{-1} P_{12}^T x_{p,0} \leq 1 \end{aligned}$$

which means that $z_0\in\mathscr{E}(P)=\mathscr{E}(W^{-1})$. The ellipsoid $\mathscr{E}(P_{11}-P_{12}P_{22}^{-1}P_{12}^T)$ corresponds to the projection of $\mathscr{E}(P)$ onto the x_p-subspace.

Moreover, it can be checked by direct calculation that

$$P^{-1}=W=\begin{bmatrix} Q^{-1} & -Q^{-1}P_{12}P_{22}^{-1} \\ \star & P_{22}^{-1}+P_{22}^{-1}P_{12}^T Q^{-1} P_{12} P_{22}^{-1} \end{bmatrix}, \tag{63}$$

where

$$Q \triangleq P_{11}-P_{12}P_{22}^{-1}P_{12}^T$$

is the Schur complement of P_{22} with respect to P. Hence, from (61) and (63), we have that

$$\mathscr{E}(P_{11}-P_{12}P_{22}^{-1}P_{12}^T)=\mathscr{E}(W_{11}^{-1}).$$

Thus, the idea is to maximize this "safe" set of plant initial states given by $\mathscr{E}(W_{11}^{-1})$, considering some size criterion. For instance, the maximization of the minor axis of the set can be considered through the following optimization problem:

$$\begin{aligned} &\max_{W,R_j,S_j,\varepsilon} \ \varepsilon \\ &\text{subject to:} \\ &(58),(59),(60), \\ &W_{11}-\varepsilon I_{n_p}\succ 0. \end{aligned} \tag{64}$$

Other size criteria, such as the volume maximization or the maximization of the set in certain directions can also be easily considered (see [TGGQ11]).

Note that problem (64) is associated to a given partition of the interval $[\tau_m,\tau_M]$. In order to find a suitable partition, the following algorithm is proposed, where the maximum value $\bar{J}$ allowed for J must be chosen empirically and is assumed to be sufficiently large:

Algorithm 3.1

Step 1: Fix λ
Step 2: Initialize J
Step 3: Compute $\tau_J=\frac{\tau_M-\tau_m}{J}$
Step 4: Fix $\alpha=\frac{1}{\tau_J}\ln(\frac{1}{\lambda})$ and solve (64)
Step 5: If (64) is feasible stop.
Step 6: If $J<\bar{J}$, $J\leftarrow J+1$ and go to Step 3. Otherwise increase λ and go to Step 2.

Note that Algorithm 3.1 tests the feasibility of the optimization problem (64) in Step 5. If (64) is not feasible, Step 6 increases either the number of partitions J or the factor λ. Moreover, the initial values of λ and J in Steps 1 and 2, respectively, must be empirically chosen. A lower bound for J is provided by Remark 3.5 below.

Remark 3.5. *As pointed out in the proof of Theorem 3.3, a necessary condition for the feasibility of (60) is that*

$$\alpha = -\frac{ln(\lambda)}{\tau_J} > \max\{2\lambda_{max}(A_c),0\}.$$

Hence, for a fixed λ, we should have

$$\tau_J < -\frac{ln(\lambda)}{\max\{2\lambda_{max}(A_c),0\}},$$

which implies, from (48), that the initialization of J in Step 2 of the algorithm should satisfy:

$$J > (\tau_m - \tau_M)\frac{\max\{2\lambda_{max}(A_c),0\}}{ln(\lambda)}.$$

It is interesting to note that Algorithm 3.1 provides a solution if a quadratic Lyapunov function with exponential decrease exists. In fact, assume that there exists a quadratic Lyapunov function $V(x) = x^T Px$, $P = P^T \succ 0$, satisfying the assumptions of Theorem 2 (and hence also of Theorem 1) for a neighborhood $\mathscr{D} \subseteq \mathbb{R}^n$ of the origin. Then LMIs (58)-(60) will have a feasible solution for $W = P^{-1}$ if the value of λ is sufficiently close to 1 and J is sufficiently large. In other words, the algorithm above has a guaranteed termination since it increases iteratively the values of λ and J.

To see this, suppose that there exists $V(x) = x^T Px$ such that:

$$V(z_{k+1}) \leq \lambda V(z_k), \quad \forall z_k \in \mathscr{D}, \forall \delta_k \in \Delta$$

where z_{k+1} is given by (46). Since the Lyapunov condition must hold also for z_k in $\mathscr{D}$ close enough to the origin and, then, such that $z_{k+1} = (A_z(\delta_k) + B_z(\delta_k)K)z_k$, it is necessary that $\lambda P \succeq (A_z(\delta) + B_z(\delta)K)^T P(A_z(\delta) + B_z(\delta)K)$ holds for all $\delta \in \Delta$. As this condition must hold in particular for $\delta = d_j$, $\forall j \in \mathbb{N}_J$, it implies the satisfaction of (58) with R_j and S_j null matrices for all $j \in \mathbb{N}_J$.

Moreover, assume without loss of generality that $\mathscr{E}(P) = \{x \in \mathbb{R}^n : \ x^T Px \leq 1\} \subseteq \mathscr{H}(K)$, where $\mathscr{H}(K) = \{x \in \mathbb{R}^n : \ \|Kx\|_\infty \leq 1\}$ is the region of linearity of the system (note that the function $V(x)$ can be scaled if necessary). Then, condition (59) is satisfied with $R_j = 0$, $\forall j \in \mathbb{N}_J$.

At last notice that, for a fixed λ, $\alpha = -\ln(\lambda)/\tau_J \to \infty$, since $\tau_J \to 0$, as $J \to \infty$. Thus also inequality (60) will be satisfied for a sufficiently large J.

Therefore, for an appropriate choice of λ close enough to 1, the LMI conditions (58)-(60) are satisfied for J sufficiently large, and thus the algorithm has finite termination.

3.3 Stabilization

The LMI problem (64) can be easily adapted if we want to design a feedback gain K that maximizes the set $\mathscr{E}(W_{11}^{-1})$. It suffices to perform the following change of variables:

$$Z \triangleq KW. \tag{65}$$

As discussed in [GT01] for the periodic sampling case, the control law computed from (64), without any additional performance constraint, can lead to a large region of stability, but will in general result in a very slow behavior. Moreover, it is not fair to demand the

same performance level when the control is saturated, since the system operates in open-loop in this case. Hence, an effective way of balancing performance and size of the region of attraction is to force some performance constraint only when the system operates in the linearity region. For instance, we can add to (64) the following LMIs:

$$\begin{bmatrix} \gamma\lambda W & WA_z^T(d_j) + Z^T B_z^T(d_j) \\ \star & W \end{bmatrix} \succeq 0, \ \forall j \in \mathbb{N}_J \tag{66}$$

where $0 < \gamma < 1$ is a parameter fixed *a priori*. Note that constraints (66) and (60) impose that $V(z_{k+1}) < \gamma V(z_k)$ when the control is not saturated, i.e. they ensure a more stringent exponential decay convergence rate at the sampling instants for the operation of the system in the linearity region.

Remark 3.6. *If we consider $K_u = 0$, we can also perform the substitution (65), but in this case, to preserve linearity, W must be block diagonal, i.e. $W_{12} = 0$, which implies that $Z = [K_p W_{11} \ 0]$.*

Remark 3.7. *It should be noticed that it is not possible to apply the change of variable in (65) when the conditions in [FG18] are considered, making rather difficult to address the design problem. This comes from the fact that the difference inclusion considered in that work is different from (46).*

3.4 Numerical example

Consider system (1),(42),(5) with the following matrices [TGGQ11]:

$$A_p = \begin{bmatrix} 0 & 1 \\ 1 & 0 \end{bmatrix}, \ B_p = \begin{bmatrix} 0 \\ -5 \end{bmatrix}, \ K_p = \begin{bmatrix} 2.6 & 1.4 \end{bmatrix}, \ K_u = \begin{bmatrix} 0 \end{bmatrix},$$

with the interval of admissible intersampling times given by $\Delta = [0.05, 0.1]$. In this case, for $\lambda = 0.98$ a feasible solution for the optimization problem (64) is obtained with a partition of Δ in 30 sub-intervals (i.e. $J = 30$), leading to:

$$W^{-1} = \begin{bmatrix} 0\,2580 & 0.1012 & -0.0204 \\ 0.1012 & 0.0868 & -0.0019 \\ -0.0204 & -0.0019 & 0.0211 \end{bmatrix}, \ \varepsilon = 3.4785.$$

Considering now the stabilization problem described in Section 3.3 with $\gamma = 0.9$ and the same values for λ and J, we obtain

$$\begin{aligned} K &= \begin{bmatrix} 1.13 & 0.94 & 0.008 \end{bmatrix} \\ W^{-1} &= \begin{bmatrix} 0.0612 & 0.0562 & -0.0037 \\ 0.0562 & 0.0608 & -0.0012 \\ -0.0037 & -0.0012 & 0.0127 \end{bmatrix}, \ \varepsilon = 8.60. \end{aligned} \tag{67}$$

Figure 6 shows the resulting estimates of the region of attraction of the origin. The ellipsoid obtained with the designed K is indeed larger than the original one, as expected. For comparison purposes, considering $K = [2.6 \ 1.4 \ 0]$, we also plotted the estimate of the RAO obtained with the method proposed in [FG18], which corresponds to the sublevel set of a piecewise quadratic function, and the one obtained with the looped-functional

approach proposed in [SG12], which is an ellipsoidal set. As it can be observed, the method proposed here resulted in a larger set for the same value of K.

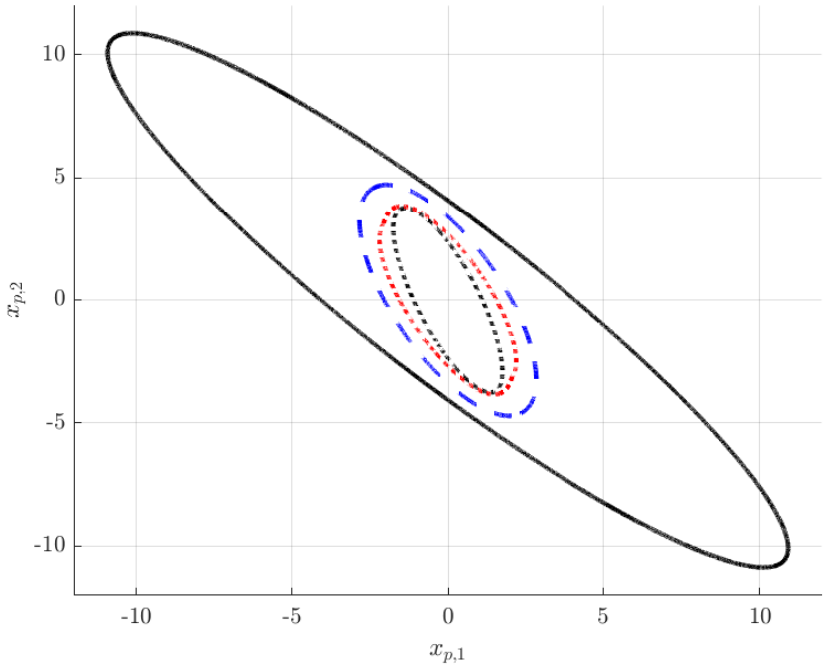

Figure 6: Estimates of the RAO obtained with the proposed method (blue-dashed for $K = [2.6\ 1.4\ 0]$ and black-continuous for $K = [1.13\ 0.94\ 0.008]$) and with the methods proposed in [SG12] (black-dotted for $K = [2.6\ 1.4\ 0]$) and [FG18] (red-dotted for $K = [2.6\ 1.4\ 0]$).

In Figure 7, several trajectories with $x_{p,0}$ at the boundary of the region $\mathscr{E}(W_{11}^{-1})$ and $u(0^-)$ chosen as in (62) considering K and W given in (67) and δ_k randomly chosen in the interval $[0.05,0.1]$ are shown. As expected, the convergence of the trajectories to the origin is ensured, which shows that $\mathscr{E}(W_{11}^{-1})$ is indeed included in its region of attraction.

Remark 3.8. *Concerning the comparison with other approaches, it has to be noticed that, in this numerical example, our method provides a better estimate of the region of attraction of the origin, but there is no formal guarantee that this will be always the case. Furthermore, the method presented in this work is particularly suitable to deal with both the stability analysis and control synthesis problems. For instance, with the looped-functional approach [SG12], to obtain tractable synthesis conditions in LMI form, the Finsler's Lemma with a particular structure of the multipliers (which is an important source of conservatism) and a fixed parameter, that has to be manually tuned, are employed. On the other hand, due to the exponential dependence of $A_z(\delta) = e^{A_c\delta}A_r$ and $B_z(\delta) = e^{A_c\delta}B_r$, which appear in (58), on A_c, it is not trivial with our method to cope with uncertainties in the system matrices A_p and B_p, that are easily manageable in the looped-functional framework. Actually, establishing a formal comparison between our method and the looped-functional one might be rather difficult as the tools and conditions are significantly different.*

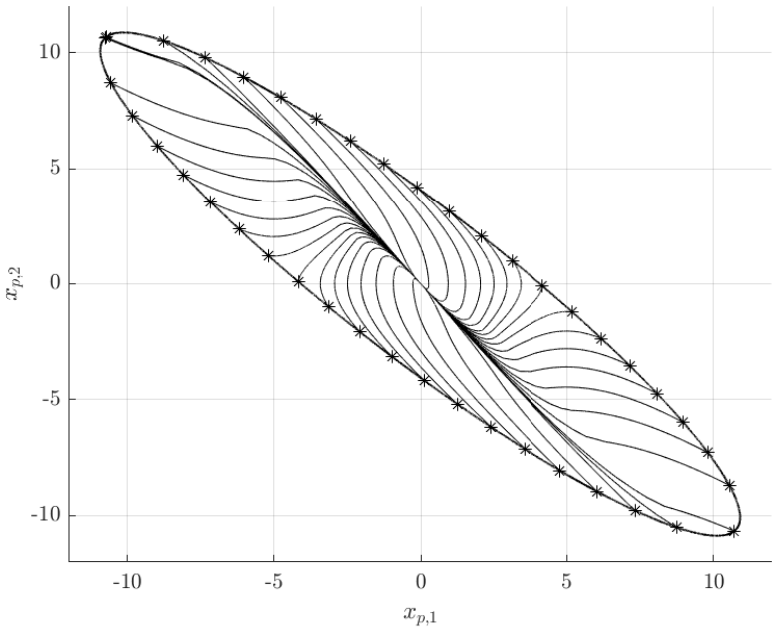

Figure 7: Trajectories starting at the boundary of $\mathscr{E}(W_{11}^{-1})$ considering (67).

3.5 Concluding remarks

A quadratic approach has been proposed to deal with sampled-data controlled linear systems under aperiodic sampling and input saturation which, unlike the method presented in [FG18], can be used not only for the stability analysis but also for the design of a stabilizing control law. By means of a numerical example, we have shown that the proposed approach can lead to a considerable conservatism reduction, in terms of estimate of the RAO, when compared to other ones reported in the literature.

The approach can be easily extended to cope with other continuous input nonlinearities, in particular sector-bounded ones. Note that in this case it suffices to replace the saturation function in model (43) by the new nonlinearity. Similar conditions to the one in Theorem 3.3 can therefore be derived using classical sector conditions.

The results in this chapter have been published in [HFG22e].

4 STABILITY ANALYSIS: POLYHEDRAL APPROACH I

In this chapter we perform the stability analysis (i.e. solve Problem 2.1) of the closed-loop system composed by (1),(3) and (5). Unlike Chapter 3, which considers ellipsoidal sets, the method presented next provides polyhedral estimates of the region of attraction of the origin, relying on the solution of linear programming problems.

Consider the closed-loop system (1),(3),(5). As explained in Section 2.1.2 (see, in particular, Lemma 2.1), it is possible to tackle the stability analysis problem using the discrete-time model (12), which assumes the following form for $f(x_{p,k}) = \text{sat}(K_p x_{p,k})$:

$$x_{p,k+1} \in \left\{A(\delta)x_{p,k} + B(\delta)\text{sat}(K_p x_{p,k}) : \ \delta \in \Delta\right\}. \tag{68}$$

As pointed out in [TGGQ11, Section 1.7], the direct handling of the saturation nonlinearity in (68), in order to obtain testable numerical conditions to assess the asymptotic stability of the origin and to compute estimates of the RAO, is a quite hard task. To overcome this problem, many representations for the saturation term, such as sector bounded nonlinearities [SG12] (also used in Chapter 3, see Lemma 3.1) and polytopic embeddings [FG18], have been successfully considered in the literature. Another representation is the saturated and nonsaturated (SNS) model [ACLC06], which is less conservative than classical polytopic embeddings [ACLC06, Section 5],[TGGQ11, Chapter 1] and will be presented in Section 4.1. Moreover, as it will be seen in Section 4.2, it is quite appropriated to compute one-step sets.

The chapter is organized as follows. Section 4.1 presents the SNS model, as mentioned above. Section 4.2 presents the main results, which are based on set invariance theory and on the concept of one-step set already introduced in Chapter 2. From the derived theoretical results, an algorithm to numerically compute polyhedral estimates of the RAO is proposed in Section 4.3. Section 4.4 presents two numerical examples. At last, Section 4.5 has some concluding remarks.

4.1 The SNS Model

Let us define $\mathscr{S} \triangleq 2^{\mathbb{N}_m}$ as the set of all subsets of $\mathbb{N}_m = \{i \in \mathbb{N} : \ 1 \leq i \leq m\}$. For example, if $m = 2$ then $\mathscr{S} = 2^{\mathbb{N}_2} = \{\emptyset, \{1\}, \{2\}, \{1,2\}\}$. The basic idea of the SNS model is to replace the saturation function $\text{sat}(\cdot)$ by another one $\text{sat}_S(\cdot)$ which depends on an additional parameter $S \in \mathscr{S}$. This parameter indicates which components of the

function are activated or not. For $m = 2$, for instance, one has:

$$\text{sat}_{\{\emptyset\}}(z) = \begin{bmatrix} z_{(1)} \\ z_{(2)} \end{bmatrix}, \ \text{sat}_{\{1\}}(z) = \begin{bmatrix} \text{sat}(z_{(1)}) \\ z_{(2)} \end{bmatrix},$$
$$\text{sat}_{\{2\}}(z) = \begin{bmatrix} z_{(1)} \\ \text{sat}(z_{(2)}) \end{bmatrix}, \ \text{sat}_{\{1,2\}}(z) = \begin{bmatrix} \text{sat}(z_{(1)}) \\ \text{sat}(z_{(2)}) \end{bmatrix},$$

where $z \in \mathbb{R}^2$. The generic expression in $\mathbb{R}^m$ is given by:

$$\text{sat}_S(z) \triangleq \sum_{i \in S^c} e_i z_{(i)} + \sum_{i \in S} e_i \text{sat}_{(i)}(z), \ S \in \mathscr{S}, \ S^c \triangleq \mathbb{N}_m \setminus S, \tag{69}$$

where e_i is the i-th canonical base vector of the Euclidean space.

Thus, the idea is to estimate the RAO of (68) by using the difference inclusion

$$\begin{aligned} x_{p,k+1} &\in \left\{ A(\delta)x_{p,k} + B(\delta)\text{sat}_S(K_p x_{p,k}) : \ \delta \in \Delta, \ S \in \mathscr{S} \right\} \\ &\triangleq \left\{ F_{SNS}(x_{p,k}, \delta, S) : \ \delta \in \Delta, \ S \in \mathscr{S} \right\} \triangleq F_{SNS}(x_{p,k}, \Delta, \mathscr{S}). \end{aligned} \tag{70}$$

The difference inclusion (70) takes into account *all* 2^m possible combinations of saturated/nonsaturated inputs given by $S \in \mathscr{S} = 2^{\mathbb{N}_m}$ simultaneously.

Notice that (70) encompasses (68): any trajectory $\{x_{p,k}\}_{k=0}^{\infty}$ satisfying (68) belongs to the family of trajectories that satisfy (70). In other words, an estimate of the RAO of (70) will also be a valid estimate of the RAO of (68). Hence, instead of directly computing an estimate for (68), we will aim at obtaining an estimate for (70) using convex analysis tools [BM15] that cannot be directly applied to (68). This estimate will correspond to a polyhedral contractive C-set, according to the Definition 2.5. In particular, the following key result holds, which can be seen as an adaptation of Corollary 2.1 to the class of SNS systems.

Lemma 4.1. *If the C-set $\Omega \subset \mathbb{R}^{n_p}$ is λ-contractive for (70), then:*

a) $\varepsilon\Omega$ also is λ-contractive for (70) for all $\varepsilon \in [0,1]$;

b) All trajectories $\{x_k\}_{k \in \mathbb{N}}$ satisfying (70) have the following property:

$$x_k \in \varepsilon\Omega \ \Rightarrow \ x_{k+p} \in \lambda^p \varepsilon\Omega, \quad \forall \varepsilon \in [0,1], \ \forall p \in \mathbb{N}. \tag{71}$$

Proof:

a) Consider the nontrivial case $\varepsilon \neq 0$. Given $x_p \in \varepsilon\Omega$, we have to prove that

$$F_{SNS}(x_p, \Delta, \mathscr{S}) = F_{SNS}(\varepsilon \bar{x}_p, \Delta, \mathscr{S}) \subseteq \lambda\varepsilon\Omega, \tag{72}$$

where $\bar{x}_p \triangleq x_p/\varepsilon \in \Omega$.

First, note that $\text{sat}(\varepsilon y) \in \varepsilon \text{Co}\{y, \text{sat}(y)\}$ for $y \in \mathbb{R}$ and $0 \leq \varepsilon \leq 1$, as it can be verified by direct calculation. More precisely:

$$\begin{cases} \text{sat}(\varepsilon y) = \varepsilon y \in \text{Co}\{\varepsilon y, \varepsilon \text{sat}(y)\}, & \text{if } \ -1 \leq \varepsilon y \leq 1, \\ \text{sat}(\varepsilon y) = 1 \in \text{Co}\{\varepsilon y, \varepsilon\}, & \text{if } \ \varepsilon y > 1, \\ \text{sat}(\varepsilon y) = -1 \in \text{Co}\{\varepsilon y, -\varepsilon\}, & \text{if } \ \varepsilon y < -1. \end{cases}$$

Thus, in the multivariable case, i.e. when $y \in \mathbb{R}^m$, it follows for $S \in \mathscr{S}$ that:

$$z \triangleq \mathrm{sat}_S(\varepsilon y) \in \varepsilon \mathrm{Co}\left\{\mathrm{sat}_{S'}(y) : \ S' \in \mathscr{S}\right\}. \tag{73}$$

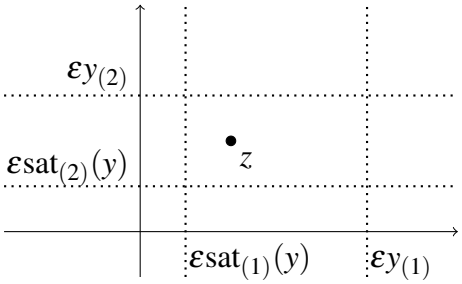

Figure 8: Sketch of property (73) for $m = 2$.

To see that (73) holds (Figure 8 shows a sketch for $m = 2$), note that

$$z_{(i)} = \begin{cases} \mathrm{sat}_{(i)}(\varepsilon y), & \text{if } i \in S, \\ \varepsilon y_{(i)}, & \text{if } i \notin S, \end{cases}$$

thus $z_{(i)}$ belongs to the interval $I_i \triangleq \varepsilon \mathrm{Co}\left\{y_{(i)}, \mathrm{sat}_{(i)}(y)\right\}$ and, consequently, z belongs to the hypercube $I \triangleq I_1 \times \cdots \times I_m \subset \mathbb{R}^m$. Note now that $I = \varepsilon \mathrm{Co}\left\{\mathrm{sat}_{S'}(y) : \ S' \in \mathscr{S}\right\}$ because the elements of $\left\{\varepsilon \mathrm{sat}_{S'}(y) : \ S' \in \mathscr{S}\right\}$ are the vertices of I.

Using relation (73), it follows that for all $\delta \in \Delta$ and $S \in \mathscr{S}$

$$\begin{aligned} F_{SNS}(\varepsilon \bar{x}_p, \delta, S) &= A(\delta)\varepsilon \bar{x}_p + B(\delta)\mathrm{sat}_S(K_p \varepsilon \bar{x}_p) \\ &\in \varepsilon A(\delta)\bar{x}_p + B(\delta)\varepsilon \mathrm{Co}\left\{\mathrm{sat}_{S'}(K_p \bar{x}_p) : \ S' \in \mathscr{S}\right\} \\ &= \varepsilon \mathrm{Co}\left\{A(\delta)\bar{x}_p + B(\delta)\mathrm{sat}_{S'}(K_p \bar{x}_p) : \ S' \in \mathscr{S}\right\} \\ &\subseteq \varepsilon \mathrm{Co}\left\{F_{SNS}(\bar{x}_p, \Delta, \mathscr{S})\right\} \subseteq \varepsilon \mathrm{Co}(\lambda \Omega) = \varepsilon \lambda \Omega \end{aligned}$$

where the last set inclusion follows from the fact that Ω is λ-contractive for (70) and $\bar{x}_p \in \Omega$ and the last equality from the fact that Ω is convex. Hence, (72) holds, as we wanted to show.

b) Follows from the recursive application of a).

■

From Lemma 4.1, if Ω is a λ-contractive C-set for (70) then it is included in the RAO of (70). Besides that, since (70) encompasses (68) as explained before, (71) also holds for the trajectories of (68) and it becomes clear that Ω is an estimate not only of the RAO of (70) but also of the RAO of (68) and, consequently, from Lemma 2.1, of the RAO of the closed-loop system (1),(3),(5)[1]. Notice that, since $0 \in \Omega^\circ$ by definition of a C-set, the origin of (68) (and, consequently, of (1),(3),(5)) is indeed asymptotically stable if Ω is contractive.

It is worth noticing that a λ-contractive C-set for (70) is also λ-contractive for (68) but the opposite is not true in general. Even so, it is possible to prove a weaker version of this statement in the other direction, as shown next.

[1]However, notice that the fact that Ω is contractive/invariant for the discrete-time system (68) does not mean that it is invariant for the continuous-time system (1),(3),(5), even if the trajectory of the continuous-time system is bounded according to (16).

Lemma 4.2. *Suppose that $m = 1$ (single input case) and consider a C-set $\Omega \subset \mathbb{R}^{n_p}$. If $\varepsilon\Omega$ is λ-contractive for (68) for all $\varepsilon \in [0,1]$, then Ω is λ-contractive for (70).*

Proof: The proof follows the same reasoning of the one of [ACLC06, Property 2] except that here the discrete-time systems (68) and (70) have an uncertain parameter δ_k. ■

Before presenting the details of the stability analysis method developed, let us introduce the following assumption with respect to the difference inclusion (70).

Assumption 4.1. *There exists a γ-contractive C-set $\Omega^\gamma \subset \mathbb{R}^{n_p}$ for (70) (where $0 \leq \gamma < 1$).*

The assumption above is not strong in the sense that it will hold for the SNS system (70) if it holds for the linear difference inclusion below

$$x_{p,k+1} \in \left\{ (A(\delta) + B(\delta)K_p)x_{p,k} : \ \delta \in \Delta \right\} \tag{74}$$

since (70) and (74) are equivalent in a sufficiently small neighborhood of the origin (where the input does not saturate).

4.2 Stability analysis

The proposed stability analysis method can be divided into two steps. The first one, presented in Section 4.2.1, consists in finding a contractive P-set $\hat{\Omega}$ for the dynamics

$$x_{p,k+1} \in F_{SNS}(x_{p,k}, \Delta_J, \mathscr{S}) \tag{75}$$

where Δ_J is defined in (48). Note that (75) considers only a finite subset Δ_J of the interval Δ and thus (75) is embedded by (70), i.e. $F_{SNS}(x_{p,k}, \Delta_J, \mathscr{S}) \subseteq F_{SNS}(x_{p,k}, \Delta, \mathscr{S})$. The second step, presented in Section 4.2.2, verifies if the set $\hat{\Omega}$ found is also contractive for (70) (not necessarily with the same contraction factor λ). If this is true, then we can conclude that $\hat{\Omega}$ is an estimate of the RAO of (68) and, consequently, of the RAO of the closed-loop system (1),(3),(5), as explained before.

4.2.1 Computation of a contractive set for $x_{p,k+1} \in F_{SNS}(x_{p,k}, \Delta_J, \mathscr{S})$

Below we particularize Definition 2.7 to system (75).

Definition 4.1. *Given $J \in \mathbb{N}_+$ and $\Omega \subseteq \mathbb{R}^{n_p}$, the one-step set $T_J(\Omega)$ of Ω for (75) is*

$$T_J(\Omega) \triangleq \left\{ x_p \in \mathbb{R}^{n_p} : \ F_{SNS}(x_p, \Delta_J, \mathscr{S}) \subseteq \Omega \right\}, \tag{76}$$

i.e. given $x_p \in T_J(\Omega)$, $A(\delta)x_p + B(\delta)sat_S(K_p x_p) \in \Omega, \forall \delta \in \Delta_J, \forall S \in \mathscr{S}$.

The following lemma provides a polyhedral characterization of $T_J(\Omega)$ when Ω is a polyhedron.

Lemma 4.3. *Consider $\Omega = \mathscr{P}(H,h)$, where $H \in \mathbb{R}^{n_h \times n_p}, h \in \mathbb{R}^{n_h}$. Then*

$$\begin{aligned} T_J(\Omega) &= \bigcap_{\delta \in \Delta_J} \bigcap_{S \in \mathscr{S}} \left\{ x_p \in \mathbb{R}^{n_p} : \ H\Big(A(\delta) + \sum_{i \in S^c} B^{(i)}(\delta) K_{p(i)}\Big) x_p - \sum_{i \in S} |HB^{(i)}(\delta)| \leq h \right\} \\ &= \bigcap_{\delta \in \Delta_J} \bigcap_{S \in \mathscr{S}} \mathscr{P}\left(H\Big(A(\delta) + \sum_{i \in S^c} B^{(i)}(\delta) K_{p(i)}\Big), \ h + \sum_{i \in S} |HB^{(i)}(\delta)| \right) \end{aligned} \tag{77}$$

Proof: The proof follows the one in [ACLC06, Theorem 1] *mutatis mutandis*. ■

The theorem below, inspired by [Bla94, Theorem 3.1], introduces the recursion used to find the maximal λ-contractive C-set for (75) in a given C-set $\Omega_0 \subset \mathbb{R}^{n_p}$. Unlike Theorem 3.1 in [Bla94], valid only for linear systems, our result applies to the nonlinear case of SNS systems.

Theorem 4.1. *Given $J \in \mathbb{N}_+$, consider the sequence of sets*

$$\Omega_{i+1} = T_J(\lambda\Omega_i) \cap \Omega_0, \ \forall i \in \mathbb{N}, \tag{78}$$

where Ω_0 is a polyhedral C-set and $\lambda \in (0,1)$. The following properties hold:

a) Ω_i is a polyhedral C-set for all $i \in \mathbb{N}$.

b) $\Omega_{i+1} \subseteq \Omega_i$ for all $i \in \mathbb{N}$.

c) If there exists a λ-contractive C-set $\Omega' \subseteq \Omega_0$ for (75), then

$$\underline{\Omega}_{\lambda,J} \triangleq \bigcap_{i\in\mathbb{N}} \Omega_i \tag{79}$$

is the maximal λ-contractive C-set for (75) in Ω_0.

Proof:

a) Let us prove it by induction. Assume Ω_i is a polyhedral C-set. Then $\lambda\Omega_i$ can be expressed as $\mathscr{P}(H_i, \mathbf{1})$ for an appropriate choice of H_i and it follows from (77) that $T_J(\lambda\Omega_i)$ is a polyhedron containing the origin in its interior. Its intersection with the polytope Ω_0 is thus a polytope (which also contains the origin in its interior since $0 \in \Omega_0^\circ$). So Ω_{i+1} is a polyhedral C-set.

b) This proof is also done by induction. If $\Omega_{i+1} \subseteq \Omega_i$ (the case $i = 0$ is clearly true), then $T_J(\lambda\Omega_{i+1}) \subseteq T_J(\lambda\Omega_i)$ and it follows that

$$\Omega_{i+2} = T_J(\lambda\Omega_{i+1}) \cap \Omega_0 \subseteq T_J(\lambda\Omega_i) \cap \Omega_0 = \Omega_{i+1}.$$

c) Consider any λ-contractive C-set $\Omega'' \subseteq \Omega_0$ for (75) (for instance $\Omega'' = \Omega'$, which exists by hypothesis). It follows by induction that $\Omega'' \subseteq \underline{\Omega}_{\lambda,J}$. In fact, if $\Omega'' \subseteq \Omega_i$ then

$$\Omega'' \subseteq T_J(\lambda\Omega'') \cap \Omega_0 \subseteq T_J(\lambda\Omega_i) \cap \Omega_0 = \Omega_{i+1},$$

i.e. $\Omega'' \subseteq \bigcap_{i\in\mathbb{N}} \Omega_i = \underline{\Omega}_{\lambda,J}$. It also follows that $0 \in \underline{\Omega}_{\lambda,J}^\circ$ because $0 \in (\Omega'')^\circ$. So $\underline{\Omega}_{\lambda,J}$ is a C-set (compact and convex because it is the intersection of nested C-sets).

We still have to prove $\underline{\Omega}_{\lambda,J}$ is λ-contractive for (75). Given $x \in \underline{\Omega}_{\lambda,J}$, it follows that $x \in \Omega_{i+1} \subseteq T_J(\lambda\Omega_i), \forall i \in \mathbb{N}$, i.e. $F_{SNS}(x, \Delta_J, \mathscr{S}) \subseteq \lambda\Omega_i, \forall i \in \mathbb{N}$. So $F_{SNS}(x, \Delta_J, \mathscr{S}) \subseteq \lambda \bigcap_{i\in\mathbb{N}} \Omega_i = \lambda\underline{\Omega}_{\lambda,J}$. Therefore $\underline{\Omega}_{\lambda,J}$ is indeed λ-contractive.

■

Remark 4.1. *It is important to keep in mind that $\Omega_i = \Omega_i(\lambda, J, \Omega_0)$ depends on the parameters λ and J and on the initial set Ω_0, even if we omit this dependence to avoid a heavy notation. A similar remark applies for $\underline{\Omega}_{\lambda,J} = \underline{\Omega}_{\lambda,J}(\Omega_0)$.*

Remark 4.2. *The result in Theorem 4.1 still holds if Ω_0 (and, in consequence, Ω_i for $i>0$) is not necessarily a polyhedron, but just a C-set. This additional assumption is important only from a practical point of view, since in this case the operators $T_J(\cdot)$ and $\cap$ in (78) can be applied using Lemma 4.3 and the MPT toolbox [HKJM13], for instance. It is important to highlight that all manipulations with polyhedral sets carried out in this study rely only on the solution of linear programming problems.*

In general, the set $\underline{\Omega}_{\lambda,J}$ might be not obtainable in a finite number of iterations by an algorithm (and in general it is not polyhedral). That is why we use the following result.

Lemma 4.4. *Assume $\underline{\Omega}_{\lambda,J}$ in (79) is a λ-contractive C-set for (75). Then, for every $\lambda^* \in (\lambda,1)$, there exists $i^* \in \mathbb{N}$ such that $\hat{\Omega}_i \triangleq \lambda/\lambda^*\Omega_i$ is λ^*-contractive for (75) for all $i \geq i^*$.*

Proof: Consider $\lambda^*/\lambda > 1$. There exists $i^* \in \mathbb{N}$ such that

$$\underline{\Omega}_{\lambda,J} \subseteq \Omega_i \subseteq \lambda^*/\lambda \underline{\Omega}_{\lambda,J}, \forall i \geq i^*$$

[Sch93, Lemma 1.8.1]. Using these set inclusions (up to scale factors) and the fact that $\underline{\Omega}_{\lambda,J}$ is λ-contractive for (75), it follows that

$$\hat{\Omega}_i = \frac{\lambda}{\lambda^*}\Omega_i \subseteq \underline{\Omega}_{\lambda,J} \subseteq T_J(\lambda \underline{\Omega}_{\lambda,J}) \subseteq T_J(\lambda\Omega_i) = T_J\left(\lambda^*\left(\frac{\lambda}{\lambda^*}\Omega_i\right)\right) = T_J(\lambda^*\hat{\Omega}_i)$$

for all $i \geq i^*$, that proves the result. ■

Lemma 4.4 ensures that, under the given assumptions, the set $\hat{\Omega}_{i^*} = \lambda/\lambda^*\Omega_{i^*}$, obtained by iterating (78) a finite number i^* of times, is a λ^*-contractive polyhedral C-set for (75).

4.2.2 Testing contractivity for system $x_{p,k+1} \in F_{SNS}(x_{p,k}, \Delta, \mathscr{S})$

The second step of the method consists in verifying if the contractive P-set found for (75) is also contractive for the dynamics (70), which takes into account all possible values for $\delta \in \Delta$ and not only the finite set Δ_J. The following property plays a key role to verify that.

Lemma 4.5. *Given $d, \tau \in \mathbb{R}$, the following identities hold:*

$$A(d+\tau) = A(d) + \Phi(\tau)e^{A_p d}A_p \tag{80}$$

$$\begin{aligned} B(d+\tau) &= B(d) + \Phi(\tau)\left(A_p \int_0^d e^{A_p s} ds B_p + B_p\right) \\ &= B(d) + \Phi(\tau)e^{A_p d}B_p \end{aligned} \tag{81}$$

where $\Phi(\tau) \triangleq \int_0^\tau e^{A_p s} ds$.

Proof: See the proof of [Fuj09, Proposition 1]. ■

Using the lemma above, it follows that

$$\begin{aligned} F_{SNS}(x_p, d+\tau, S) &= \begin{bmatrix} A(d+\tau) & B(d+\tau) \end{bmatrix} \begin{bmatrix} x_p \\ \text{sat}_S(K_p x_p) \end{bmatrix} \\ &= \left(\begin{bmatrix} A(d) & B(d) \end{bmatrix} + \Phi(\tau) e^{A_p d} \begin{bmatrix} A_p & B_p \end{bmatrix} \right) \begin{bmatrix} x_p \\ \text{sat}_S(K_p x_p) \end{bmatrix} \\ &= F_{SNS}(x_p, d, S) + \Phi(\tau) \underbrace{e^{A_p d} \begin{bmatrix} A_p & B_p \end{bmatrix}}_{\triangleq N(d)} \begin{bmatrix} x_p \\ \text{sat}_S(K_p x_p) \end{bmatrix}. \end{aligned} \tag{82}$$

Define now the logarithmic norm of A_p associated with the 2-norm [Van77]: $\mu(A_p) \triangleq \lambda_{max}\left(\frac{A_p + A_p^T}{2}\right)$. Notice in particular that $\mu(A_p)$ can be negative. The following theorem can now be stated.

Theorem 4.2. *Consider $J \in \mathbb{N}_+$ and a λ^*-contractive polyhedral C-set $\hat{\Omega}$ for the dynamics (75). If*

$$\nu(\hat{\Omega}, J, \lambda^*) \triangleq \lambda^* + c_1(J) c_2 c_3(\hat{\Omega}) c_4(\hat{\Omega}) < 1, \tag{83}$$

where

$$\begin{aligned} c_1(J) &\triangleq \begin{cases} \dfrac{e^{\mu(A_p)\tau_J} - 1}{\mu(A_p)} & \text{if } \mu(A_p) \neq 0, \\ \tau_J & \text{if } \mu(A_p) = 0, \end{cases} \\ c_2 &\triangleq \max\left(e^{\mu(A_p)\tau_m}, e^{\mu(A_p)\tau_M} \right) \sqrt{\|A_p\|^2 + \|B_p\|^2}, \\ c_3(\hat{\Omega}) &\triangleq \max_{x_p \in \hat{\Omega}} \left\| \begin{bmatrix} I_{n_p} \\ K_p \end{bmatrix} x_p \right\|, \\ c_4(\hat{\Omega}) &\triangleq \Psi_{\hat{\Omega}}(\mathscr{B}), \quad \mathscr{B} \triangleq \{x_p \in \mathbb{R}^{n_p} : \ \|x_p\| \leq 1\}, \end{aligned} \tag{84}$$

then $\hat{\Omega}$ is $\nu(\hat{\Omega}, J, \lambda^*)$-contractive for the dynamics (70).

Proof: To prove that $\hat{\Omega}$ is $\nu(\hat{\Omega}, J, \lambda^*)$-contractive for (70), we have to show that $x_{p,k+1}$ given by (70) satisfies

$$\Psi_{\hat{\Omega}}(x_{p,k+1}) \leq \nu(\hat{\Omega}, J, \lambda^*), \quad \forall x_{p,k} \in \hat{\Omega}, \ \forall \delta_k \in \Delta, \ \forall S_k \in \mathscr{S}.$$

Given $x_{p,k} \in \hat{\Omega}, \delta_k \in \Delta, S_k \in \mathscr{S}$, there exist $d_k \in \Delta_J$ and $\tau_k \in [0, \tau_J]$ such that $\delta_k = d_k + \tau_k$. Then using (82) it follows that

$$\begin{aligned} x_{p,k+1} &= F_{SNS}(x_{p,k}, d_k + \tau_k, S_k) \\ &= \underbrace{F_{SNS}(x_{p,k}, d_k, S_k)}_{\triangleq y_{k+1}} + \underbrace{\Phi(\tau_k) N(d_k) \begin{bmatrix} x_{p,k} \\ \text{sat}_{S_k}(K_p x_{p,k}) \end{bmatrix}}_{\triangleq z_{k+1}}. \end{aligned} \tag{85}$$

From the fact that $\hat{\Omega}$ is λ^*-contractive for (75), $d_k \in \Delta_J$ and $x_{p,k} \in \hat{\Omega}$, it follows that

$$\Psi_{\hat{\Omega}}(y_{k+1}) \leq \Psi_{\hat{\Omega}}(F_{SNS}(x_{p,k}, \Delta_J, \mathscr{S})) \leq \lambda^*. \tag{86}$$

Considering that $\|e^{A_p s}\| \leq e^{\mu(A_p)s}$ for all $s \geq 0$ (see [Van77]), and since $\tau_k \in [0, \tau_J]$, one obtains:

$$\|\Phi(\tau_k)\| = \left\| \int_0^{\tau_k} e^{A_p s} \mathrm{d}s \right\| \leq \int_0^{\tau_k} \left\| e^{A_p s} \right\| \mathrm{d}s \leq \int_0^{\tau_J} e^{\mu(A_p)s} \mathrm{d}s = c_1(J). \tag{87}$$

Moreover, one has that

$$\begin{aligned} \|N(d_k)\| &\leq \left\| e^{A_p d_k} \right\| \left\| \begin{bmatrix} A_p & B_p \end{bmatrix} \right\| \leq e^{\mu(A_p)d_k} \left\| \begin{bmatrix} A_p & B_p \end{bmatrix} \right\| \\ &\leq \max_{d \in \Delta_J} \left(e^{\mu(A_p)d} \right) \sqrt{\|A_p\|^2 + \|B_p\|^2} \\ &\leq \max \left(e^{\mu(A_p)\tau_m}, e^{\mu(A_p)\tau_M} \right) \sqrt{\|A_p\|^2 + \|B_p\|^2} = c_2. \end{aligned}$$

Using the inequalities above we conclude that

$$\|z_{k+1}\| \leq \|\Phi(\tau_k)\| \, \|N(d_k)\| \left\| \begin{bmatrix} x_{p,k} \\ \mathrm{sat}_{S_k}(K_p x_{p,k}) \end{bmatrix} \right\| \leq c_1(J) c_2 \left\| \begin{bmatrix} x_{p,k} \\ K_p x_{p,k} \end{bmatrix} \right\| \leq c_1(J) c_2 c_3(\hat{\Omega}),$$

i.e. $z_{k+1} \in c_1(J) c_2 c_3(\hat{\Omega}) \mathscr{B}$. Then, from (85), (86) and the properties in Lemma 2.2:

$$\Psi_{\hat{\Omega}}(x_{p,k+1}) \leq \Psi_{\hat{\Omega}}(y_{k+1}) + \Psi_{\hat{\Omega}}(z_{k+1}) \leq \lambda^* + c_1(J) c_2 c_3(\hat{\Omega}) \Psi_{\hat{\Omega}}(\mathscr{B}) = \nu(\hat{\Omega}, J, \lambda^*),$$

as we wanted to show. ■

Remark 4.3. *The constant $c_3(\Omega)$ can be obtained, in practice, by taking the maximum over the vertices of the polytope Ω or by solving a quadratic programming problem with linear constraints. In turn, $c_4(\Omega)$ can be computed as follows*

$$\begin{aligned} c_4(\Omega) = \Psi_\Omega(\mathscr{B}) &= \min\{\alpha \geq 0 : \ \mathscr{B} \subseteq \alpha\Omega\} \\ &= \min\{\alpha \geq 0 : \ Hx \leq \alpha h, \forall x \in \mathscr{B}\} = \max_{i \in \mathbb{N}_{n_h}} \frac{\|H_{(i)}^T\|}{h_{(i)}} \end{aligned}$$

where $\Omega = \mathscr{P}(H,h), H \in \mathbb{R}^{n_h \times n_p}, h \in \mathbb{R}^{n_h}$, assuming without loss of generality that $h > 0$.

The next theorem makes a connection between the preceding results. It states that, under some conditions, the recursion (78) not only will result in a λ^*-contractive polyhedral C-set $\hat{\Omega}_{i^*} = \lambda / \lambda^* \Omega_{i^*}$ for (75) but also that this set $\hat{\Omega}_{i^*}$ will indeed satisfy the hypothesis (83) of Theorem 4.2, that is, it will indeed be contractive for system (70).

Theorem 4.3. *Consider that Assumption 4.1 holds with $\Omega^\gamma \subseteq \Omega_0$,*[2] *where Ω_0 is the P-set that initializes recursion (78). Define*[3]

$$\bar{J} = \bar{J}(\lambda, \lambda^*) : (0,1) \times (0,1) \mapsto \mathbb{N}_+$$

as the smallest positive integer such that

$$c_1(J) c_2 \bar{c}_3 \bar{c}_4(\lambda, \lambda^*) < (1 - \lambda^*), \quad \forall J \geq \bar{J}, \tag{88}$$

[2] The set inclusion $\Omega^\gamma \subseteq \Omega_0$ can be assumed to be true without loss of generality. If it does not hold, it suffices to scale down the set Ω^γ, which will remain γ-contractive for (70) in view of Lemma 4.1.

[3] $\bar{J}$ is well-defined since $c_1(J) \overset{J \to \infty}{\to} 0$.

where

$$\bar{c}_3 \triangleq \max_{x_p \in \Omega_0} \left\| \begin{bmatrix} I_{n_p} \\ K_p \end{bmatrix} x_p \right\|, \quad \bar{c}_4(\lambda, \lambda^*) \triangleq \Psi_{\lambda/\lambda^*\Omega^\gamma}(\mathscr{B}). \tag{89}$$

Then, given (λ, λ^*, J) *satisfying*

$$\gamma \leq \lambda < \lambda^* < 1, \quad J \geq \bar{J}(\lambda, \lambda^*), \tag{90}$$

there exists $i^* = i^*(\lambda, \lambda^*, J) \in \mathbb{N}$ *such that for all* $i \geq i^*$ *the set* $\hat{\Omega}_i = \lambda/\lambda^*\Omega_i(\lambda, J, \Omega_0)$ *obtained by the recursion* (78)*:*

a) is λ^**-contractive for* (75)*;*

b) satisfies (83)*;*

c) is $\nu(\hat{\Omega}_i, J, \lambda^*)$*-contractive for* (70)*.*

Proof:

a) Since Ω^γ is γ-contractive for (70) and $\lambda \geq \gamma$, it also is λ-contractive for (75) for the given value of J. So from item c) of Theorem 4.1 it follows that

$$\Omega^\gamma \subseteq \underline{\Omega}_{\lambda,J} \tag{91}$$

where $\underline{\Omega}_{\lambda,J}$ is the maximal λ-contractive C-set for (75) in Ω_0. Applying now Lemma 4.4 we conclude that there exists $i^* \in \mathbb{N}$ such that $\hat{\Omega}_i = \lambda/\lambda^*\Omega_i$ is λ^*-contractive for (75) for all $i \geq i^*$, i.e. $\hat{\Omega}_i \subseteq T_J\left(\lambda^*\hat{\Omega}_i\right)$.

b) We have to show that $\nu(\hat{\Omega}_i, J, \lambda^*) < 1$ for all $i \geq i^*$. Next we will show that the inequality holds not only for $i \geq i^*$ but for all $i \in \mathbb{N}$.

Recalling that $\hat{\Omega}_i = \lambda/\lambda^*\Omega_i \subset \Omega_i \subseteq \Omega_0$, we have that:

$$\bar{c}_3 = \max_{x_p \in \Omega_0} \left\| \begin{bmatrix} I_{n_p} \\ K_p \end{bmatrix} x_p \right\| \geq \max_{x_p \in \hat{\Omega}_i} \left\| \begin{bmatrix} I_{n_p} \\ K_p \end{bmatrix} x_p \right\| = c_3(\hat{\Omega}_i). \tag{92}$$

Moreover, as

$$\lambda/\lambda^*\Omega^\gamma \underbrace{\subseteq}_{(91)} \lambda/\lambda^*\underline{\Omega}_{\lambda,J} \subseteq \lambda/\lambda^*\Omega_i = \hat{\Omega}_i, \tag{93}$$

it follows that:

$$\bar{c}_4(\lambda, \lambda^*) = \Psi_{\lambda/\lambda^*\Omega^\gamma}(\mathscr{B}) \geq \Psi_{\hat{\Omega}_i}(\mathscr{B}) = c_4(\hat{\Omega}_i). \tag{94}$$

Then,

$$\nu(\hat{\Omega}_i, J, \lambda^*) = \lambda^* + c_1(J)c_2c_3(\hat{\Omega}_i)c_4(\hat{\Omega}_i) \underbrace{\leq}_{(92),(94)} \lambda^* + c_1(J)c_2\bar{c}_3\bar{c}_4(\lambda, \lambda^*) \underbrace{<}_{(88)} 1,$$

which concludes the proof.

c) It suffices to apply Theorem 4.2 using properties a) and b).

■

As a byproduct of the proof, note that the existence of a γ-contractive C-set $\Omega^\gamma \subseteq \Omega_0 \subset \mathbb{R}^{n_p}$ for (70) not only guarantees that the proposed recursion (78) will result in a $\nu(\hat{\Omega}_i, J, \lambda^*)$-contractive P-set $\hat{\Omega}_i$ for (70), with appropriate choices of λ, λ^* and J, but also ensures that the obtained estimate of the RAO $\hat{\Omega}_i$ will include the estimate Ω^γ up to the scaling factor λ/λ^*, i.e. $\lambda/\lambda^*\Omega^\gamma \subseteq \hat{\Omega}_i$ (see (93)). This observation is formalized below.

Corollary 4.1. *If all the assumptions of Theorem 4.3 hold, the set $\hat{\Omega}_i$ contains $\lambda/\lambda^*\Omega^\gamma$.*

It is important to highlight that the ellipsoidal estimate $\mathscr{E}(W_{11}^{-1})$ of the RAO of the system provided by the method of Chapter 3 is, if $K_u = 0$, contractive for the difference inclusion (68) (as well as $\varepsilon\mathscr{E}(W_{11}^{-1})$ for all $\varepsilon \in [0,1]$) due to the exponential decrease of the quadratic Lyapunov function related to this set at the sampling instants t_k. In other words, in the single input case Lemma 4.2 guarantees that $\mathscr{E}(W_{11}^{-1})$ is a contractive C-set for (70). Consequently, according to Corollary 4.1, the polyhedral estimate $\hat{\Omega}_i$ of the RAO of the system obtained as described above will contain $\lambda/\lambda^*\mathscr{E}(W_{11}^{-1})$ if λ, λ^* and J are appropriately chosen. That is, the polyhedral estimate tends to be less conservative than the ellipsoidal one if the ratio λ/λ^* is close to 1.

4.3 Numerical algorithm

Algorithm 4.1

Step 1: Choose $J_0, \bar{i} \in \mathbb{N}_+$, a P-set Ω_0 and λ, λ^* s.t. $0 < \lambda < \lambda^* < 1$
Step 2: $J \leftarrow J_0$
Step 3: $i = 0$
Step 4: Compute Ω_{i+1} using (78)
  if $\hat{\Omega} \triangleq \lambda/\lambda^*\Omega_{i+1}$ satisfies $\hat{\Omega} \subseteq T_J\left(\lambda^*\hat{\Omega}\right)$ **then**
    Compute $\nu(\hat{\Omega}, J, \lambda^*)$ using (83)
    if $\nu(\hat{\Omega}, J, \lambda^*) < 1$ **then**
      Stop successfully
    else
      $J \leftarrow J + 1$ and go to Step 3
    end if
  else
    $i \leftarrow i + 1$
    if $i < \bar{i}$ **then**
      Go to Step 4
    else

$$\lambda \leftarrow \frac{\lambda + 1}{2}, \quad \lambda^* \leftarrow \frac{\lambda^* + 1}{2} \tag{95}$$

      and go to Step 3
    end if
  end if
Output: Contractive P-set $\hat{\Omega}$ for (70)

Based on the previously presented results, Algorithm 4.1 is proposed to obtain a

$\nu(\hat{\Omega}, J, \lambda^*)$-contractive polyhedral C-set $\hat{\Omega}$ for (70), which can be used as an estimate of the RAO of (1),(3),(5).

Notice that (78) is recursively applied until a λ^*-contractive P-set $\hat{\Omega}$ is found for (75) or until the maximum number of iterations $\bar{i}$ is reached, where $\bar{i}$ is empirically chosen and assumed to be a large enough constant (such that $\bar{i} > i^*$ will most likely be true where i^* is defined in Lemma 4.4). If $\bar{i}$ is reached, the algorithm increases the value of λ with the aim of making $\lambda \geq \gamma$ according to the statement of Theorem 4.3, where γ is not known *a priori*. The update rule (95) is just a possible choice and can be modified by the users of the method.

On the other hand, if a λ^*-contractive P-set is found for (75) but constraint (83) is violated, the algorithm increases the value of J. This choice is also inspired by the assumptions of Theorem 4.3, which guarantees that $\nu(\hat{\Omega}, J, \lambda^*) < 1$ for J sufficiently large if the other hypothesis hold, see (90).

4.4 Numerical examples

Two numerical examples are presented next.

4.4.1 Example I

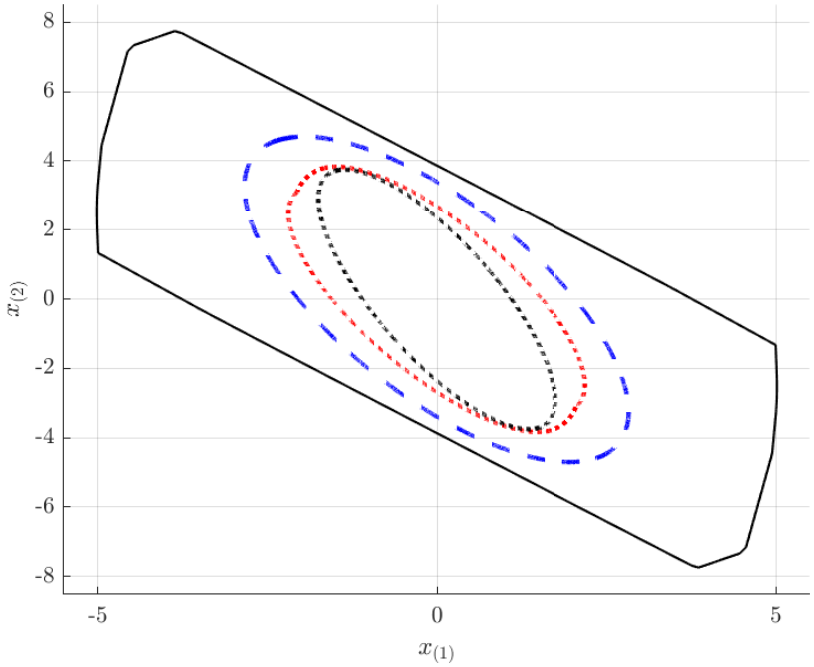

Figure 9: Estimates of the RAO of (1),(3),(5),(96) given by the proposed approach (black-continuous) and by the methods proposed in [SG12] (black-dotted), [FG18] (red-dotted) and Chapter 3 (blue-dashed).

Consider the system taken from [FG18] (also considered in Chapter 3), where:

$$A_p = \begin{bmatrix} 0 & 1 \\ 1 & 0 \end{bmatrix}, \; B_p = \begin{bmatrix} 0 \\ -5 \end{bmatrix}, \; K_p = \begin{bmatrix} 2.6 & 1.4 \end{bmatrix}, \; \Delta = [0.05, 0.1]. \tag{96}$$

Choosing $\lambda = 0.98$ and $\lambda^* = 0.99$ and considering as initial set Ω_0 a square with side of size 20 centered at the origin, the algorithm above gives, for $J = 140$, the polytope $\hat{\Omega}_{35}$ displayed in Figure 9, which is an estimate of the RAO of system (1),(3),(5). In this case, the contractivity factor of $\hat{\Omega}_{35}$ is given by $\nu(\hat{\Omega}_{35},140,0.99) \cong 0.999 < 1$. For comparison purposes, the figure also shows the piecewise quadratic estimate obtained with the conditions proposed in [FG18] and the ellipsoidal estimates obtained through the methods presented in [SG12] and in Chapter 3. Notice that the approach presented here resulted in an estimate of the RAO that includes the other ones.

In Figure 10, several trajectories of system (1),(3),(5),(96) considering δ_k randomly chosen in the interval Δ are shown. As expected, the trajectories initialized at the boundary of the set $\hat{\Omega}_{35}$ converge to the origin. Among the ones initialized outside $\hat{\Omega}_{35}$, some of them converge to the origin while others diverge.

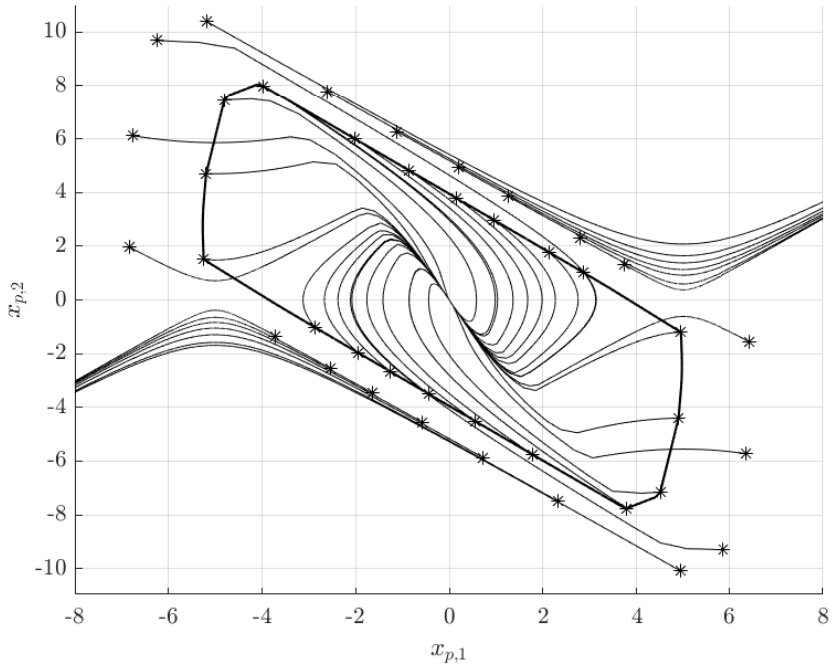

Figure 10: Trajectories of (1),(3),(5),(96), where the initial conditions are depicted by the symbol *.

4.4.2 Example II

Consider the three-dimensional system (1),(3),(5) with:

$$A_p = \begin{bmatrix} 0.75 & 0.35 & 1.75 \\ 0.7 & 0 & 0.7 \\ 0.75 & -1.1 & 1.75 \end{bmatrix}, \; B_p = \begin{bmatrix} 0.7 \\ 0 \\ 0.7 \end{bmatrix}, \; K_p = \begin{bmatrix} -24.82 & -22.85 & 11.13 \end{bmatrix}, \; \Delta = [0.1,0.2].$$

Choosing $\lambda = 0.8$ and $\lambda^* = 0.95$ and considering as initial set Ω_0 a square with side of size 1 centered at the origin, the algorithm leads, for $J = 100$, to the polytope $\hat{\Omega}_{12}$ displayed in Figure 11, where $\nu(\hat{\Omega}_{12},100,0.95) \cong 0.99 < 1$.

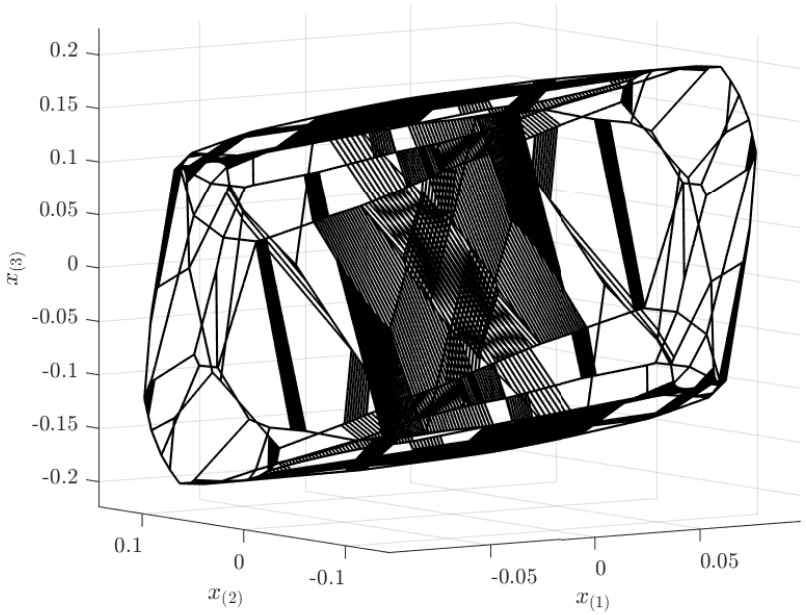

Figure 11: Estimate of the RAO of (1),(3),(5) given by the proposed approach.

4.5 Concluding remarks

A method for the computation of polyhedral estimates of the RAO of aperiodic sampled-data systems subject to control input saturation was presented. As shown in the first example, the obtained polytope provided an estimate of the RAO that is less conservative than other ones from the literature (including the one of Chapter 3).

The main drawback of this approach is its numerical complexity, as usual with methods based on polyhedrons [BM15]. In particular, the polytopes generated by the proposed recursion (78) become more complex at each iteration. Thus, even if there is a theoretical guarantee that the algorithm will finish after a finite number of steps if Assumption 4.1 holds, in practice this may not always be the case, since the execution time of the computer code grows significantly at each iteration. In order to circumvent this problem, another approach is developed in the next chapter, which is also iterative but provides at each iteration a new contractive polytope of increased size that *can* be used as estimate of the RAO, unlike the intermediary sets generated by recursion (78).

The results in this chapter have been published in [HFG22d].

5 STABILITY ANALYSIS: POLYHEDRAL APPROACH II

The objective of this chapter is analogous to the one of Chapter 4, but the polyhedral estimates of the RAO of the system are computed using a quite different approach. A comparison between the methods is presented in the section of numerical examples at the end of the chapter. As explained in the Introduction, we recall that there is no formal guarantee that the method of Chapter 5 outperforms the one of Chapter 4 in all cases. What motivated the development of this new approach is the numerical applicability of the corresponding algorithm rather than the quality of the estimate of the RAO itself.

Differently from Chapter 4, to derive the results, an impulsive system representation is employed, as shown in Section 5.1. Section 5.2 presents the main theoretical results, which lead to the proposition of an algorithm to generate an increasing sequence of polyhedral estimates of the RAO of the closed-loop system. The theory is then applied in numerical examples in Section 5.3. The chapter ends with some concluding remarks.

5.1 Closed-loop system representation

Consider the system composed by (1),(3) and (5) and its impulsive representation, given by (43) with $K_u = 0$ (see also (9)):

$$\begin{cases} \dot{x}(t) = A_c x(t), & \forall t \in \mathbb{R}_+ \setminus \mathscr{T}, \\ x(t) = x(t^+) = A_r x(t^-) + B_r \text{sat}(Kx(t^-)), & \forall t \in \mathscr{T}, \\ x(0) = [x_{p,0}^T \ \text{sat}^T(K_p x_{p,0})]^T \in \mathbb{R}^n \end{cases} \tag{97}$$

where $x = [x_p^T \ u^T]^T \in \mathbb{R}^n$, $n = n_p + m$, is the overall system state and $A_c, A_r \in \mathbb{R}^{n\times n}$, $B_r \in \mathbb{R}^{n\times m}$ and $K \in \mathbb{R}^{m\times n}$ are given by:

$$A_c = \begin{bmatrix} A_p & B_p \\ 0 & 0 \end{bmatrix}, \ A_r = \begin{bmatrix} I_{n_p} & 0 \\ 0 & 0 \end{bmatrix}, \ B_r = \begin{bmatrix} 0 \\ I_m \end{bmatrix}, \ K = \begin{bmatrix} K_p & 0 \end{bmatrix}. \tag{98}$$

From the analytical solution of (97), the dynamics between two successive sampling instants is given by:

$$\begin{aligned} x(t_{k+1}^+) &= A_r x(t_{k+1}^-) + B_r \text{sat}(Kx(t_{k+1}^-)) \\ &= A_r e^{A_c \delta_k} x(t_k^+) + B_r \text{sat}(K e^{A_c \delta_k} x(t_k^+)), \quad \delta_k \in \Delta. \end{aligned}$$

Equivalently, we obtain the following difference inclusion [FG18]:

$$\begin{aligned} x_{k+1} &\in \{A_x(\delta)x_k + B_r \text{sat}(K_x(\delta)x_k) : \ \delta \in \Delta\} \\ &\triangleq \{\mathscr{F}(x_k, \delta) : \ \delta \in \Delta\} \\ &\triangleq \mathscr{F}(x_k, \Delta) \end{aligned} \tag{99}$$

where $A_x(\delta) \triangleq A_r e^{A_c \delta}$, $K_x(\delta) \triangleq K e^{A_c \delta}$ and

$$x_k \triangleq \begin{bmatrix} x_{p,k} \\ u_k \end{bmatrix} \triangleq \begin{bmatrix} x_p(t_k) \\ u(t_k) \end{bmatrix} = x(t_k) = x(t_k^+). \tag{100}$$

Notice that the difference inclusion (99) is different from the one used in Chapter 3, which is given by (46), because $x_k = x(t_k) \neq x(t_k^-) = z_k$, where x_k and z_k correspond to the state just after and just before the impulse, respectively. It is also different from (68), which is used in Chapter 4 and considers only the plant state $x_{p,k}$ instead of the augmented vector x_k.

Following a reasoning similar to the one of the preceding chapters, we will perform next the stability analysis of the sampled-data system (97) considering the discrete-time system (99). In particular, it is straightforward to adapt the proof of Lemma 2.1 to the present case (see also [FG18]). Moreover, the RAO of (99), which will be denoted by Γ_d from now on, coincides with the RAO of (97), denoted by Γ_c, i.e. $\Gamma_d = \Gamma_c$.

5.2 SNS invariant and contractive sets

Below we particularize Definition 2.7 to system (99).

Definition 5.1. *Given $\Omega \subseteq \mathbb{R}^n$, the one-step set $P(\Omega)$ with respect to (99) is given by*

$$P(\Omega) \triangleq \{x \in \mathbb{R}^n : \ \mathscr{F}(x, \Delta) \subseteq \Omega\} \tag{101}$$

Given an invariant C-set Ω_0 for the discrete-time system (99) that belongs to the RAO of it, the increasing sequence of nested sets

$$\Omega_{i+1} = P(\Omega_i), \quad i \in \mathbb{N}, \tag{102}$$

gives approximations of increasing accuracy of the RAO of this system. However, the computation of such sets is in general not possible in practice. In particular, $P(\Omega)$ may be nonconvex even if Ω is a C-set because of the saturation function. That is why we use, as in Chapter 4, the concept of SNS system. The SNS system that corresponds to (99) is given by

$$\begin{aligned} x_{k+1} &\in \{A_x(\delta)x_k + B_r \mathrm{sat}_S(K_x(\delta)x_k) : \ \delta \in \Delta, \ S \in \mathscr{S}\} \\ &\triangleq \{\mathscr{F}_{SNS}(x_k, \delta, S) : \ \delta \in \Delta, \ S \in \mathscr{S}\} \\ &\triangleq \mathscr{F}_{SNS}(x_k, \Delta, \mathscr{S}) \end{aligned} \tag{103}$$

where $\mathrm{sat}_S : \mathbb{R}^m \to \mathbb{R}^m$ is defined in (69) and $\mathscr{S} = 2^{\mathbb{N}_m}$.

Consider the definitions below.

Definition 5.2. *(SNS invariance) A SNS invariant (contractive) set for system (99) is an invariant (contractive) set for (103).*

Definition 5.3. *(SNS Region of Attraction of the Origin) The SNS RAO of system (99), denoted by Γ_{SNS}, is the RAO of (103).*

Following the same line of argument of Chapter 4, the dynamics of the SNS system (103) includes the one of (99), i.e.

$$\begin{aligned} \mathscr{F}(x_k, \Delta) &= \{A_x(\delta)x_k + B_r \mathrm{sat}(K_x(\delta)x_k) : \ \delta \in \Delta\} \\ &= \{A_x(\delta)x_k + B_r \mathrm{sat}_S(K_x(\delta)x_k) : \ \delta \in \Delta, \ S = \mathbb{N}_m\} \\ &\subseteq \{A_x(\delta)x_k + B_r \mathrm{sat}_S(K_x(\delta)x_k) : \ \delta \in \Delta, \ S \in \mathscr{S}\} = \mathscr{F}_{SNS}(x_k, \Delta, \mathscr{S}) \end{aligned}$$

where the second equality follows from the definition of $\mathrm{sat}_S(\cdot)$ in (69) and the set inclusion from the fact that $\mathbb{N}_m \in \mathscr{S} = 2^{\mathbb{N}_m}$. That is why the notions of SNS invariance and SNS RAO are more conservative than the concepts of invariance and RAO. Consequently, $\Gamma_{SNS} \subseteq \Gamma_d$. This fact will be exploited by the method presented here. More precisely, to obtain a numerical tractable procedure, the idea is to compute polyhedral estimates of Γ_d through the computation of estimates of Γ_{SNS}.

The one-step set related to (103) is defined below.

Definition 5.4. *Given $\Omega \subseteq \mathbb{R}^n$, the one-step set $Q(\Omega)$ with respect to (103) is given by*

$$Q(\Omega) \triangleq \{x \in \mathbb{R}^n : \mathscr{F}_{SNS}(x, \Delta, \mathscr{S}) \subseteq \Omega\}. \tag{104}$$

Analogously to (102), we can consider the recursion:

$$\Omega_{i+1} = Q(\Omega_i), \quad i \in \mathbb{N}. \tag{105}$$

The next theorem states some properties of the sequence $\{\Omega_i\}_{i\in\mathbb{N}}$ defined above.

Theorem 5.1. *Consider the recursion (105) where $\Omega_0 \subseteq \Gamma_{SNS}$ is an initial SNS invariant C-set for (99). Then:*

- *Ω_i is a SNS invariant set for (99) for all $i \in \mathbb{N}$;*
- *$\Omega_i \subseteq \Omega_{i+1}$, $\forall i \in \mathbb{N}$;*
- *$\Omega_i \subseteq \Gamma_{SNS}$, $\forall i \in \mathbb{N}$;*
- *The sequence $\{\Omega_i\}_{i\in\mathbb{N}}$ converges to Γ_{SNS}.*[1]

Proof: The proof is analogous to the one of [ACLC06, Th. 2]. The only difference is that, besides S, there is an additional degree of freedom δ in the difference inclusion (103). ■

Unfortunately, as discussed in [FM16] for the linear case, under aperiodic sampling the one-step set $Q(\Omega)$ is in general not polyhedral even if Ω is a polytope. This is due to the dependence of the discrete-time model (103) on an uncertain matrix exponential term $e^{A_c\delta}$, where the value of δ varies within an interval Δ. A common approach to deal with this term consists in obtaining convex embeddings for it, which can be polytopic [CVHN09, LONH12] or norm-bounded [Fuj09, FO11, KF13]. In the present case, in order to obtain numerically tractable conditions for the stability analysis, it will be convenient to adopt the same strategy of Chapters 3 and 4, which is based on the grid Δ_J of Δ defined in (48). Hence, consider the following approximation of $Q(\Omega)$:

Definition 5.5. *Given $\Omega \subseteq \mathbb{R}^n$ and $J \in \mathbb{N}_+$,*

$$Q_J(\Omega) \triangleq \{x \in \mathbb{R}^n : \mathscr{F}_{SNS}(x, \Delta_J, \mathscr{S}) \subseteq \Omega\} \tag{106}$$

Notice that $Q_J(\Omega)$ takes into account only the finite subset Δ_J of possible values for the intersampling time δ_k. So $Q(\Omega) \subseteq Q_J(\Omega)$ but these sets are different in general. In the next section we see how to deal with this fact. Notice also that, using (48), (103) can be expressed as:

$$x_{k+1} \in \bigcup_{\tau\in[0,\tau_J]} \mathscr{F}_{SNS}(e^{A_c\tau}x_k, \Delta_J, \mathscr{S}). \tag{107}$$

[1] That is, given $x \in \Gamma_{SNS}$, there exists $i^*(x)$ such that $x \in \Omega_i, \forall i \geq i^*(x)$.

To understand why, notice first that

$$\begin{aligned}\mathscr{F}_{SNS}(e^{A_c\tau}x_k,\Delta_J,\mathscr{S}) &= \{A_x(d)e^{A_c\tau}x_k + B_r\mathrm{sat}_S(K_x(d)e^{A_c\tau}x_k) :\ d\in\Delta_J,\ S\in\mathscr{S}\}\\ &= \{A_x(d+\tau)x_k + B_r\mathrm{sat}_S(K_x(d+\tau)x_k) :\ d\in\Delta_J,\ S\in\mathscr{S}\}\\ &= \{A_x(\delta)x_k + B_r\mathrm{sat}_S(K_x(\delta)x_k) :\ \delta\in\Delta_J+\tau,\ S\in\mathscr{S}\}\\ &= \mathscr{F}_{SNS}(x_k,\Delta_J+\tau,\mathscr{S})\end{aligned}$$

where $\delta \triangleq d+\tau$. Moreover, for any two sets of real numbers $\Delta_A,\Delta_B\subseteq\mathbb{R}$ one has

$$\mathscr{F}_{SNS}(x_k,\Delta_A,\mathscr{S})\cup\mathscr{F}_{SNS}(x_k,\Delta_B,\mathscr{S}) = \mathscr{F}_{SNS}(x_k,\Delta_A\cup\Delta_B,\mathscr{S}).$$

Using the properties above we conclude that

$$\begin{aligned}\bigcup_{\tau\in[0,\tau_J]}\mathscr{F}_{SNS}(e^{A_c\tau}x_k,\Delta_J,\mathscr{S}) &= \bigcup_{\tau\in[0,\tau_J]}\mathscr{F}_{SNS}(x_k,\Delta_J+\tau,\mathscr{S})\\ &= \mathscr{F}_{SNS}(x_k,\Delta_J+[0,\tau_J],\mathscr{S}) = \mathscr{F}_{SNS}(x_k,\Delta,\mathscr{S})\end{aligned}$$

and it follows that (103) and (107) are indeed equivalent.

The following lemma, derived straightforwardly from [ACLC06, Th. 1], is similar to Lemma 4.3 and provides a polyhedral characterization of $Q_J(\Omega)$ when Ω is a polyhedron.

Lemma 5.1. *Consider $\Omega=\mathscr{P}(H,h)$, where $H\in\mathbb{R}^{n_h\times n}, h\in\mathbb{R}^{n_h}$. Then*

$$\begin{aligned}Q_J(\Omega) &= \bigcap_{\delta\in\Delta_J}\bigcap_{S\in\mathscr{S}}\left\{x\in\mathbb{R}^n : H\Big(A_x(\delta)+\sum_{i\in S^c}B_r^{(i)}K_{x(i)}(\delta)\Big)x - \sum_{i\in S}|HB_r^{(i)}| \le h\right\}\\ &= \bigcap_{\delta\in\Delta_J}\bigcap_{S\in\mathscr{S}}\mathscr{P}\left(H\Big(A_x(\delta)+\sum_{i\in S^c}B_r^{(i)}K_{x(i)}(\delta)\Big),\ h+\sum_{i\in S}|HB_r^{(i)}|\right).\end{aligned}\tag{108}$$

Moreover, we have the following technical results, which will be used later and whose proofs are in Appendices A.3 and A.4, respectively. They provide some basic properties of the operators $Q(\cdot)$ and $Q_J(\cdot)$.

Lemma 5.2. *Consider $\Delta=[\tau_m,\tau_M]$ with $\tau_m<\tau_M$ and define $J^\star$ as the number of elements of the finite set*

$$\Delta^\star \triangleq \{\tau_m,\tau_M\}\cup(\{\tau_m+2\pi r/\omega_l :\ l\in\mathbb{N}_{n_\omega}, r\in\mathbb{Z}\}\cap\Delta)$$

where $\pm j\omega_l$ is the l-th pair of pure imaginary eigenvalues of A_p with $l=1,\dots,n_\omega$. Given a P-set Ω,

a) $Q(\Omega)$ and $Q_J(\Omega)$ are both C-sets for all $J\ge J^\star$;

b) For $\gamma>0$ such that $\Omega\subseteq\mathscr{B}_\gamma$, there exists $r=r(\gamma)>0$ such that

$$Q(\Omega)\subseteq Q_J(\Omega)\subseteq\mathscr{B}_r, \forall J\ge J^\star.$$

Among all properties that $Q_J(\Omega)$ has to satisfy to be a C-set, the requirement $J\ge J^\star$ in the lemma above is important only to guarantee that $Q_J(\Omega)$ is bounded, avoiding some "pathological" cases where it would be unbounded even if Ω is bounded. In the simplest case, where A_p has no pure imaginary eigenvalues, $\Delta^\star=\{\tau_m,\tau_M\}$ and $J^\star=2$. Otherwise,

it is possible to show that $J^\star = 2$ if the frequencies $f_{s,k} \triangleq 2\pi/\delta_k \in [2\pi/\tau_M, 2\pi/\tau_m]$ are larger than the natural frequencies ω_l of the open-loop system.

Given two C-sets Θ_1, Θ_2 such that $\Theta_1 \subset \Theta_2^\circ$, it follows straightforwardly that $Q(\Theta_1) \subseteq Q(\Theta_2^\circ)$. However, it is not trivial to see if the set inclusion still holds inverting the order of the operators $Q(\cdot)$ and $(\cdot)^\circ$, i.e. $Q(\Theta_1) \subset Q(\Theta_2)^\circ$. The role of Lemma 5.3 below is to prove this relation.

Lemma 5.3. *Given two C-sets Θ_1, Θ_2 such that $\Theta_1 \subset \Theta_2^\circ$, it follows that*

$$Q(\Theta_1) \subset Q(\Theta_2)^\circ.$$

5.2.1 Computation of estimates of the RAO

We want to obtain estimates of the RAO of (99), i.e. Γ_d, through the computation of polyhedral estimates of the SNS RAO of (99), i.e. Γ_{SNS}. As explained before, it is not possible to simply replace the operator $Q(\cdot)$ by $Q_J(\cdot)$ in the recursion (105) and use the result of Theorem 5.1 since $Q_J(\cdot)$ does not take into account all possible values of δ_k, except in the trivial case where $\tau_m = \tau_M$. Thus, from now on, we will only deal with the nontrivial case $\tau_m < \tau_M$, i.e. δ_k is uncertain. For technical reasons, we will also consider that the number of partitions J of Δ satisfies $J \geq J^\star$, where $J^\star$ is defined in Lemma 5.2, in which case $Q_J(\cdot)$ is a C-set.

The objective of this section is to show how to construct, in a numerically tractable way, an increasing sequence $\{\Omega_i\}_{i\in\mathbb{N}}$ of SNS λ_i-contractive polyhedral C-sets for (99) using an initial SNS λ_0-contractive polyhedral C-set Ω_0. From the contractivity property, it follows that these sets are included in $\Gamma_{SNS} \subseteq \Gamma_d = \Gamma_c$, being therefore estimates of Γ_c, the RAO of (97). This statement is a direct consequence of the lemma below.

Lemma 5.4. *If the C-set $\Omega \subset \mathbb{R}^n$ is SNS λ-contractive for (99):*

a) $\varepsilon\Omega$ also is SNS λ-contractive for (99) for all $\varepsilon \in [0,1]$;

b) All trajectories of (103) have the following property:

$$x_k \in \varepsilon\Omega \;\Rightarrow\; x_{k+p} \in \lambda^p \varepsilon\Omega, \quad \forall \varepsilon \in [0,1],\ \forall p \in \mathbb{N}. \tag{109}$$

c) All trajectories of (99) have property (109).

Proof: The proof of a) follows the one of Lemma 4.1 *mutatis mutandis*; b) is implied by the recursive application of a); and c) follows directly from b) and the fact that every trajectory of (99) is also a trajectory of (103). ■

Corollary 5.1. *If the C-set $\Omega \subset \mathbb{R}^n$ is SNS contractive for (99), then $\Omega \subseteq \Gamma_{SNS} \subseteq \Gamma_d = \Gamma_c$.*

Proof: Follows from item b) of Lemma 5.4 and the fact that $\lambda \in [0,1)$ and Ω is bounded by definition. ■

In order to construct the sequence $\{\Omega_i\}_{i\in\mathbb{N}}$, the operator $Q(\Omega)$ in (105) will be replaced not by $Q_J(\Omega)$ (as already explained, this strategy would not work) but by the set $\hat{Q}_J(\Omega)$ defined below. The main difference is that $\hat{Q}_J(\Omega)$ corresponds to an inner approximation of $Q(\Omega)$ while $Q_J(\Omega)$ corresponds to an outer approximation of $Q(\Omega)$. The set $\hat{Q}_J(\Omega)$ will be obtained by scaling down $Q_J(\Omega)$.

Definition 5.6. *Given the polyhedral C-set $\Omega \subset \mathbb{R}^n$, $J \geq J^\star$ and the H-representation*[2] *$Q_J(\Omega) = \mathscr{P}(H, \mathbf{1})$, $H \in \mathbb{R}^{n_h \times n}$,*

$$\beta^J(\Omega) \triangleq \inf_{T,\beta} \beta \text{ s.t. } \begin{cases} HA_c = TH \\ T\mathbf{1} \leq \beta \mathbf{1} \\ T_{(i,j)} \geq 0, \qquad \forall i \neq j \end{cases} \tag{110}$$

$$\alpha^J(\Omega) \triangleq \max\{1, e^{\beta^J(\Omega)\tau_J}\} \tag{111}$$

$$\hat{Q}_J(\Omega) \triangleq Q_J(\Omega)/\alpha^J(\Omega) \tag{112}$$

where $T \in \mathbb{R}^{n_h \times n_h}, \beta \in \mathbb{R}$, A_c is defined in (98) and τ_J in (48).

Remark 5.1. *According to Lemma 2.5, the constraints in (110) are feasible for some $\beta \in \mathbb{R}$ if and only if the polyhedral C-set $Q_J(\Omega) = \mathscr{P}(H, \mathbf{1})$ is β-invariant for $\dot{x}(t) = A_c x(t)$. Therefore, $\beta^J(\Omega)$ is the smallest number β such that $Q_J(\Omega)$ (or equivalently $\hat{Q}_J(\Omega)$) is β-invariant for this system.*

The theorem below guarantees that $\hat{Q}_J(\Omega) = Q_J(\Omega)/\alpha^J(\Omega) \subseteq Q(\Omega)$. The motivation for choosing the scale factor $\alpha^J(\Omega)$ will become clear in the proof of this theorem. The number $\alpha^J(\Omega)$ is related to the possible expansion of the set $\hat{Q}_J(\Omega)$ along the trajectories of (31) in a time interval $[0, \tau] \subseteq [0, \tau_J]$.

Theorem 5.2. *Given a polyhedral C-set $\Omega \subset \mathbb{R}^n$ and $J \geq J^\star$, it follows that*

$$\hat{Q}_J(\Omega) \subseteq Q(\Omega). \tag{113}$$

Proof: Given $x_k \in \hat{Q}_J(\Omega)$, we have to prove that $x_k \in Q(\Omega)$. This is equivalent to show that $x_{k+1} \in \Omega$ for all possible values of $\delta_k \in \Delta$ and $S_k \in \mathscr{S}$, where x_{k+1} is given by (103).

Given $\delta_k \in \Delta$ and $S_k \in \mathscr{S}$, we know from (107) that there exists $\tau \in [0, \tau_J]$ such that

$$x_{k+1} \in \mathscr{F}_{SNS}(e^{A_c \tau} x_k, \Delta_J, \mathscr{S}). \tag{114}$$

Consider now that $x_k \in \hat{Q}_J(\Omega) = Q_J(\Omega)/\alpha^J(\Omega)$ where $\hat{Q}_J(\Omega)$ is $\beta^J(\Omega)$-invariant for $\dot{x}(t) = A_c x(t)$. Applying Corollary 2.2 (with $\Omega = \hat{Q}_J(\Omega)$, $\beta = \beta^J(\Omega)$, $\bar{\tau} = \tau_J$ and $\alpha = \alpha^J(\Omega)$), we conclude that

$$e^{A_c \tau} x_k \in e^{A_c \tau} \hat{Q}_J(\Omega) \subseteq \alpha^J(\Omega) \hat{Q}_J(\Omega) = Q_J(\Omega).$$

Since $e^{A_c \tau} x_k \in Q_J(\Omega)$, it follows from (106) that

$$\mathscr{F}_{SNS}(e^{A_c \tau} x_k, \Delta_J, \mathscr{S}) \subseteq \Omega.$$

Combining this set inclusion with (114), we conclude that $x_{k+1} \in \Omega$, that is, $x_k \in Q(\Omega)$, proving the result. ■

Considering the result below it is possible to conclude that the set $\hat{Q}_J(\Omega) \subseteq Q(\Omega)$ converges to $Q(\Omega)$ as $J \to \infty$.

Lemma 5.5. *Given a polyhedral C-set $\Omega \subset \mathbb{R}^n$ and $c \in [0,1)$, there exists $\bar{J} \in \mathbb{N}, \bar{J} \geq J^\star$, such that*

$$cQ(\Omega) \subset \hat{Q}_J(\Omega)^\circ, \quad \forall J \geq \bar{J}. \tag{115}$$

[2] $Q_J(\Omega)$ is a polyhedral C-set according to Lemmas 5.1 and 5.2 and we can assume without loss of generality that $h = \mathbf{1}$ in the H-representation $Q_J(\Omega) = \mathscr{P}(H, h)$ because $0 \in Q_J(\Omega)^\circ$.

Proof: See Appendix A.5. ■

The lemma above leads directly to the next theorem.

Theorem 5.3. *Given a SNS contractive polyhedral C-set $\Omega \subset \mathbb{R}^n$ for (99), there exists $\bar{J} \in \mathbb{N}, \bar{J} \geq J^\star$, such that*

$$\Omega \subset \hat{Q}_J(\Omega)^\circ, \quad \forall J \geq \bar{J}. \tag{116}$$

Proof: Since Ω is contractive for the SNS system (103), there exists $\lambda \in (0,1)$ such that $\Omega \subseteq Q(\lambda\Omega)$. Moreover, using the relation $\lambda\Omega \subset \Omega^\circ$, Lemma 5.3 guarantees that $Q(\lambda\Omega) \subset Q(\Omega)^\circ$. Combining these two set inclusions we conclude that $\Omega \subset Q(\Omega)^\circ$, so there exists $c \in (0,1)$ such that $\Omega \subseteq cQ(\Omega)$. Combining this relation with the result from Lemma 5.5, it follows that

$$\Omega \subseteq cQ(\Omega) \subset \hat{Q}_J(\Omega)^\circ$$

for J sufficiently large. ■

Figure 12 presents a geometrical interpretation of Theorems 5.2 and 5.3 and Lemma 5.5. As the value of J increases, the set $\hat{Q}_J(\Omega)$ converges to $Q(\Omega)$ from the inside, while $Q_J(\Omega)$ converges to $Q(\Omega)$ from the outside. Therefore, for J sufficiently large, $\Omega \subset \hat{Q}_J(\Omega)^\circ$, as illustrated in the right image. The complexity of sets $Q_J(\Omega)$ and $\hat{Q}_J(\Omega)$ will, in principle, increase as $J \to \infty$, as implied by the expression (108).

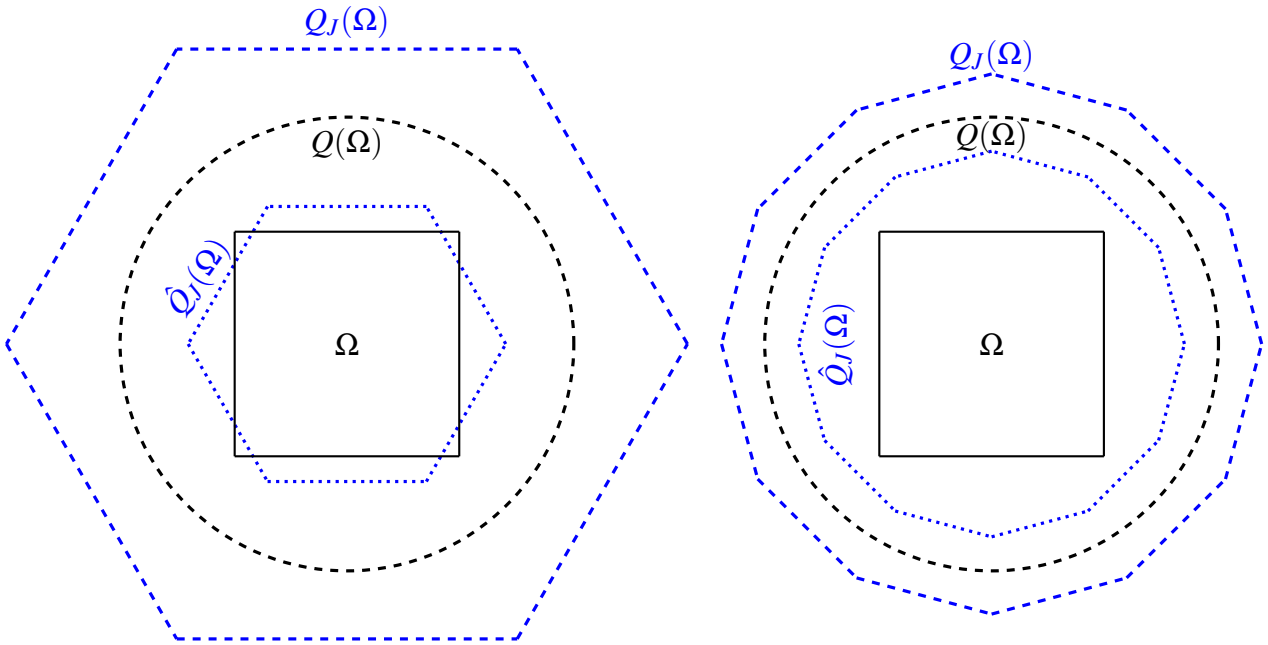

Relatively small J Relatively large J

Figure 12: Geometrical interpretation of Theorems 5.2 and 5.3 and Lemma 5.5.

Theorem 5.4 combines the results of Theorems 5.2 and 5.3 in order to guarantee the contractivity of the set $\hat{Q}_J(\Omega)$.

Theorem 5.4. *Given a polyhedral C-set $\Omega \subset \mathbb{R}^n$ and $J \geq J^\star$, if $\Omega \subset \hat{Q}_J(\Omega)^\circ$ then $\hat{Q}_J(\Omega) \subset \mathbb{R}^n$ is a SNS contractive polyhedral C-set for (99).*

Proof: Relation $\Omega \subset \hat{Q}_J(\Omega)^\circ$ guarantees the existence of $\hat{\lambda} \in (0,1)$ such that

$$\Omega \subseteq \hat{\lambda}\hat{Q}_J(\Omega).$$

Then, from (113),

$$\hat{Q}_J(\Omega) \subseteq Q(\Omega) \subseteq Q(\hat{\lambda}\hat{Q}_J(\Omega))$$

and we conclude from the definition of contractivity that $\hat{Q}_J(\Omega)$ is SNS $\hat{\lambda}$-contractive for (99). ■

The properties above are used in Algorithm 5.1, which applies them recursively to provide an increasing sequence of estimates of the (SNS) RAO of the system. The MPT toolbox [HKJM13], which has functions to manipulate polyhedral sets, can be used. Moreover, an initial SNS contractive polyhedral C-set $\Omega_0 \subset \mathbb{R}^n$ for (99) is required. It is suggested to obtain this set in the region of linearity

$$\mathscr{L} \triangleq \{x \in \mathbb{R}^n : \ |K_x(\delta)x| \leq \mathbf{1}, \ \forall \delta \in \Delta\}$$

of (99), i.e. the region where the control input does not saturate, using the method proposed in [FM16], which allows to compute a contractive polyhedral C-set for the linear difference inclusion

$$x_{k+1} \in \{(A_x(\delta) + B_r K_x(\delta))\, x_k : \ \delta \in \Delta\}$$

provided that it is exponentially stable.

Algorithm 5.1 Increasing sequence of estimates of $\Gamma_{SNS} \subseteq \Gamma_c$

Input: Initial SNS contractive polyhedral C-set $\Omega_0 \subset \mathbb{R}^n$ for (99), $\bar{i} \in \mathbb{N}$, $J_0 \geq J^\star$

$i \leftarrow 0$, $J \leftarrow J_0$

while $i < \bar{i}$ **do**

Compute $\hat{Q}_J(\Omega_i)$ according to Definition 5.6

if

$$\Omega_i \subset \hat{Q}_J(\Omega_i)^\circ \tag{117}$$

then

$$\Omega_{i+1} \triangleq \hat{Q}_J(\Omega_i), \ \ J_{i+1} \triangleq J \tag{118}$$

$i \leftarrow i+1$

end if

Increment J

end while

Output: Estimate of the RAO: $\Omega_{\bar{i}}$

Remark 5.2. *Algorithm 5.1 generates a sequence* $\{\Omega_i\}_{i=0}^{\bar{i}}$ *of polyhedral C-sets and a corresponding strictly increasing sequence of integers* $\{J_i\}_{i=1}^{\bar{i}}$ *that satisfy for all i:*

$\Omega_{i+1} \subseteq Q(\Omega_i)$	*(from* (118) *and Theorem 5.2)*	(119a)
$\Omega_i \subset \Omega_{i+1}^\circ$	*(from* (117) *and* (118)*)*	(119b)
Ω_{i+1} *is SNS* λ_{i+1}*-contractive for* (99)	*(from* (117),(118) *and Theorem 5.4)*	(119c)
$\Omega_{i+1} \subseteq \Gamma_{SNS} \subseteq \Gamma_c$	*(from* (119c) *and Corollary 5.1)*	(119d)
$\Omega_{i+1} = \hat{Q}_{J_{i+1}}(\Omega_i)$	*(from* (118)*)*	(119e)

where in (119c) *the sets* Ω_i *have not necessarily the same contraction factor* λ_i *since* $\lambda \in (0,1)$ *in Theorem 5.4 depends on* Ω *and* J.

Theorem 5.3 guarantees that the test (117) (the *if* statement) will eventually be true since J is always incremented, thus the algorithm has a finite execution time. Recall that Algorithms 3.1 and 4.1 of the preceding chapters also increment the value of J.

The estimate $\Omega_{\bar{i}}$ of the RAO is related to

$$x_0 = [x_p^T(0)\ u^T(0)]^T \tag{120}$$

but $x_p(0)$ and $u(0)$ are actually coupled by the relation $u(0) = \text{sat}(K_p x_p(0))$. That is, considering the H-representation $\Omega_{\bar{i}} = \mathscr{P}(H,h) = \{x \in \mathbb{R}^n :\ Hx \leq h\}$, the "safe" set of plant initial states is given by:

$$\Omega_{\bar{i},x_p} \triangleq \left\{ x_p \in \mathbb{R}^{n_p} :\ H \begin{bmatrix} x_p \\ \text{sat}(K_p x_p) \end{bmatrix} \leq h \right\}, \tag{121}$$

which corresponds to the union of 3^m polytopes. To understand why, notice that $\text{sat}(K_p x_p)$ is a piecewise affine function of x_p. More precisely, with appropriately chosen matrices R_j and vectors r_j, the space $\mathbb{R}^{n_p}$ can be partitioned into 3^m polyhedral sets $S_j \triangleq \mathscr{P}(R_j, r_j), j \in \mathbb{N}_{3^m}$, called regions of saturation in [GT99], such that:

$$\begin{aligned} &\text{sat}(K_p x_p) = P_j x_p + p_j, \quad \forall x_p \in S_j,\ \forall j \in \mathbb{N}_{3^m} \\ &\textstyle\bigcup_{j=1}^{3^m} S_j = \mathbb{R}^{n_p} \\ &(S_j \cap S_l)^\circ = \emptyset, \quad \forall j,l \in \mathbb{N}_{3^m},\ j \neq l \end{aligned} \tag{122}$$

where $P_j \in \mathbb{R}^{m \times n_p}$ and $p_j \in \mathbb{R}^m$ can be obtained as described in [GT99]. Substituting (122) in (121), we get:

$$\begin{aligned} \Omega_{\bar{i},x_p} = \mathbb{R}^{n_p} \cap \Omega_{\bar{i},x_p} &= \left(\textstyle\bigcup_{j=1}^{3^m} S_j \right) \cap \left\{ x_p \in \mathbb{R}^{n_p} :\ H \begin{bmatrix} x_p \\ \text{sat}(K_p x_p) \end{bmatrix} \leq h \right\} \\ &= \textstyle\bigcup_{j=1}^{3^m} \left(S_j \cap \left\{ x_p \in \mathbb{R}^{n_p} :\ H \begin{bmatrix} x_p \\ \text{sat}(K_p x_p) \end{bmatrix} \leq h \right\} \right) \\ &= \textstyle\bigcup_{j=1}^{3^m} \left(S_j \cap \left\{ x_p \in \mathbb{R}^{n_p} :\ H \begin{bmatrix} x_p \\ P_j x_p + p_j \end{bmatrix} \leq h \right\} \right) \\ &= \textstyle\bigcup_{j=1}^{3^m} \left(S_j \cap \left\{ x_p \in \mathbb{R}^{n_p} :\ \begin{bmatrix} H_1 & H_2 \end{bmatrix} \begin{bmatrix} I_{n_p} \\ P_j \end{bmatrix} x_p \leq h - H_2 p_j \right\} \right) \\ &= \textstyle\bigcup_{j=1}^{3^m} \left(\mathscr{P}(R_j, r_j) \cap \mathscr{P}(H_1 + H_2 P_j, h - H_2 p_j) \right) \\ &= \textstyle\bigcup_{j=1}^{3^m} \mathscr{P}\left(\begin{bmatrix} R_j \\ H_1 + H_2 P_j \end{bmatrix}, \begin{bmatrix} r_j \\ h - H_2 p_j \end{bmatrix} \right) \end{aligned}$$

where $H = [H_1\ H_2]$ and H_1 and H_2 have appropriate dimensions.

Notice that the bigger $\bar{i}$ is, the bigger will be the estimate $\Omega_{\bar{i},x_p}$ of the RAO of the system. However, the polytopes Ω_i computed by the algorithm above tend to become more complex at each iteration. Consequently, the execution time of the computer code also grows at each iteration and, in practice, the maximum number of iterations $\bar{i}$ cannot be arbitrarily large. The method presented in Chapter 4 has a similar problem. The main difference between these two polyhedral approaches is that the method of Chapter 4 will only provide a valid estimate of the RAO of the system upon termination of Algorithm 4.1, while the method proposed in this chapter provides, at each iteration of Algorithm 5.1, a

new estimate Ω_{i,x_p} of the RAO which encompasses the preceding one Ω_{i-1,x_p}. One of the numerical examples of Section 5.3 presents a case where the execution of Algorithm 4.1 becomes prohibitively complex before its stopping criterion $\nu(\Omega, J, \lambda^*) < 1$ is reached. That is, Algorithm 4.1 fails to provide an estimate of the RAO. On the other hand, the application of Algorithm 5.1 is successful, even if $\bar{i}$ is relatively small.

5.2.2 Convergence properties

Consider the non-truncated version of the sequence $\{\Omega_i\}$ generated by Algorithm 5.1 (i.e. with $\bar{i} \equiv \infty$), which satisfies (119). We will show that $\{\Omega_i\}_{i\in\mathbb{N}}$ converges to the SNS RAO Γ_{SNS} of (99) under the following assumption.

Assumption 5.1. *Γ_{SNS} is bounded, i.e. there exists $\gamma > 0$ such that $\Gamma_{SNS} \subseteq \mathscr{B}_\gamma$.*

The convergence will be proved starting with the lemma below, whose proof is in Appendix A.6.

Lemma 5.6. *Given the sequence $\{\Omega_i\}_{i\in\mathbb{N}}$ generated by Algorithm 5.1 and $i_1 \in \mathbb{N}$, $\exists i_2 \geq i_1$ such that*

$$Q(\Omega_{i_1}) \subseteq \Omega_{i_2}.$$

It is worth saying that, according to our experience, the result above may also be true even if Assumption 5.1 does not hold. Using this lemma we obtain the following theorem.

Theorem 5.5. *The sequence $\{\Omega_i\}_{i\in\mathbb{N}}$ generated by Algorithm 5.1 converges to Γ_{SNS}.*

Proof: Denote the sequence generated by (105) as $\{\Theta_i\}_{i\in\mathbb{N}}$ to avoid confusion with $\{\Omega_i\}_{i\in\mathbb{N}}$, generated by Algorithm 5.1. The initial SNS contractive polyhedral C-set $\Omega_0 \subset \mathbb{R}^n$ for (99) satisfies the hypothesis of Theorem 5.1. Thus, Theorem 5.1 guarantees the convergence of $\{\Theta_i\}_{i\in\mathbb{N}}$ with $\Theta_0 = \Omega_0$ to Γ_{SNS}. Therefore, since $\{\Theta_i\}_{i\in\mathbb{N}}$ and $\{\Omega_i\}_{i\in\mathbb{N}}$ are both increasing sequences of nested sets, it suffices to show that for each $i_A \geq 0$ there exists $i_B \geq 0$ such that $\Theta_{i_A} \subseteq \Omega_{i_B}$. This implies that $\{\Omega_i\}_{i\in\mathbb{N}}$ converges to Γ_{SNS} from the inside, like $\{\Theta_i\}_{i\in\mathbb{N}}$. Let us prove the relation $\Theta_{i_A} \subseteq \Omega_{i_B}$ by induction.

The case $i_A = 0$ is clearly true since $\Theta_0 = \Omega_0$. Let us assume that $\Theta_{i_A} \subseteq \Omega_{i_B}$ for $i_A, i_B \in \mathbb{N}$ and show that there exists $i_C \in \mathbb{N}$ such that $\Theta_{i_A+1} \subseteq \Omega_{i_C}$. From Lemma 5.6, there exists $i_C \in \mathbb{N}$ satisfying $Q(\Omega_{i_B}) \subseteq \Omega_{i_C}$. Thus, from (105),

$$\Theta_{i_A+1} = Q(\Theta_{i_A}) \subseteq Q(\Omega_{i_B}) \subseteq \Omega_{i_C},$$

that proves the result. ■

5.3 Numerical examples

This section presents two numerical examples where the method of this chapter is compared to other ones. At each iteration of Algorithm 5.1 the value of J is incremented using the rule $J \leftarrow \lceil 1.05J \rceil$, where $\lceil c \rceil$ is the smallest integer greater than or equal to c. Moreover, the initial set Ω_0 required by Algorithm 5.1 was obtained using the method in [FM16].

5.3.1 Example I

Consider the system given by (96):

$$A_p = \begin{bmatrix} 0 & 1 \\ 1 & 0 \end{bmatrix}, \; B_p = \begin{bmatrix} 0 \\ -5 \end{bmatrix}, \; K_p = \begin{bmatrix} 2.6 & 1.4 \end{bmatrix}, \; \Delta = [0.05, 0.1].$$

Algorithm 5.1 with $J_0 = 20$ and $\bar{i} = 21$ resulted in the estimate of the RAO $\Omega_{\bar{i},x_p}$ shown in Figure 13, which also depicts the estimates obtained with the methods of Chapters 3 and 4 and with the methods in [FG18, SG12]. In this case the application of the approach presented in this chapter has no particular advantage over the one of Chapter 4. Even so, the resulting estimate encompasses the ones of [FG18] and [SG12].

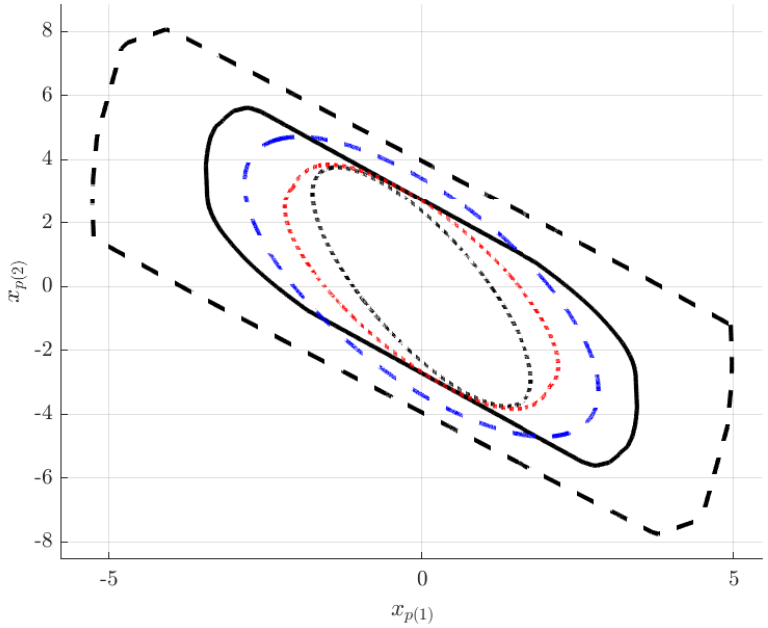

Figure 13: Estimates of the RAO of (96) obtained with the proposed approach (black-continuous) and with the methods of Chapter 3 (blue-dashed), Chapter 4 (black-dashed), [FG18] (red-dotted) and [SG12] (black-dotted).

5.3.2 Example II

Consider the system borrowed from [SG12], where

$$A_p = \begin{bmatrix} 1.1 & -0.6 \\ 0.5 & -1 \end{bmatrix}, \; B_p = \begin{bmatrix} 1 \\ 1 \end{bmatrix}, \; K_p = \begin{bmatrix} -1.7491 & 0.5417 \end{bmatrix}, \; \Delta = [0.5, 2]. \tag{123}$$

Considering $J_0 = 20$ and $\bar{i} = 9$, Figure 14 shows the increasing sequence $\{\Omega_{i,x_p}\}_{i=0}^{\bar{i}}$ of estimates of the RAO, computed from $\{\Omega_i\}_{i=0}^{\bar{i}}$ according to (121). For ease of viewing we performed in the plot the transformation of coordinates $z_p \triangleq T x_p$, where matrix

$$T = \begin{bmatrix} 0.9093 & -0.2792 \\ -0.2792 & 0.1407 \end{bmatrix}$$

corresponds to a contraction in the direction of $[\cos(72^\circ) \;\; \sin(72^\circ)]^T$ by a factor of 20.

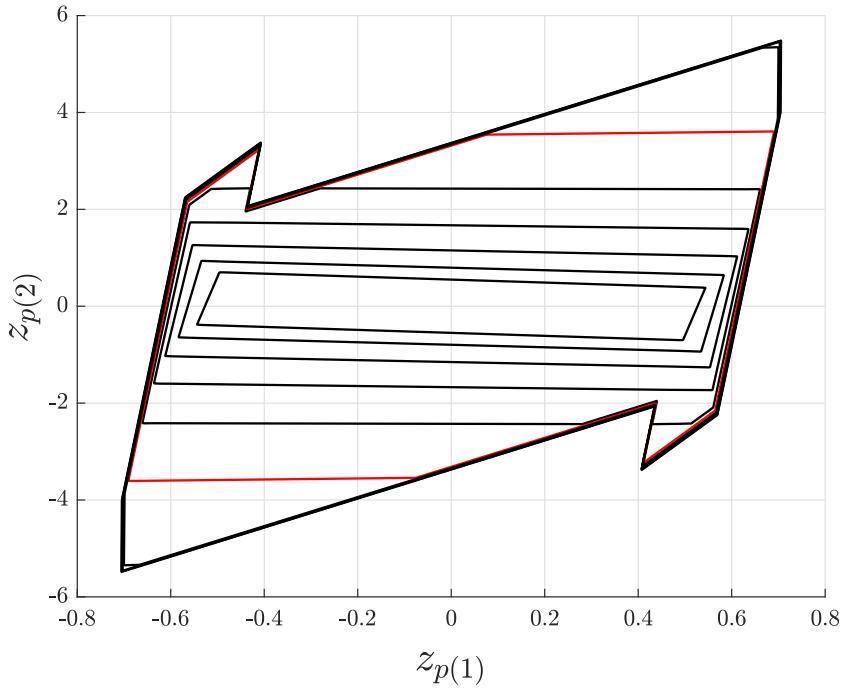

Figure 14: Sequence $\{\Omega_{i,x_p}\}_{i=0}^{9}$, where Ω_{5,x_p} is in red.

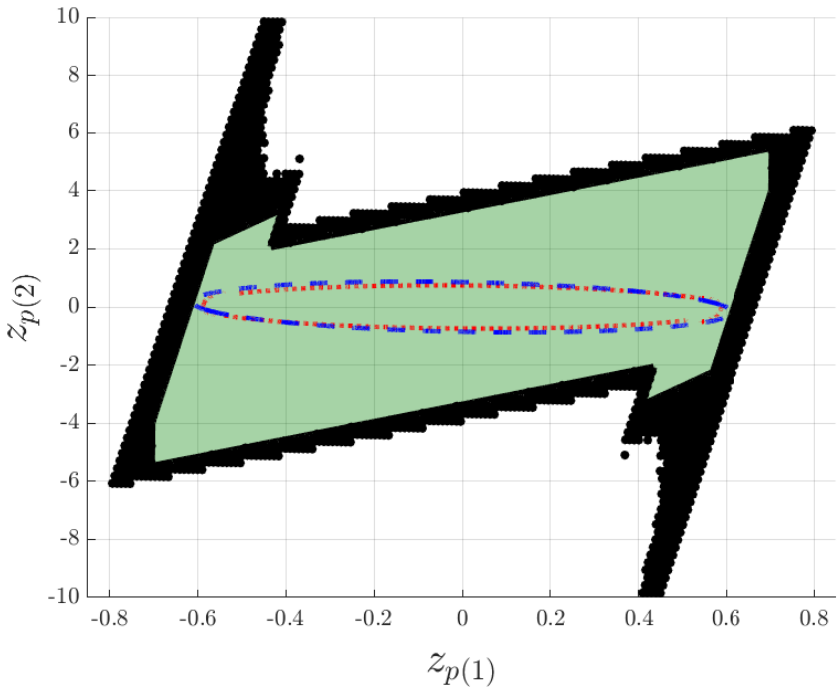

Figure 15: Estimates of the RAO of (123) obtained with the proposed approach (filled in green) and with the methods of Chapter 3 (blue-dashed line) and [FG18] (red-dotted line). A numerically evaluated approximation of the RAO is depicted by black circles.

Notice that Ω_{6,x_p} is considerably close to the last 3 sets of the sequence. However, its

complexity is significantly smaller, since the H-representation of Ω_6 has 154 hyperplanes, while the one of Ω_9 has 302 hyperplanes, which shows the trade-off between number of iterations and complexity.

In Figure 15, the estimate $\Omega_{\bar{i},x_p}$ of the RAO is compared to other ones from the literature. We plotted the piecewise quadratic estimate obtained with the method from [FG18] and the ellipsoidal estimate obtained with the one from Chapter 3. The approach presented here resulted in an estimate of the RAO that encompasses these other two. On the other hand, it was not possible to obtain a valid estimate using the method in [SG12] since the corresponding matrix inequalities are not feasible for this example. Moreover, the stopping criterion of Algorithm 4.1 (which corresponds to the method of Chapter 4) was not satisfied after nearly 3 days of execution on a computer with a `Intel® Core™ i7` processor, i.e. it was not possible to obtain a valid estimate of the RAO using the method of Chapter 4 either.

A numerically evaluated approximation of the RAO is shown in Figure 15 through black circles, where, for each point of a grid of the state space, 2000 trajectories of the closed-loop system starting at it were simulated, considering $\{\delta_k\}_{k\in\mathbb{N}}$ to be a sequence of independent, identically distributed (i.i.d.) random variables with uniform distribution on the interval Δ. As it can be seen, the proposed approach provided a considerably accurate estimate of the RAO (specially if compared to the methods of Chapter 3 and [FG18]).

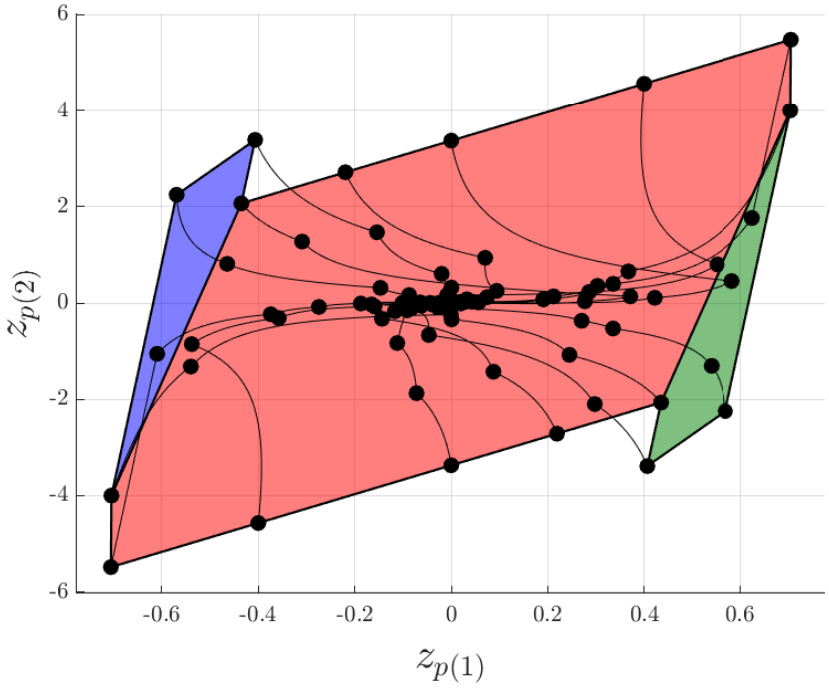

Figure 16: Trajectories starting at the boundary of $\Omega_{\bar{i},x_p}$.

Figure 16 shows several continuous-time trajectories of system (123) with $x_p(0) \in \partial\Omega_{\bar{i},x_p}$ and δ_k randomly chosen in the interval Δ. It should be noticed that the set $\Omega_{\bar{i},x_p}$ is not invariant for the continuous-time system. It is only invariant with respect to the discrete-time trajectory $\{x_p(t_k)\}_{k\in\mathbb{N}}$ that models the behavior of $x_p(t)$ at the sampling instants t_k, represented in the figure by black circles. Nevertheless, it is ensured that for

all initial conditions in $\Omega_{\bar{i},x_p}$ the corresponding continuous-time trajectories converge to the origin.

Figure 16 also shows the division of $\Omega_{\bar{i},x_p}$ in $3^m = 3$ polytopes. Notice that, even if $\Omega_{\bar{i}}$ is convex, $\Omega_{\bar{i},x_p}$ is not convex in general.

5.4 Concluding remarks

A new method to obtain estimates of the RAO of linear aperiodic sampled-data systems subject to input saturation was developed. It relies on the use of a convex embedding of the difference inclusion that models the behavior of the system state between consecutive sampling instants, leading to a computational algorithm based on linear programming only. As shown by the numerical examples, it depends on the case whether or not it will be advantageous to use it instead of other approaches. In the second example, in particular, the proposed method outperformed the ones of [SG12, FG18] and of Chapters 3 and 4.

Compared to the method of Chapter 4, the main advantage of the one presented here is related to the numerical applicability of Algorithm 5.1, where at each iteration a valid estimate of the RAO is generated. Hence, it is possible to manage the trade-off between number of iterations and complexity of the resulting polytope. Algorithm 4.1 of Chapter 4, on the other hand, depends on the satisfaction of a stopping criterion in order to provide a valid estimate of the RAO and there is no guarantee its execution will finish after an acceptable amount of time, as already discussed.

The results in this chapter have been published in [HFG22c].

6 STABILIZATION: POLYHEDRAL APPROACH

In this chapter we consider the system composed by (1),(2) and (5) and focus on the control design problem (Problem 2.2). More precisely, we intend to design a piecewise linear state-feedback control law $f : \mathbb{R}^{n_p} \to \mathscr{U} \subset \mathbb{R}^m$ (where $\mathscr{U}$ represents the set of input constraints) that guarantees the asymptotic stability of the origin and optimizes the size of a polyhedral estimate Ω of the RAO of the resulting closed-loop system. As explained in Section 2.1.2, according to Lemma 2.1, if $f(\cdot)$ is locally Lipschitz at the origin, then Problem 2.2 can be solved considering the equivalent discrete-time uncertain system (12), which is rewritten below:

$$\begin{aligned} x_{p,k+1} &\in \left\{A(\delta)x_{p,k} + B(\delta)f(x_{p,k}) : \ \delta \in \Delta\right\} \\ &\triangleq F(x_{p,k}) \end{aligned} \tag{124}$$

where $x_{p,k} = x_p(t_k)$, $A(\delta) = e^{A_p \delta}$ and $B(\delta) = \int_0^\delta e^{A_p s} \mathrm{d}s B_p$. Therefore, in the next sections we solve the control design problem for (124). It will be useful to consider the controlled version of the difference inclusion above, i.e.

$$\begin{aligned} x_{p,k+1} &\in \left\{A(\delta)x_{p,k} + B(\delta)u_k : \ \delta \in \Delta\right\} \\ &\triangleq G(x_{p,k}, u_k) \end{aligned} \tag{125}$$

where $u_k \in \mathscr{U}$ will be a function of the state, i.e. $u_k = f(x_{p,k})$.

The design of the state feedback can be divided into two steps. The first one, presented in Section 6.1, consists in finding a controlled contractive polyhedral C-set Ω and a corresponding control law $u_k = f(x_{p,k})$ for the difference inclusion

$$x_{p,k+1} \in \left\{A(\delta)x_{p,k} + B(\delta)u_k : \ \delta \in \Delta_J\right\}, \tag{126}$$

where $u_k \in \mathscr{U}$, $J \in \mathbb{N}_+$, $\Delta_J = \{d_j = \tau_m + (j-1)\tau_J : \ j \in \mathbb{N}_J\}$ and $\tau_J = \frac{\tau_M - \tau_m}{J}$. Notice that (126) considers only a finite subset Δ_J with J elements of the interval Δ. Moreover, recall that the definition of Δ_J is also used in the preceding chapters (it appears for the first time in (48)). The second step of the method regards the guarantee that Ω is controlled contractive not only for (126) but also for (125) (not necessarily with the same contraction factor λ). A sufficient condition to ensure this is derived in Section 6.2. At last, in Section 6.3, it will be shown that the obtained set Ω is included in the RAO of the closed-loop system formed by (125) and the designed state feedback $u_k = f(x_{p,k})$. Equivalently, Ω is included in the RAO of (124).

Section 6.4 presents two numerical examples and the chapter ends with some concluding remarks.

6.1 Computation of a controlled contractive set for system (126)

Given a polyhedral C-set Ω and its vertex representation $\Omega = \mathcal{V}_0(V), V \in \mathbb{R}^{n_p \times n_v}$, where the vertices of Ω are represented by columns of V (see (20)), the following result holds.[1]

Lemma 6.1. [BM15, Proposition 7.26] *The polyhedral C-set $\Omega = \mathcal{V}_0(V), V \in \mathbb{R}^{n_p \times n_v}$, is controlled λ-contractive for (126) if and only if there exist $U \in \mathbb{R}^{m \times n_v}$ and nonnegative matrices $Y_j, j \in \mathbb{N}_J$, such that*

$$A(d_j)V + B(d_j)U = VY_j, \quad \forall j \in \mathbb{N}_J \tag{127}$$

$$\mathbf{1}^T Y_j \leq \lambda \mathbf{1}^T, \quad \forall j \in \mathbb{N}_J \tag{128}$$

$$U^{(i)} \in \mathscr{U}, \quad \forall i \in \mathbb{N}_{n_v} \tag{129}$$

where $U^{(i)}$ is the i-th column of U.

The lemma above can be used in order to obtain a controlled λ-contractive P-set Ω for (126). The idea will be to fix *a priori* the number of vertices n_v of $\Omega = \mathcal{V}_0(V)$ and look for a matrix V that satisfies (127)-(129). Since V and Y_j are both variables, constraints (127) are bilinear while (128)-(129) are both linear (since $\mathscr{U}$ is a given polyhedron). In order to optimize the size of $\Omega = \mathcal{V}_0(V)$, we propose the following optimization problem:

$$\max_{V,U,Y_j,\Gamma,L} \sum_{r=1}^{n_r} \Gamma_{(r,r)} w_{(r)} \tag{130}$$

subject to (127) – (129)

$$R\Gamma = VL, \ \mathbf{1}^T L \leq \mathbf{1}^T, \ L \geq 0 \tag{131}$$

$$\Gamma_{(r,r)} \geq \eta, \ \forall r \in \mathbb{N}_{n_r} \tag{132}$$

where $\eta > 0$, $L \in \mathbb{R}^{n_v \times n_r}$, $\Gamma \in \mathbb{R}^{n_r \times n_r}$ is diagonal, $w \in \mathbb{R}^{n_r}$ is a vector of positive weights ($w \geq 0$) for the elements of Γ and $R \in \mathbb{R}^{n_p \times n_r}$ is chosen such that

$$0 \in \mathcal{V}_0(R)^\circ, \tag{133}$$

where $\mathcal{V}_0(R)^\circ$ denotes the interior of $\mathcal{V}_0(R)$.

The columns of R, defined *a priori*, are directions along which the polyhedron Ω will be maximized. Notice that (131) means that each column $\Gamma_{(r,r)} R^{(r)}$ of $R\Gamma$ can be represented as a convex combination of the columns of V and of the zero vector. That is, (131) is equivalent to

$$\Gamma_{(r,r)} R^{(r)} \in \mathcal{V}_0(V) = \Omega, \ \forall r \in \mathbb{N}_{n_r},$$

where $\Gamma_{(r,r)}$ is a scale factor. Consequently, $\mathcal{V}_0(R\Gamma) \subseteq \Omega$. Thus, the optimization problem maximizes a linear combination of the scale factors $\Gamma_{(r,r)}$, where $w_{(r)}$ are positive weights for each factor, i.e. they weight the maximization of Ω along each one of the directions given by the columns of R. Since some of the constraints are bilinear, this is a nonlinear programming problem and, in principle, only a local maximum can be found. On the other hand, it is possible to obtain an initial feasible solution to the constraints using for instance the method presented in [BCM10]. Therefore, the solution of (130) will be at least as good as the one of [BCM10] with respect to the chosen size criterion of the polyhedron.

Moreover, constraints (131), (132) (where η is a relatively small number) and (133) guarantee that $0 \in \Omega^\circ$.

[1] Since Ω has a nonempty interior, $n_v \geq n_p + 1$ by construction.

6.1.1 Design of the control law

Lemma 6.1 gives a necessary and sufficient condition for the λ-contractivity of the polyhedral C-set $\Omega = \mathscr{V}_0(V)$, but does not provide the control law $u_k = f(x_{p,k})$. One of the possible choices of construction of $f(\cdot)$ corresponds to the concept of control "at the vertices" [BM15, Pages 158-159]. Assume without loss of generality that the vertex representation $\Omega = \mathscr{V}_0(V)$ is minimal (otherwise it is possible to discard the redundant columns of matrix V and the corresponding ones of matrix U). The idea is to interpolate the control value at the vertices as follows:

a) For any pair $(V^{(i)}, U^{(i)})$ of columns of V and U (defined in the statement of the Lemma 6.1), $f(V^{(i)}) = U^{(i)}$;

b) for $x_{p,k} \in \Omega$, $f(x_{p,k}) = U\alpha$, where $\alpha \in \mathbb{R}^{n_v}$ is such that

$$\begin{cases} x_{p,k} = V\alpha, \\ \mathbf{1}^T\alpha = \Psi_\Omega(x_{p,k}), \\ \alpha \geq 0. \end{cases}$$

This control law can be constructed as described next [BM15]. Firstly, Ω can be partitioned into simplices[2] formed by n_p vertices and the origin:

$$\Omega^l \triangleq \{x_p = \bar{V}^l\bar{\alpha} : \ \bar{\alpha} \geq 0, \ \mathbf{1}^T\bar{\alpha} \leq 1, \ \bar{\alpha} \in \mathbb{R}^{n_p}\} \tag{134}$$

where $\bar{V}^l$ is a matrix formed by the n_p columns of V corresponding to the l-th simplex (to be not confused with $V^{(l)}$). We also denote as $\bar{U}^l$ the n_p columns of U that correspond to the selected columns of V. Each simplex generates a polyhedral cone as follows:

$$C^l \triangleq \{x_p = \bar{V}^l\bar{\alpha} : \ \bar{\alpha} \geq 0, \ \bar{\alpha} \in \mathbb{R}^{n_p}\}. \tag{135}$$

The sets above can be chosen such that (see a sketch in Figure 17):

- Ω^l and C^l have non-empty interiors;
- $\Omega^l \bigcap \Omega^h$ and $C^l \bigcap C^h$ have empty interiors for $l \neq h$;
- $\bigcup_l \Omega^l = \Omega$ and $\bigcup_l C^l = \mathbb{R}^{n_p}$.

Then, the piecewise linear control law below is Lipschitz continuous, guarantees the λ-contractivity of Ω and satisfies the constraint $u_k \in \mathscr{U}$ and properties a) and b) above [BM15]:

$$u_k = f(x_{p,k}) \triangleq F^l x_{p,k} \triangleq \bar{U}^l(\bar{V}^l)^{-1}x_{p,k}, \quad x_{p,k} \in \Omega^l, \tag{136}$$

where the inverse of $\bar{V}^l$ exists because Ω^l has a non-empty interior. Notice that (136) satisfies property b), indeed. To see this, assume that simplex 1 (for the other simplices the same considerations apply) Ω^1 is generated by the first n_p columns $\bar{V}^1$ of $V = [\bar{V}^1 \ \tilde{V}]$. Then, if $x_{p,k} \in \Omega^1$,

$$x_{p,k} = \bar{V}^1\bar{\alpha} = \begin{bmatrix} \bar{V}^1 & \tilde{V} \end{bmatrix} \begin{bmatrix} \bar{\alpha} \\ 0 \end{bmatrix} = V\alpha,$$

where $\bar{\alpha} \in \mathbb{R}^{n_p}$, $\bar{\alpha} \geq 0$, $\mathbf{1}^T\bar{\alpha} = \Psi_\Omega(x_{p,k})$ and $\alpha \triangleq [\bar{\alpha}^T \ 0^T]^T \in \mathbb{R}^{n_v}$. It follows that

$$u_k = F^1 x_{p,k} = \bar{U}^1(\bar{V}^1)^{-1}\bar{V}^1\bar{\alpha} = \bar{U}^1\bar{\alpha} = \begin{bmatrix} \bar{U}^1 & \tilde{U} \end{bmatrix} \begin{bmatrix} \bar{\alpha} \\ 0 \end{bmatrix} = U\alpha.$$

[2] A simplex (plural: simplices or simplexes) is the simplest kind of polytope with nonempty interior. In $\mathbb{R}^{n_p}$ it corresponds to the convex hull of $n_p + 1$ affinely independent points.

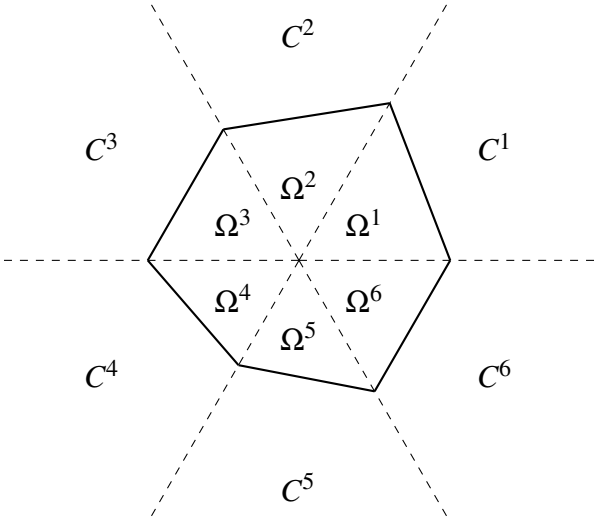

Figure 17: Partitions of $\Omega = \bigcup_{l=1}^{6} \Omega^l$ and of $\mathbb{R}^2 = \bigcup_{l=1}^{6} C^l$.

6.2 Testing contractivity

The second step of the method consists in verifying if the control law (136) guarantees the contractivity of Ω for (125), which takes into account all possible values for $\delta_k \in \Delta$ and not only the finite set Δ_J.

Theorem 6.1. *Consider a controlled λ-contractive polyhedral C-set Ω for (126) and the corresponding control law (136). If*

$$\theta(\Omega, J, \lambda) \triangleq \lambda + c_1(J) k_2 k_3(\Omega) c_4(\Omega) < 1, \tag{137}$$

where

$$c_1(J) = \begin{cases} \dfrac{e^{\mu(A_p)\tau_J} - 1}{\mu(A_p)} & \text{if } \mu(A_p) \neq 0, \\ \tau_J & \text{if } \mu(A_p) = 0, \end{cases}$$

$$c_4(\Omega) = \Psi_\Omega(\mathscr{B})$$

(already defined in the statement of Theorem 4.2) and

$$k_2 \triangleq \max\left(e^{\mu(A_p)\tau_m}, e^{\mu(A_p)\tau_M}\right), \; k_3(\Omega) \triangleq \max_{x_p \in \Omega} \left\| A_p x_p + B_p f(x_p) \right\|,$$

then:

a) Ω is controlled $\theta(\Omega, J, \lambda)$-contractive for (125);

b) The control law (136) guarantees the $\theta(\Omega, J, \lambda)$-contractivity of Ω for (125) (equivalently, Ω is $\theta(\Omega, J, \lambda)$-contractive for (124), which represents the closed loop composed by (125) and (136)).

Proof: We will prove items a) and b) simultaneously. We have to show that $x_{p,k+1}$ given by (125) with u_k given by (136) satisfies

$$\Psi_\Omega(x_{p,k+1}) \leq \theta(\Omega, J, \lambda), \quad \forall x_{p,k} \in \Omega, \; \forall \delta_k \in \Delta.$$

Given $x_{p,k} \in \Omega, \delta_k \in \Delta$, there exist $d_k \in \Delta_J$ and $\tau_k \in [0, \tau_J]$ such that $\delta_k = d_k + \tau_k$. From Lemma 4.5, the following identity holds for all $(x_p, u, d, \tau) \in \mathbb{R}^{n_p+m+2}$:

$$A(d+\tau)x_p + B(d+\tau)u = A(d)x_p + B(d)u + \Phi(\tau)e^{A_p d}(A_p x_p + B_p u).$$

Using the relation above, one has:

$$\begin{aligned} x_{p,k+1} &= A(d_k+\tau_k)x_{p,k} + B(d_k+\tau_k)f(x_{p,k}) \\ &= \underbrace{A(d_k)x_{p,k} + B(d_k)f(x_{p,k})}_{\triangleq y_{k+1}} + \underbrace{\Phi(\tau_k)e^{A_p d_k}(A_p x_{p,k} + B_p f(x_{p,k}))}_{\triangleq z_{k+1}} \end{aligned} \tag{138}$$

From the fact that $u_k = f(x_{p,k})$ given by (136) assures the λ-contractivity of Ω for (126), $d_k \in \Delta_J$ and $x_{p,k} \in \Omega$, it follows that

$$\Psi_\Omega(y_{k+1}) \leq \lambda. \tag{139}$$

Since $\tau_k \in [0, \tau_J]$, we also know that (see (87)):

$$\|\Phi(\tau_k)\| \leq c_1(J).$$

Moreover, considering that $\|e^{A_p s}\| \leq e^{\mu(A_p)s}$ for all $s \geq 0$ (see [Van77]), one has:

$$\left\|e^{A_p d_k}\right\| \leq \max\left(e^{\mu(A_p)\tau_m}, e^{\mu(A_p)\tau_M}\right) = k_2.$$

Using the inequalities above we conclude that

$$\|z_{k+1}\| \leq \|\Phi(\tau_k)\| \left\|e^{A_p d_k}\right\| \left\|A_p x_{p,k} + B_p f(x_{p,k})\right\| \leq c_1(J)k_2 k_3(\Omega),$$

i.e. $z_{k+1} \in c_1(J)k_2k_3(\Omega)\mathscr{B}$. Then, from (138), (139) and the properties in Lemma 2.2, we get that

$$\Psi_\Omega(x_{p,k+1}) \leq \Psi_\Omega(y_{k+1}) + \Psi_\Omega(z_{k+1}) \leq \lambda + c_1(J)k_2k_3(\Omega)\Psi_\Omega(\mathscr{B}) = \theta(\Omega, J, \lambda),$$

as we wanted to show. ■

Notice that $J \in \mathbb{N}_+$ can be freely chosen by the user of the method. Thus, if (137) is not satisfied for some value of J, we recommend to increment it (as it is done in the other chapters) and to recompute the solution of (130).

The constant $k_3(\Omega)$ can be obtained, in practice, as follows:

$$k_3(\Omega) = \max_i \left\|A_p V^{(i)} + B_p U^{(i)}\right\|.$$

To see why, notice that, given arbitrary $x_p \in \Omega$, property b) of $f(\cdot)$ guarantees the existence of $\alpha \in \mathbb{R}^{n_v}, \alpha \geq 0$, $\mathbf{1}^T\alpha = \Psi_\Omega(x_p) \leq 1$, such that

$$\begin{bmatrix} x_p \\ f(x_p) \end{bmatrix} = \begin{bmatrix} V \\ U \end{bmatrix} \alpha.$$

Then

$$\begin{aligned} \left\|A_p x_p + B_p f(x_p)\right\| &= \left\|(A_p V + B_p U)\alpha\right\| = \left\|\sum_{i=1}^{n_v} (A_p V + B_p U)\alpha_{(i)} e_i\right\| \\ &= \left\|\sum_{i=1}^{n_v} \alpha_{(i)}(A_p V^{(i)} + B_p U^{(i)})\right\| \leq \sum_{i=1}^{n_v} \alpha_{(i)} \left\|A_p V^{(i)} + B_p U^{(i)}\right\| \\ &\leq \left(\sum_{i=1}^{n_v} \alpha_{(i)}\right) \max_i \left\|A_p V^{(i)} + B_p U^{(i)}\right\| \leq \max_i \left\|A_p V^{(i)} + B_p U^{(i)}\right\| = k_3(\Omega), \end{aligned}$$

where e_i is the i-th canonical base vector of the Euclidean space and

$$\sum_{i=1}^{n_v} \alpha_{(i)} \leq 1 \;\text{ since }\; \mathbf{1}^T \alpha = \Psi_\Omega(x_p) \leq 1.$$

6.3 Stability of the closed-loop system

We know from the preceding discussion that, if the P-set Ω and the corresponding control law (136) obtained in Section 6.1 satisfy the condition of Theorem 6.1, then Ω is θ-contractive for (124) with $f(x_{p,k})$ given by (136). From the piecewise linear structure of (136) and the shape of the simplices Ω^l, the control law is positively homogeneous of order 1 inside Ω, i.e.

$$f(cx_p) = cf(x_p),\ \forall x_p \in \Omega,\ \forall c \in [0,1].$$

Thus, it follows that the closed-loop system (124) satisfies

$$F(cx_p) = cF(x_p),\ \forall x_p \in \Omega,\ \forall c \in [0,1].$$

Applying Corollary 2.1 (with λ replaced by θ), we conclude that all trajectories $\{x_{p,k}\}_{k\in\mathbb{N}}$ of (124) have the following property:

$$x_{p,k} \in \varepsilon\Omega \;\Rightarrow\; x_{p,k+m} \in \theta^m \varepsilon\Omega, \quad \forall \varepsilon \in [0,1],\ \forall m \in \mathbb{N},$$

that is, the origin of (124) is asymptotically stable and Ω is included in its region of attraction. This is also true for the continuous-time system composed by (1) and (2) with $f(x_p(t_k))$ given by (136), as explained at the beginning of the chapter.

6.4 Numerical examples

Two numerical examples are presented next to validate the proposed method.

6.4.1 Example I

Consider system (1),(2),(5) with

$$A_p = \begin{bmatrix} 0 & 1 \\ 1 & 0 \end{bmatrix},\ B_p = \begin{bmatrix} 0 \\ -5 \end{bmatrix},\ \Delta = [0.05, 0.1],$$

where $\mathscr{U} = \{u \in \mathbb{R} :\ \|u\|_\infty \leq 1\}$. Problem (130) was solved using the KNITRO toolbox [BNW06] and considering $n_v = 10,\ \lambda = 0.99,\ J = 50$ and $w = \mathbf{1}$. The columns of R, i.e. the directions along which the polyhedron is maximized, correspond to the elements of the following set:

$$\left\{ \begin{bmatrix} \cos(\theta) \\ \sin(\theta) \end{bmatrix} : \theta = \frac{(q-1)\pi}{24}, q \in \mathbb{N}_{48} \right\}.$$

The resulting $\theta(\Omega, J, \lambda)$-contractive polyhedron Ω is shown in Figure 18, where $\theta \cong 0.999$. Notice that, even if $n_v = 10$, Ω has only 6 vertices (there are 4 redundant columns in the vertex representation $\Omega = \mathscr{V}_0(V)$). This set belongs to the RAO of the closed-loop system with the piecewise linear control law (136), whose gains are presented in Table 1. The corresponding simplices are depicted in Figure 19.

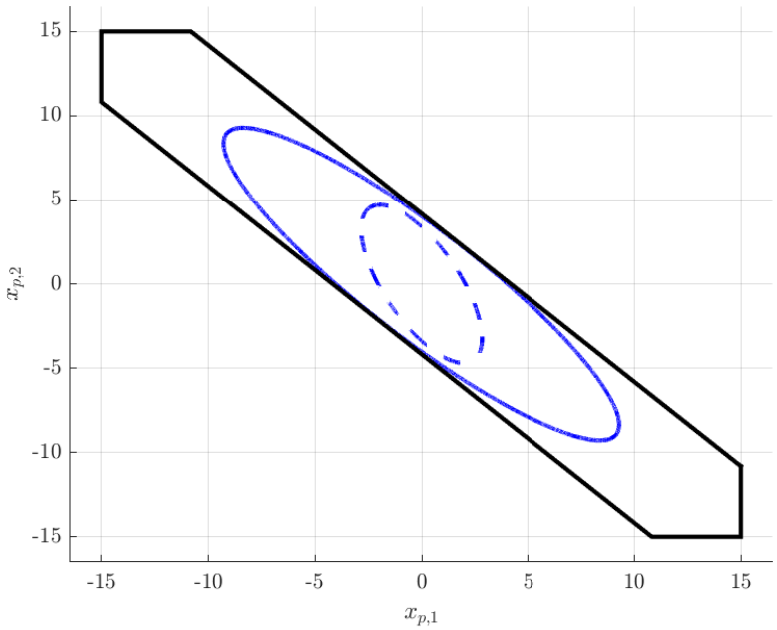

Figure 18: Estimates of the RAO of the closed-loop system considering (136) and the proposed method (black-continuous) and considering the linear saturated control (3) and the method of Chapter 3 (blue-dashed for $K_p = [2.6\ 1.4]$ and blue-continuous for $K_p = [1.13\ 0.94]$).

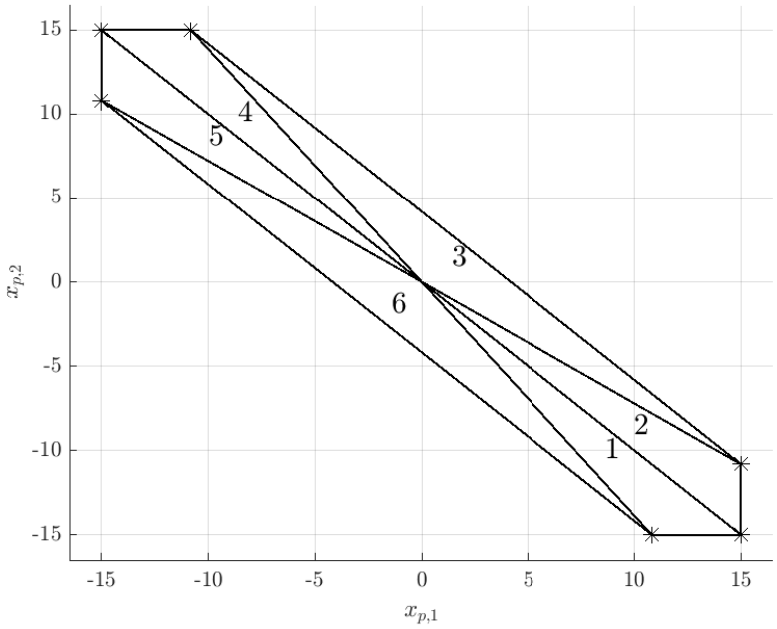

Figure 19: Partition of Ω into simplices for Example I.

For comparison purposes, we also show in Figure 18 the estimates of the RAO of the closed-loop system with the linear saturated control law (3) obtained with the control

design method of Chapter 3, which considers quadratic Lyapunov functions. The gains $K_p = [2.6\ 1.4]$ and $K_p = [1.13\ 0.94]$ are the ones considered in that chapter. As it can be seen, the method presented in Chapter 6 was able to provide a feedback control law of low complexity for which the corresponding estimate of the RAO of the closed-loop system contains the estimates obtained with the method of Chapter 3 considering a linear saturated state feedback.

Table 1: Feedback gains of the piecewise linear control law (136) for Example I.

Simplex	F^l	Simplex	F^l
1	[0.0064464 0.071316]	4	[0.0081126 0.072518]
2	[0.40709 0.47196]	5	[0.40589 0.4703]
3	[0.23921 0.23921]	6	[0.23921 0.23921]

In Figure 20, the trajectories with $x_p(0)$ at the vertices of Ω and considering (136) with δ_k randomly chosen in the interval Δ are shown. As expected, the convergence of the trajectories to the origin is ensured showing that Ω is indeed included in its region of attraction.

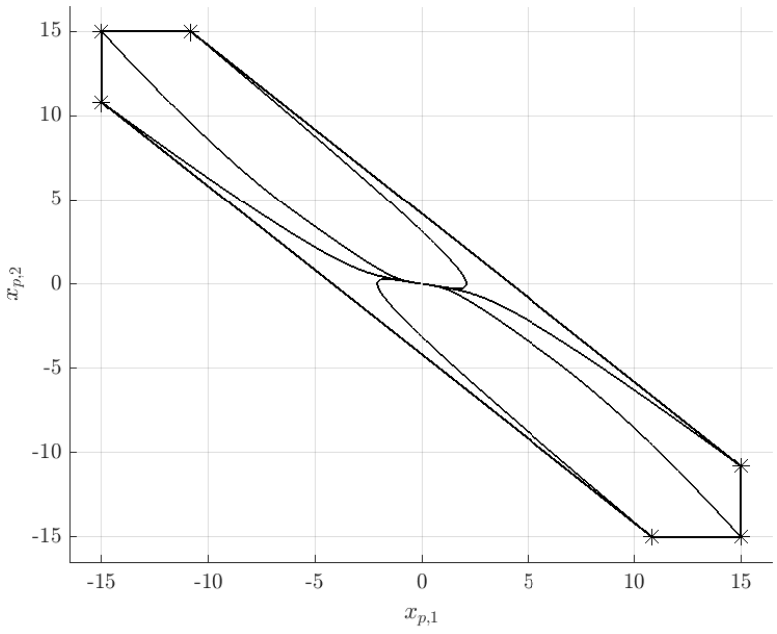

Figure 20: Trajectories starting at the vertices of Ω for Example I.

6.4.2 Example II

Consider system (1),(2),(5) with

$$A_p = \begin{bmatrix} 1 & 0 \\ 0 & 0.2 \end{bmatrix}, \ B_p = \begin{bmatrix} 1 \\ 1 \end{bmatrix}, \ \Delta = [0.05, 0.1],$$

and the set $\mathscr{U} = \{u \in \mathbb{R} : \ |u| \leq 1\}$. Problem (130) was solved considering

$$n_v = 10, \ \lambda = 0.98, \ J = 20 \text{ and } w = \mathbf{1}.$$

The chosen columns of R are the same as in the previous example.

The resulting $\theta(\Omega, J, \lambda)$-contractive polyhedron Ω is shown in Figure 21, where

$$\theta \cong 0.996.$$

This set belongs to the RAO of the closed-loop system with the piecewise linear control law (136), whose gains are presented in Table 2.

For comparison purposes we show again (in Figure 21) the estimate of the RAO of the closed-loop system with the linear saturated control law (3) obtained with the control design method presented in Chapter 3. As it can be seen, the approach of this chapter was able to provide a feedback control law for which the corresponding estimate of the RAO of the closed-loop system is considerably larger than the estimate obtained with the other method considering a linear saturated state feedback. If we replace the number of vertices $n_v = 10$ by $n_v = 20$, then the resulting polyhedron includes the latter estimate, as it is also shown in Figure 21.

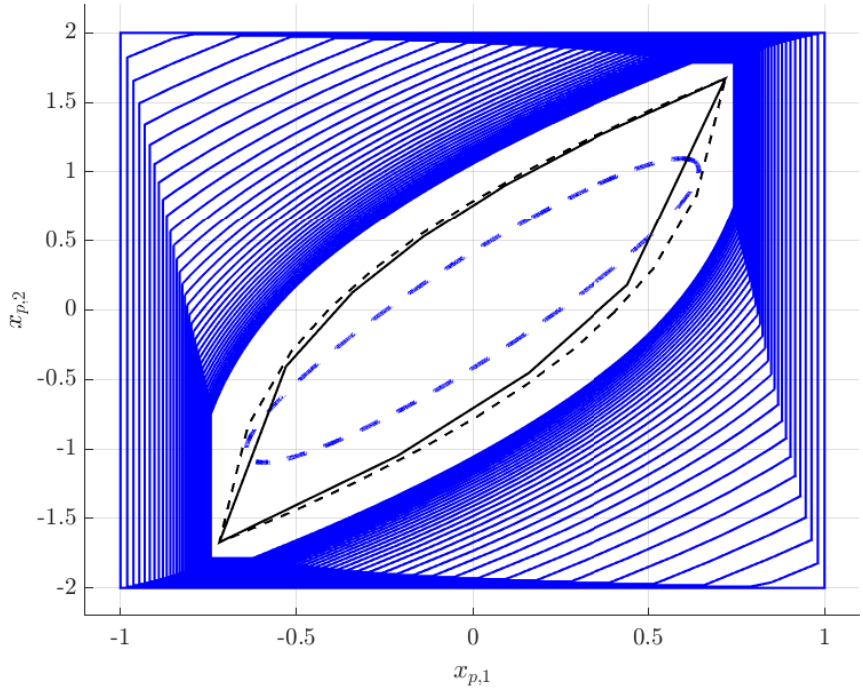

Figure 21: Estimates of the RAO of the closed-loop system considering (136) and the proposed method (black-continuous for $n_v = 10$ and black-dashed for $n_v = 20$) and considering the linear saturated control (3) and the method of Chapter 3 (blue-dashed for $K_p = [-10.70\ 4.38]$). Outer approximations of the maximal controlled λ-contractive C-set for (126) in blue-continuous.

Moreover, Figure 21 depicts a decreasing sequence of outer approximations of the maximal controlled λ-contractive C-set for (126) (with $J = 20,\ \lambda = 0.98$) obtained with the method proposed in [Bla94]. By visual inspection it is possible to have an idea about the conservatism of our method. Notice that the obtained set Ω is an inner approximation (of low complexity) of the maximal controlled λ-contractive C-set for (126). Furthermore, we guarantee that Ω also is controlled contractive for (125) applying the result of Theorem 6.1.

The division of the polyhedron Ω into simplices is illustrated in Figure 22.

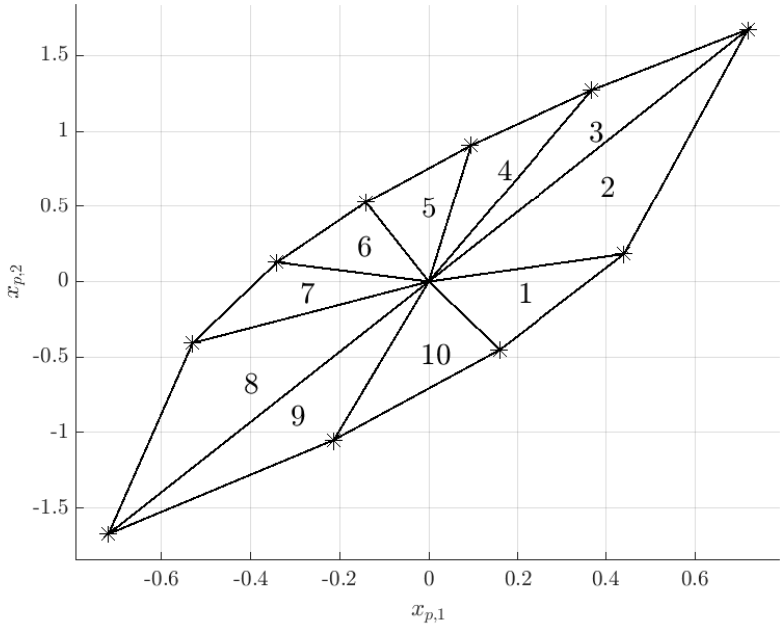

Figure 22: Partition of Ω into simplices for Example II.

Figure 23 is analogous to Figure 20, that is, it shows several trajectories of the closed-loop system with $x_p(0)$ at the boundary of Ω and with δ_k randomly chosen in the interval Δ. As expected, the trajectories converge to the origin.

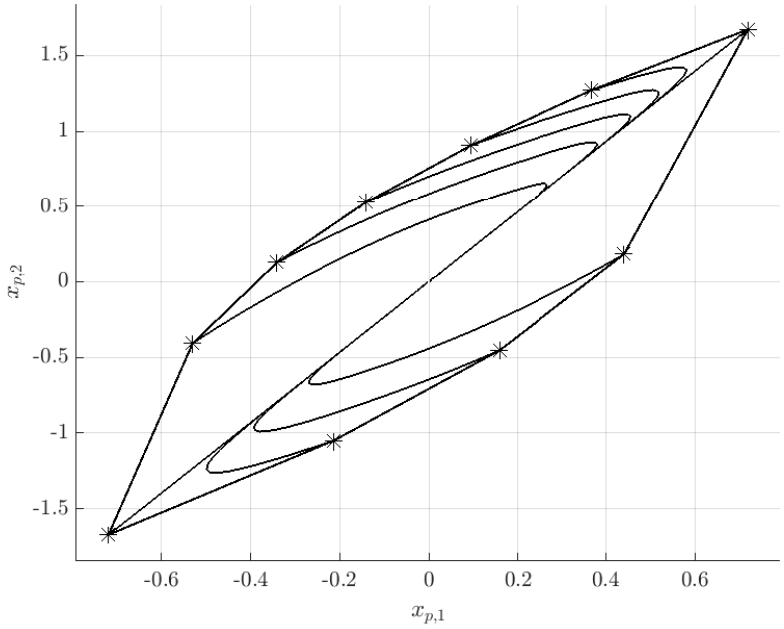

Figure 23: Trajectories starting at the vertices of Ω for Example II.

Table 2: Feedback gains of the piecewise linear control law (136) for Example II.

Simplex	F^l	Simplex	F^l
1	[-2.7763 1.23]	6	[-2.4724 1.2333]
2	[-2.4569 0.45893]	7	[-2.5903 0.91817]
3	[-9.8438 3.6367]	8	[-2.1301 0.31834]
4	[-1.712 1.2823]	9	[-6.8346 2.3422]
5	[-2.1273 1.3258]	10	[-2.2615 1.4124]

6.5 Concluding remarks

The problem of stabilization of aperiodic sampled-data linear systems subject to input constraints was tackled using a polyhedral framework. The proposed method finds a polytope of fixed complexity which is controlled contractive for the dynamics of the system between two consecutive sampling instants. From this polytope it is possible to derive a feedback control law for the system. Among the different existing approaches to do that (e.g. [BM15]), we chose to construct a piecewise linear control law. As explained at the beginning of the chapter, the obtained polytope is included in the RAO of the continuous-time plant in closed loop with the computed sampled-data control law. Even if, in principle, only a local optimum will be found for the optimization problem on which the method relies, numerical examples show the efficiency of the resulting feedback control, for which the corresponding estimates of the RAO were larger than the ones obtained with the method presented in Chapter 3 considering linear saturated feedback control laws.

As a future work, it would be possible to analyze the numerical issues related to the solution of (130), which depends on bilinear constraints, specially for systems of higher dimension. It would also be interesting to consider the case where the system dynamics is subject to additive disturbances.

The results in this chapter have been published in [HFG21].

7 STABILIZATION IN A STOCHASTIC FRAMEWORK

As explained in the Introduction, a common feature of the preceding chapters is that they consider a *non-stochastic framework*, where hard bounds are imposed for the sampling interval of the system. This assumption, however, can be quite conservative in some cases. Thus, the aim of the present chapter (and of the paper to be submitted [HFG22a]) is to consider a *stochastic framework*, where the sampling intervals are assumed to be random variables with the Erlang distribution. As it will be shown, this distribution allows to model sampling intervals whose probability density function has unbounded support and is concentrated around a value, which may represent the nominal sampling interval of the system in the ideal case where there is no uncertainties. Moreover, the Poisson sampling process, considered in detail in [HFG22b], corresponds to a particular case, as it will also be discussed in this chapter.

The stochastic framework in this chapter leads to quite different theoretical developments, which are based on the theory of SHSs (stochastic hybrid systems) or, more precisely, PDMPs (Piecewise Deterministic Markov Processes). The aim of the proposed method is to provide convex conditions for the global stabilization in the mean square sense of the closed-loop sampled-data system, where the control input is subject to a sector bounded nonlinearity. Moreover, the possibility of packet dropouts is explicitly taken into account and modeled through a Bernoulli distribution.

The chapter is organized as follows. Section 7.1 presents basic definitions and proposes an equivalent SHS representation for the closed-loop sampled-data system. Section 7.2 presents the main results related to the control design method. Section 7.3 shows some numerical examples. At last, some concluding remarks end the chapter.

7.1 Problem Formulation

Consider the linear model (1), recalled here for ease of reference:

$$\dot{x}_p(t) = A_p x_p(t) + B_p u(t) \tag{140}$$

where $x_p \in \mathbb{R}^{n_p}$ and $u \in \mathbb{R}^m$ are the state and the input of the plant, respectively. The control input is updated at the sampling instants t_k and kept constant (by means of a zero-order-hold) for all $t \in [t_k, t_{k+1})$ according to the law:

$$\begin{aligned} u(t) &= u(t_k), \text{ for } t \in [t_k, t_{k+1}) \\ u(t_k) &= \begin{cases} \phi(K_p x_p(t_k^-) + K_u u(t_k^-)), & \text{if no packet dropout} \\ u(t_k^-), & \text{otherwise} \end{cases} \end{aligned} \tag{141}$$

where K_p and K_u are matrices of appropriate dimensions and $\phi : \mathbb{R}^m \to \mathbb{R}^m$ denotes an actuator nonlinearity (e.g. saturation, deadzone, quantization, etc.). Note in (141) that

$u(t)$ is updated at time t_k only if the corresponding packet of measurement data from the sensors is not lost due to some misbehavior of the control network, otherwise the controller maintains the current input until the next sampling instant t_{k+1}. It is assumed that ϕ is decentralized, i.e.

$$\phi(\zeta) = [\phi_1(\zeta_{(1)})\ \phi_2(\zeta_{(2)})\ \dots\ \phi_m(\zeta_{(m)})],\ \zeta \in \mathbb{R}^m, \tag{142}$$

and satisfies a sector condition (see the List of Symbols):

$$\phi_i(\cdot) \in \operatorname{sec}[\underline{d}_i, \bar{d}_i], \quad \forall i \in \mathbb{N}_m. \tag{143}$$

Note that (141) is based not only on the sampled value of the state x_p, but also on the value of the last control input applied to the plant, where the use of the term $K_u u(t_k^-)$ has already showed its benefits in Chapter 3, which considers a non-stochastic framework. The probability of packet dropout is $\mu_0 \in (0,1)$ for all t_k and the events of packet dropout for each t_k are mutually independent between them.

We recall that by convention $t_0 = 0$ and that the sampling interval is denoted by $\delta_k = t_{k+1} - t_k$. It is assumed that $\{\delta_k\}_{k\in\mathbb{N}}$ is a sequence of i.i.d. random variables with the Erlang distribution (see details, for instance, in [PP02, Pgs. 87-89]) of *degree* $\nu \in \mathbb{N}_+$ and *rate* $\lambda \in \mathbb{R}_+$, i.e. $\delta_k \sim \mathtt{E}(\nu,\lambda)$. The corresponding probability density function in this case is given by [PP02, Pg. 87]:

$$f_\delta(s) \triangleq \begin{cases} \dfrac{\lambda^\nu s^{\nu-1} e^{-\lambda s}}{(\nu-1)!}, & s \geq 0, \\ 0, & \text{otherwise.} \end{cases} \tag{144}$$

The Erlang distribution has been successfully used to model the stochastic behavior of networked control systems under random sampling in [STWH17]. As illustrated in Figure 24, it allows to model an event whose probability density function is concentrated around a value, which may represent the nominal sampling interval of the system in the ideal case where there is no uncertainties. In particular, note that the mean and the variance of the sampling interval $\delta_k \sim \mathtt{E}(\nu,\lambda)$ are, respectively, ν/λ and ν/λ^2. Moreover, the exponential distribution, considered for instance in [TCL18] and [HFG22b], is a particular case for $\nu = 1$, as it can be seen from (144), see also Figure 24.

It will be convenient to define $\underline{D} \triangleq \operatorname{Diag}(\underline{d}_1,\dots,\underline{d}_m)$, $\overline{D} \triangleq \operatorname{Diag}(\overline{d}_1,\dots,\overline{d}_m)$, $D \triangleq \overline{D} - \underline{D}$ and $\bar{\phi}(\zeta) \triangleq \phi(\zeta) - \underline{D}\zeta$. From these definitions and (143), the i-th component of the nonlinearity $\bar{\phi}$ belongs to the sector $\operatorname{sec}[0, \overline{d}_i - \underline{d}_i]$. In other words, $\bar{\phi}$ satisfies the following sector condition, adapted from [TGGQ11, Lemma 1.4].

Lemma 7.1. *Given a diagonal matrix $T \in \mathbb{R}^{m\times m}, T \succeq 0$,*

$$\bar{\phi}^T(\zeta) T (D\zeta - \bar{\phi}(\zeta)) \geq 0,\ \forall \zeta \in \mathbb{R}^m. \tag{145}$$

Consider now $x = [x_p^T\ u^T]^T \in \mathbb{R}^n,\ n = n_p + m$. The dynamics (140)-(141) can be described by the following impulsive system, where the packet dropouts are modeled by a Bernoulli process $\{\alpha_k\}_{k\in\mathbb{N}_+}$ (i.e. a sequence of i.i.d. Bernoulli random variables) with $P[\alpha_k = 0] = \mu_0$ and $P[\alpha_k = 1] = \mu_1 \triangleq 1 - \mu_0$, where $\alpha_k = 0$ means that a packet dropout occurs:

$$\dot{x}(t) = A_c x(t), \qquad \forall t \geq 0,\ t \neq t_k,\ \forall k \in \mathbb{N}_+ \tag{146a}$$

$$x(t_k) = \begin{cases} g(x(t_k^-)), & \text{if } \alpha_k = 1, \\ x(t_k^-), & \text{if } \alpha_k = 0, \end{cases} \qquad \forall k \in \mathbb{N}_+ \tag{146b}$$

$$g(x) \triangleq A_d x + B_r \bar{\phi}(Kx) \tag{146c}$$

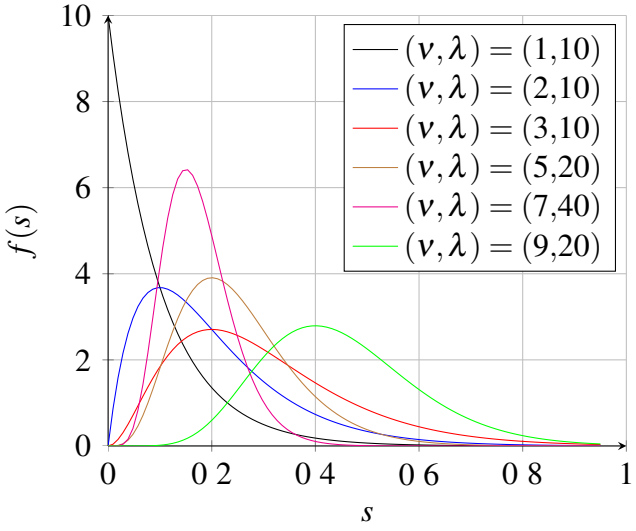

Figure 24: Probability density function (144) of the Erlang distribution for different values of the parameters ν and λ.

where $x(0) = x_0 \in \mathbb{R}^n$, $A_d \triangleq A_r + B_r \underline{D} K$ and, cf. also (10) and (44):

$$A_c = \begin{bmatrix} A_p & B_p \\ 0 & 0 \end{bmatrix} \in \mathbb{R}^{n\times n}, \quad A_r = \begin{bmatrix} I_{n_p} & 0 \\ 0 & 0 \end{bmatrix} \in \mathbb{R}^{n\times n},$$
$$B_r = \begin{bmatrix} 0 \\ I_m \end{bmatrix} \in \mathbb{R}^{n\times m}, \qquad K = \begin{bmatrix} K_p & K_u \end{bmatrix} \in \mathbb{R}^{m\times n}.$$

Definition 7.1. *The equilibrium point $x = 0$ of (146) is mean exponentially stable (MES) if there exist constants $c, \gamma > 0$ such that for every initial condition $x_0 \in \mathbb{R}^n$:*

$$\mathbb{E}[\|x(t)\|^2] \leq ce^{-\gamma t}\|x_0\|^2, \ \forall t \geq 0 \tag{147}$$

where $\gamma > 0$ will be referred to as a decay rate of the trajectories of the system.

From Markov's inequality [Dav93, Pg. 12],

$$P[\|x(t)\| > r] \leq \frac{\mathbb{E}[\|x(t)\|^2]}{r^2},$$

that is, the decay rate corresponds to a measure of how fast the probability of $\|x(t)\|$ being large decays with time.

The problem we focus on in this chapter can now be stated.

Problem 7.1 (Mean square exponential stabilization)**.** *Given the parameters μ_0, ν and λ, provide convex conditions for the design of the feedback gain K such that the resulting closed-loop system (146) is MES.*

7.1.1 Equivalent SHS representation

Next we present a SHS representation for (146), where we use the fact that a Erlang-distributed random variable $X \sim \mathtt{E}(\nu,\lambda)$ of degree ν is statistically equivalent to the sum of ν mutually independent exponentially distributed random variables $X_i \sim \mathtt{E}(1,\lambda)$, i.e. (cf. [Bil95, Exercise 23.2]):

$$X \sim \sum_{i=1}^{\nu} X_i. \tag{148}$$

This feature will be important to derive convex conditions for the stabilization of the closed-loop system.

Consider the augmented state $(q,x) \in \mathbb{N}_\nu \times \mathbb{R}^n$ and a sequence $\{\theta_k\}_{k\in\mathbb{N}_+}$ with the same distribution of $\{\alpha_k\}_{k\in\mathbb{N}_+}$. Consider also a sequence $\{r_k\}_{k\in\mathbb{N}}$ of *reset* (or *jump*) *times*, with $r_0 = 0$, for the proposed SHS model given by:

$$(\dot{q}(t),\dot{x}(t)) = (0,\, A_c x(t)), \qquad \forall t \geq 0,\ t \neq r_k,\ \forall k \in \mathbb{N}_+ \tag{149a}$$

$$(q(r_k),x(r_k)) = \Psi(q(r_k^-),x(r_k^-),\theta_k), \qquad \forall k \in \mathbb{N}_+ \tag{149b}$$

$$\Psi(q,x,\theta) \triangleq \begin{cases} (q+1,x), & \text{if } q < \nu \\ (1,g(x)), & \text{if } (q,\theta) = (\nu,1) \\ (1,x), & \text{if } (q,\theta) = (\nu,0) \end{cases} \tag{149c}$$

where $(q_0,x_0) \triangleq (q(0),x(0))$ and $\{\rho_k\}_{k\in\mathbb{N}} \triangleq \{r_{k+1} - r_k\}_{k\in\mathbb{N}}$ is a sequence of i.i.d. random variables with $\rho_k \sim \mathrm{E}(1,\lambda)$ exponentially distributed, i.e. the *counting process*

$$N_t \triangleq \sup\{k \in \mathbb{N} :\ r_k \leq t\} \tag{150}$$

is a Poisson process [Dav93, Pg. 37],[PP02, Pg. 378] of rate $\lambda > 0$, for which

$$P[N_t = n] = e^{-\lambda t}\frac{(\lambda t)^n}{n!}.$$

Moreover, since ρ_k has the exponential distribution [PP02, Pg. 88]:

$$F_\rho(s) \triangleq P[\rho_k \leq s] = 1 - e^{-\lambda s}, \quad \forall k \in \mathbb{N},\ \forall s \geq 0. \tag{151}$$

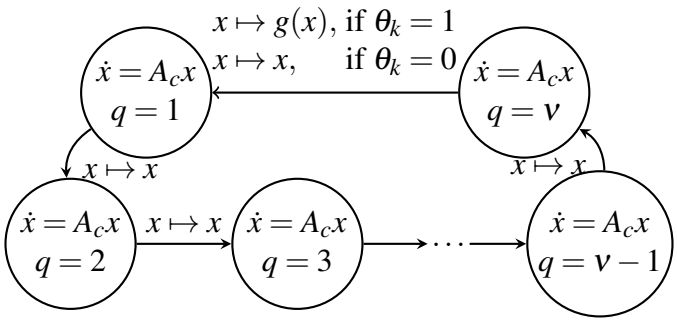

Figure 25: Graphical representation of the SHS (149).

Figure 25 presents a graphical illustration of the dynamics described by (149). The sampling instants t_k of (146) are represented by the transition from $q = \nu$ to $q = 1$ while the other jumps of (149), which do not affect $x(t)$, allow to express the behavior of system (146) through exponentially distributed random variables $\rho_k \sim \mathrm{E}(1,\lambda)$. Indeed, we claim that $x(t)$ in (146) is statistically equivalent to $x(t)$ in (149) if $q_0 = 1$. To understand why, let us denote by $\{\bar{t}_k\}_{k\in\mathbb{N}}$ the sequence of times at which the transitions from $q = \nu$ to $q = 1$ of (149) take place. Then, it suffices to notice that, if $q_0 = 1$, $\{\bar{t}_k\}_{k\in\mathbb{N}}$, given in this case by $\{\bar{t}_k\}_{k\in\mathbb{N}} = \{r_{\nu k}\}_{k\in\mathbb{N}}$, has the same distribution of $\{t_k\}_{k\in\mathbb{N}}$ in (146). This is a direct consequence of the discussion at the beginning of this subsection and of the way

these sequences are defined:

$$\begin{aligned}\{\bar{t}_{k+1}-\bar{t}_k\}_{k\in\mathbb{N}} &= \{r_{\nu(k+1)}-r_{\nu k}\}_{k\in\mathbb{N}}\\ &= \left\{\sum_{i=\nu k}^{\nu(k+1)-1}\rho_i\right\}_{k\in\mathbb{N}} \underbrace{\sim}_{(148)} \{\delta_k\}_{k\in\mathbb{N}}\\ &= \{t_{k+1}-t_k\}_{k\in\mathbb{N}}.\end{aligned}$$

These facts allow to address Problem 7.1 considering model (149), which involves the exponential distribution, as in the next section.

Remark 7.1. *Note that model* (149) *is slightly more general than* (146)*, since the time elapsed until the first transition from $q=\nu$ to $q=1$ can have any one of the distributions $\bar{t}_1 \sim E(\hat{\nu},\lambda), \hat{\nu}\in\mathbb{N}_\nu$, depending on the initial condition of $q(t)$. More precisely, using a reasoning similar to the one outlined above, one concludes that:*

$$\bar{t}_1 \sim E(\hat{\nu},\lambda) \Leftrightarrow q_0 = \nu-\hat{\nu}+1,\ \hat{\nu}\in\mathbb{N}_\nu.$$

7.2 Mean Square Exponential Stabilization

The main results of the chapter are presented next. Section 7.2.1 considers the nonlinear case and Section 7.2.2 shows that in the linear case, that is, when

$$\phi(K_p x_p + K_u u) = K_p x_p + K_u u,$$

the proposed stabilization conditions are non-conservative (i.e. necessary and sufficient).

7.2.1 The general case

According to the definitions in [Dav93, Section 24], system (149) belongs to the class of PDMPs (which is a subclass of SHSs, cf. [TSS14, Table 1]), where the state space and the boundary set are, respectively,

$$E \triangleq \mathbb{N}_\nu \times \mathbb{R}^n \text{ and } \Gamma \triangleq \emptyset.$$

Assumption 24.4 of [Dav93] is indeed satisfied since N_t, defined in (150), is a Poisson process, for which $\mathbb{E}[N_t]=\lambda t<\infty$ [PP02, Pg. 378]. Given a function

$$V(q,x),$$

these facts allow to establish the following key result, which is closely related to Theorem 2 of [Hes14].

Theorem 7.1. *Consider system* (149) *and a continuously differentiable function $V: E\to\mathbb{R}$ such that*

$$\mathbb{E}\left[\sum_{r_k\le T}\left|V(q(r_k),x(r_k))-V(q(r_k^-),x(r_k^-))\right|\right]<\infty,\ \forall T\ge 0,\ \forall (q_0,x_0)\in E, \tag{152}$$

where $q(r_0^-)=q(r_0)=q_0$ by convention and similarly for $x(r_0^-)$. Then, for $t\ge 0$,

$$\mathbb{E}[V(q(t),x(t))] = V(q_0,x_0)+\mathbb{E}\left[\int_0^t \mathfrak{U}V(q(s),x(s))ds\right],\ \forall (q_0,x_0)\in E \tag{153}$$

where

$$\mathfrak{U}V(q,x) \triangleq \frac{\partial V(q,x)}{\partial x} A_c x + \lambda \left(QV(q,x) - V(q,x) \right), \tag{154}$$

$$QV(q,x) \triangleq \begin{cases} V(q+1,x), & \text{if } q < \nu, \\ \mu_1 V(1,g(x)) + \mu_0 V(1,x), & \text{if } q = \nu. \end{cases} \tag{155}$$

Proof: The result follows from [Dav93, Theorem 26.14] and [Dav93, Remark 26.16], which guarantee, under condition (152), that Eq. (14.17) in [Dav93] holds (which corresponds to (153)). ■

Relation (153) is known as the Dynkin's formula [Dav93, Pg. 33] and can be intuitively interpreted as a stochastic version of the fundamental theorem of calculus. The first term of the right-hand side of (154) is just the usual time derivative of $V(q,x)$ along the trajectories of $\dot{x}(t) = A_c x(t)$ while the second term accounts for the jumps at the reset times. Note also that one of the transitions of (149) (the jump from $q = \nu$ to $q = 1$) is stochastic and depends on a Bernoulli random variable (that is why there are two terms in the second line of (155)).

Now we are ready to state our main stabilization result, whose proof is in Appendix A.7.

Theorem 7.2. *If there exist $\gamma > 0$, $Y \in \mathbb{R}^{m\times n}$ and positive definite matrices $W_q \in \mathbb{R}^{n\times n}, \forall q \in \mathbb{N}_\nu$, and $S \in \mathbb{R}^{m\times m}$ diagonal such that*

$$\begin{bmatrix} A_c W_q + W_q A_c^T + (\gamma - \lambda) W_q & \star \\ W_q & -\frac{W_{q+1}}{\lambda} \end{bmatrix} \preceq 0, \quad \forall q < \nu, \tag{156a}$$

$$\begin{bmatrix} A_c W_\nu + W_\nu A_c^T + (\gamma - \lambda) W_\nu & \star & \star & \star \\ DY & -2S & \star & \star \\ A_r W_\nu + B_r \underline{D} Y & B_r S & -\frac{W_1}{\lambda \mu_1} & \star \\ W_\nu & 0 & 0 & -\frac{W_1}{\lambda \mu_0} \end{bmatrix} \preceq 0, \tag{156b}$$

then for $K = Y W_\nu^{-1}$ the system (146) is MES with decay rate γ.

The proof of the theorem above, based in Theorem 7.1, considers a Lyapunov function of the form

$$V(q,x) = x^T P_q x$$

for the SHS (149). This choice is not arbitrary but motivated by the fact that it leads to non-conservative (i.e. necessary and sufficient) stabilization conditions in the linear case, as we will show next.

Remark 7.2. *Until now we have considered that $\mu_0 \in (0,1)$. If $\mu_0 = 0$ (that is, zero probability of packet dropouts), then LMI (156b) is replaced by*

$$\begin{bmatrix} A_c W_\nu + W_\nu A_c^T + (\gamma - \lambda) W_\nu & \star & \star \\ DY & -2S & \star \\ A_r W_\nu + B_r \underline{D} Y & B_r S & -\frac{W_1}{\lambda} \end{bmatrix} \preceq 0. \tag{157}$$

7.2.2 The linear case

Consider the case where $\phi(\zeta) = \zeta$ and (146c) reduces to

$$g(x) = A_d x = (A_r + B_r K) x. \tag{158}$$

The following theorem provides necessary and sufficient conditions for the mean square exponential stabilization of the closed-loop system in this case.

Theorem 7.3. *There exists a gain K such that the system (146) with $g(x)$ given by (158) is MES if and only if there exist $Y \in \mathbb{R}^{m\times n}$ and positive definite matrices $W_q^L \in \mathbb{R}^{n\times n}, \forall q \in \mathbb{N}_\nu$, such that*

$$\begin{bmatrix} A_c W_q^L + W_q^L A_c^T - \lambda W_q^L & \star \\ W_q^L & -\frac{W_{q+1}^L}{\lambda} \end{bmatrix} \prec 0, \quad \forall q < \nu, \tag{159a}$$

$$\begin{bmatrix} A_c W_\nu^L + W_\nu^L A_c^T - \lambda W_\nu^L & \star & \star \\ A_r W_\nu^L + B_r Y & -\frac{W_1^L}{\lambda\mu_1} & \star \\ W_\nu^L & 0 & -\frac{W_1^L}{\lambda\mu_0} \end{bmatrix} \prec 0, \tag{159b}$$

with $K = Y(W_\nu^L)^{-1}$.

Proof: See Appendix A.8. ■

Remark 7.3. *As in Theorem 7.2, it is possible to guarantee a specific decay rate $\gamma^L > 0$ in (147) replacing (159) by*

$$\begin{bmatrix} A_c W_q^L + W_q^L A_c^T + (\gamma^L - \lambda) W_q^L & \star \\ W_q^L & -\frac{W_{q+1}^L}{\lambda} \end{bmatrix} \preceq 0, \quad \forall q < \nu, \tag{160a}$$

$$\begin{bmatrix} A_c W_\nu^L + W_\nu^L A_c^T + (\gamma^L - \lambda) W_\nu^L & \star & \star \\ A_r W_\nu^L + B_r Y & -\frac{W_1^L}{\lambda\mu_1} & \star \\ W_\nu^L & 0 & -\frac{W_1^L}{\lambda\mu_0} \end{bmatrix} \preceq 0. \tag{160b}$$

7.2.2.1 Poisson sampling process

The Poisson sampling process corresponds to the particular case where $\mu_0 = 0$ and $\nu = 1$, that is, zero probability of packet dropouts and exponentially distributed sampling intervals. Consider the following corollary of Theorem 7.3, where $W \equiv W_1^L = W_\nu^L$ [HFG22b].

Corollary 7.1. *There exists a gain K such that the system (146) with $\mu_0 = 0$, δ_k exponentially distributed and $g(x)$ given by (158) is MES if and only if there exist $Y \in \mathbb{R}^{m\times n}$ and a positive definite matrix W such that*

$$\begin{bmatrix} A_c W + W A_c^T - \lambda W & \star \\ A_r W + B_r Y & -\frac{W}{\lambda} \end{bmatrix} \prec 0 \tag{161}$$

with $K = YW^{-1}$.

After application of the Schur's complement, (161) becomes, with $P = W^{-1}$:

$$PA_c + A_c^T P + \lambda (A_d^T P A_d - P) \prec 0,$$

which is a known necessary and sufficient condition for the mean square exponential stability of a impulsive system of the form

$$\dot{x}(t) = A_c x(t), \qquad \forall t \geq 0,\ t \neq t_k,\ \forall k \in \mathbb{N}_+ \tag{162}$$

$$x(t_k) = A_d x(t_k^-), \qquad \forall k \in \mathbb{N}_+ \tag{163}$$

when the intervals between the impulses are exponentially distributed (see, for instance, [TCL18, Theorem 5.1] or [AHS13, Theorem 7]).

Moreover, the mean square stabilization problem of system (140) subject to a Poisson sampling process has already been dealt with in [TCL18] considering the control law

$$u(t) = K_p x_p(t_k^-), \quad \forall t \in [t_k, t_{k+1}), \tag{164}$$

which is a particular case of

$$u(t) = K_p x_p(t_k^-) + K_u u(t_k^-), \quad \forall t \in [t_k, t_{k+1}). \tag{165}$$

It should be noticed that the results in [TCL18] are derived from a different impulsive system, where the error between $x_p(t)$ and its last sampled value until time t is considered as an additional state variable (see [TCL18, Eq. 14]). In this case, due to a different problem structure, it is not possible to obtain non-conservative convex conditions for the computation of K_p. In our method, this problem is overcome by considering a different impulsive representation and a more generic control law, which also depends on the past value of the control input. We briefly recall below the method of [TCL18], which provides only a partial solution to the stabilization problem, since it is based on the assumption below.

Assumption 7.1. *There exist positive definite matrices $R = R^T$ and $P = P^T$ which solve the algebraic Riccati equation*

$$A_p^T P + P A_p - 2 P B_p R^{-1} B_p^T P = -\alpha P, \ \alpha > 0, \tag{166}$$

and such that $(A_p - B_p R^{-1} B_p^T P)$ is Hurwitz. Moreover, the matrix $P = P(\alpha)$ has the property that for some $p > \frac{2}{3}$

$$\limsup_{\alpha \downarrow 0} \frac{\lambda_{max}(P)}{\alpha^p} < \infty, \tag{167}$$

i.e. $\lambda_{max}(P) = O(\alpha^p)$ as $\alpha \downarrow 0$.

This assumption is rather strong, as recognized in [TCL18, Pg. 239]. Indeed, in general, Assumption 7.1 is not expected to hold for systems where A_p has eigenvalues on the open right-half complex plane (see Remark 6.4 in [TCL18]). Note that even verifying Assumption 7.1 is not a simple task. It is necessary not only to solve the Riccati equation (166) to obtain the matrix $P = P(\alpha) \succ 0$, but also to analyze property (167). It is possible to get some insight about the behavior of the ratio $\lambda_{max}(P)/\alpha^p$ computing it for a grid of values of the pair $(\alpha, p) \in (0, \infty) \times (\frac{2}{3}, \infty)$. However, this numerical procedure does not formally guarantee that (167) holds.

In case Assumption 7.1 is satisfied, the stabilizing control law is given by the result below [TCL18, Theorem 6.5].

Lemma 7.2. *Suppose that Assumption 7.1 holds and that the sampling intervals are exponentially distributed. Then there exists $\alpha > 0$ (sufficiently small) such that the feedback gain*

$$K_p = -R^{-1} B_p^T P(\alpha) \tag{168}$$

where $P(\alpha)$ solves (166) renders the closed-loop system (140)-(164) mean exponentially stable.

Notice that Lemma 7.2 is non-constructive in the sense that it does not provide a valid value for $\alpha > 0$, which difficults the use of this result in practice. On the other hand, the results derived in this chapter do not have this limitation and can be easily applied, since they rely on semidefinite programming problems, like Corollary 7.1 in the particular case of a Poisson sampling process or Theorems 7.2 and 7.3 if the sampling intervals have the Erlang distribution. Moreover, these results are valid in the general case and not only for the class of systems which satisfy Assumption 7.1.

7.3 Numerical Examples

This section presents two numerical examples to illustrate the applicability of the proposed stabilization method, where the control law (141) is initialized with $u(0^-) = 0$.

7.3.1 Example I

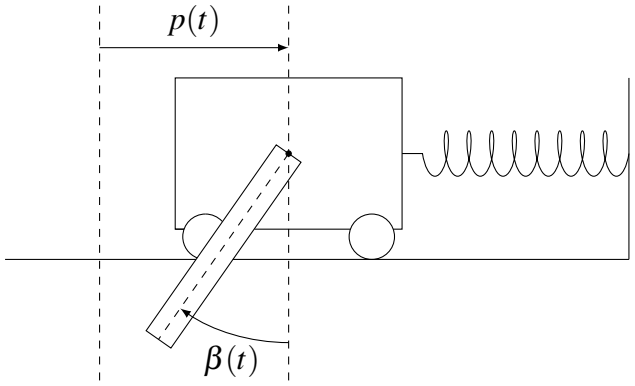

Figure 26: Cart–spring–pendulum system. Adapted from [TGGQ11, Example 8.3].

Consider the system matrices

$$A_p = \begin{bmatrix} 0 & 1 & 0 & 0 \\ -330.46 & -12.15 & -2.44 & 0 \\ 0 & 0 & 0 & 1 \\ -812.61 & -29.87 & -30.10 & 0 \end{bmatrix}, \quad B_p = \begin{bmatrix} 0 \\ 2.71762 \\ 0 \\ 6.68268 \end{bmatrix} \tag{169}$$

taken from a cart–spring–pendulum system (see Fig. 26), which has been fully described in [GHP+03] and has also been used in [DHTZ10] and [TGGQ11, Example 8.3], for instance. The state is given by $x_p = [p \ \dot{p} \ \beta \ \dot{\beta}]^T$, where $p(t)$ is the linear position of the cart and $\beta(t)$ is the angular position of the pendulum. The control input $u(t)$ is the voltage applied to the armature of the DC motor of the cart. Consider the parameters $\nu = 3$, $\lambda = 10$, $\mu_0 = 0.05$ and $\mu_1 = 0.95$ to model the stochastic sampling effects and recall that, as shown in Figure 24, the Erlang distribution allows to model an event whose probability density function is concentrated around a value. Assume that $u(t)$ is subject to saturation, that is, the nonlinearity $\phi(\cdot)$ in (141) satisfies the sector condition (143) with $\overline{D} = I_m$ and $\underline{D} = 0$.

The feedback matrix $K = [K_p \ K_u] \in \mathbb{R}^{m \times n}$ will be computed such that the resulting closed-loop system (140)-(141) is MES. Moreover, as a second control objective, the gain K will be designed to maximize the decay rate of the trajectories of the linear model composed by (140) and (141) with $\phi(\cdot)$ replaced by the identity function, which corresponds

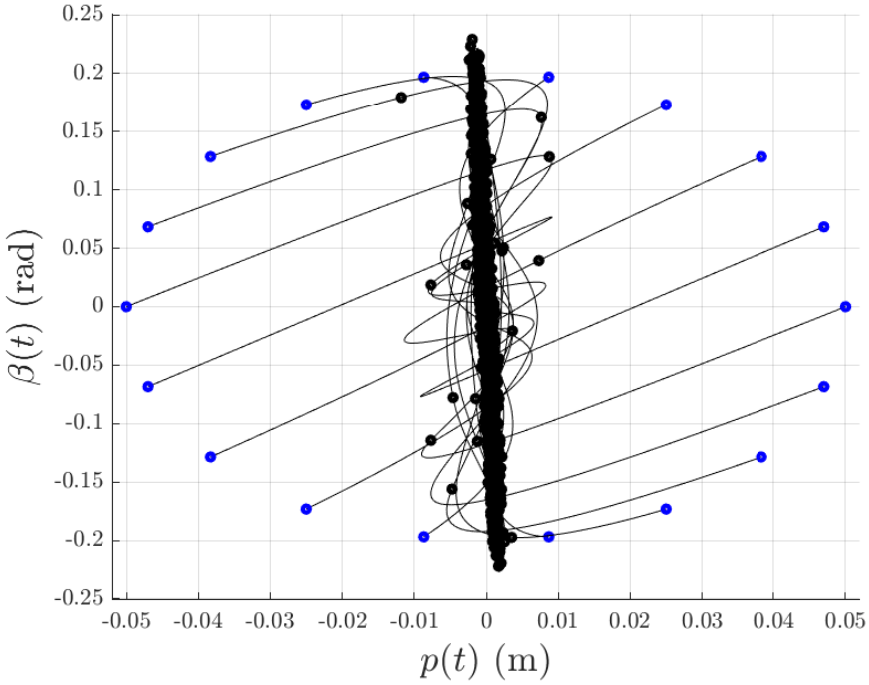

Figure 27: Trajectories of the closed-loop system composed by (140)-(141), (169) and (171) in the subspace of $[p(t)\ \beta(t)]^T$, where the initial conditions are depicted by blue circles and the state at the sampling instants t_k by black ones.

to the behavior of the nonlinear closed-loop system (140)-(141) when the control input does not saturate. Combining the results of Theorems 7.2 and 7.3 and Remark 7.3, the following optimization problem is proposed:

$$\begin{aligned} \max_{\gamma^L, Y, S, W_q, W_q^L} \quad & \gamma^L \\ \text{subject to:} \quad & (156), (160), \\ & S \succ 0 \text{ (diagonal)}, \\ & W_q \succ 0,\ W_q^L \succ 0,\ \forall q \in \mathbb{N}_v, \\ & W_v = W_v^L \end{aligned} \tag{170}$$

where $\gamma > 0$ in (156) is fixed *a priori*. Then the resulting feedback gain is given by

$$K = Y(W_v)^{-1} = Y(W_v^L)^{-1}.$$

Note that the use of a common Lyapunov matrix $W_v = W_v^L$ allows to construct an optimization problem with LMI constraints for each fixed value of γ^L. More precisely, (170) corresponds to a generalized eigenvalue problem [BEFB94, Section 2.2.3] and can be solved using bisection on γ^L and a semidefinite programming algorithm.

Applying (170) with $\gamma = 0.01$, one obtains $\gamma^L = 0.0225$ and

$$K = \begin{bmatrix} 12.87 & 0.24 & -0.21 & 0.032 & -0.00076 \end{bmatrix}, \tag{171}$$

which makes the closed-loop system (140)-(141) MES. Figure 27 shows several trajectories of the closed-loop system in the subspace of $[p(t)\ \beta(t)]^T$ for different initial conditions (depicted by blue circles, with $\dot{p}(0) = 0$ and $\dot{\beta}(0) = 0$) and different realizations

of the sequences $\{\delta_k\}_{k\in\mathbb{N}}$ and $\{\alpha_k\}_{k\in\mathbb{N}_+}$, where the black circles represent the sampling instants. As it can be seen, the trajectories converge to the origin, and $p(t)$ converges to zero faster than $\beta(t)$.

7.3.2 Example II

Consider the linear, Poisson sampling case described in Section 7.2.2.1 with the parameter $\lambda = 3$. Recall that the control law (141) reduces to (165). Consider also the following system matrices, already used in previous chapters:

$$A_p = \begin{bmatrix} 0 & 1 \\ 1 & 0 \end{bmatrix}, \quad B_p = \begin{bmatrix} 0 \\ -5 \end{bmatrix}. \tag{172}$$

Assumption 7.1 was numerically tested and does not seem to hold, what is in accordance with Remark 6.4 of [TCL18], since one of the eigenvalues of A_p is equal to 1. Thus, the stabilization result proposed in [TCL18], i.e. Lemma 7.2, cannot be applied in this case. On the other hand, applying the results of Corollary 7.1 and Remark 7.3 (which is also valid for (161) *mutatis mutandis*), one obtains the following feedback gain:

$$K = \begin{bmatrix} 0.2536 & 0.2574 & 0.0032 \end{bmatrix}, \tag{173}$$

which renders the closed-loop system mean exponentially stable with decay rate $\gamma^L = 0.49$.

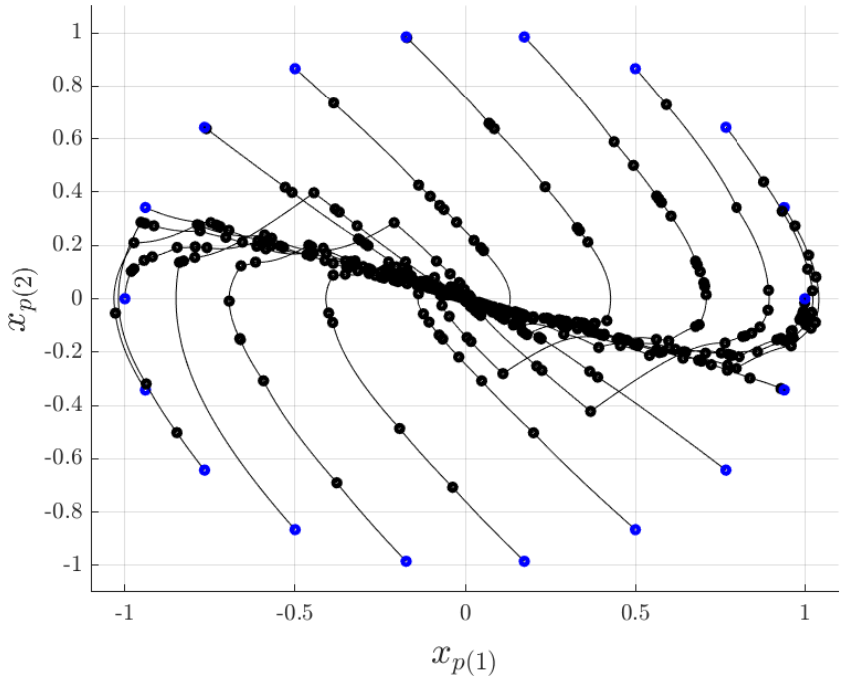

Figure 28: Trajectories of the closed-loop system composed by (140), (165), (172) and (173) in the x_p-subspace, where the initial conditions $x_p(0)$ are depicted by blue circles and the state at the sampling instants t_k by black ones.

Figure 28 shows several trajectories of the closed-loop system in the x_p-subspace for some realizations of the sequence $\{\delta_k\}_{k\in\mathbb{N}}$, where the initial conditions, depicted by blue

circles, satisfy $\|x_p(0)\| = 1$. As one should expect, the trajectories converge to the origin. We recall that $x_p(t)$ is continuous. On the other hand, its derivative is discontinuous at the sampling instants (represented by black circles) because of the update of the control input $u(t)$ using the law (165).

7.4 Concluding remarks

In this chapter, LMI conditions are proposed for the mean square exponential stabilization of randomly sampled linear systems subject to control input nonlinearities and packet dropouts, where the sampling intervals are considered to be Erlang-distributed random variables. Unlike [SWH16, STWH17, HRDL22, SSC21], which focus on the discrete-time trajectories of the system, our method formally guarantees the exponential stabilization of the continuous-time system. Moreover, it is non-conservative in the linear case. Besides that, the proposed approach has some advantages over the one of [TCL18], which deals with the particular case of a Poisson sampling process, as explained in Section 7.2.2.1.

As a future work, it would be interesting to consider other (and more general) distribution functions for the sampling interval of the system as well as the presence of measurement noise. Another idea consists in dealing with the case where only local stabilization (in a probabilistic sense) around the origin is possible.

The results in this chapter have been published in [HFG22b] and are also the subject of a new paper to be submitted [HFG22a].

8 CONCLUSIONS

This study has proposed methods for the stability analysis and stabilization of linear aperiodic sampled-data systems subject to input saturation (in Chapters 3–5) or more general input constraints (in Chapters 6 and 7) considering in most cases a non-stochastic framework but also a stochastic one in Chapter 7. The associated numerical algorithms were based on semidefinite or linear programming (with the exception of Chapter 6) and can therefore be easily applied using off-the-shelf optimization softwares. It should be noticed that there is an extensive literature on the subject, specially in the non-stochastic case to the best of the author's knowledge (see, for instance, the survey [HFO+17]). In other words, this work has proposed some new contributions to this research field but it is by no means exhaustive (some ideas of future works are discussed afterwards).

The problem of computing estimates of the region of attraction of the origin of the sampled-data system under input saturation was dealt with in Chapter 3 considering a quadratic approach (which can be seen as an evolution and generalization of the previous work in [FG18]) and in Chapters 4 and 5 considering polyhedral ones, which employ the SNS embedding of the saturation function [ACLC06] and some concepts on set invariance theory [BM15]. As explained in [Kha02, Pg. 122], the notion of RAO is important because it gives an idea about the robustness of the equilibrium point of the system, i.e. how far from the equilibrium point the trajectory can start and still converge to it as t goes to ∞. As pointed out in [TGGQ11], the estimates of the RAO can be seen as safe regions of operation for the closed-loop nonlinear system. The analytic characterization of these estimates is therefore important to manage the trade-off between performance and stability. A control law that guarantees an extremely good performance can be useless if the associated RAO is too small.

Even if the open-loop system is not unstable, to satisfy performance criteria around the origin, it may be interesting to use a control law that ensures only local stability of the origin and to compute the corresponding estimate of the RAO [TGGQ11]. In this case, one can also use a switched control law, where we start with a global stabilizing control law and, as the state approaches the origin, we switch to a more performing one. The estimate of the RAO will then define the switching region.

As already mentioned in the Introduction, because of their flexibility, adopting polyhedrons instead of ellipsoids allows a reduction of conservatism regarding the estimates of the RAO but is very demanding in terms of computational complexity [BM15]. Thus, it depends on the case whether or not it is advantageous to use the methods of Chapters 4 and 5 instead of the one of Chapter 3. It also depends on the case whether or not the method of Chapter 5 is useful compared to the one of Chapter 4, as shown by the simulation examples of Chapter 5. There is no formal guarantee that the approach of Chapter 5 outperforms the one of Chapter 4 in all cases. What motivated the development of the for-

mer is, as already explained, the numerical applicability of the corresponding algorithm rather than the quality of the estimate of the RAO itself. In Algorithm 5.1 of Chapter 5, it is possible to manage the trade-off between number of iterations and complexity of the resulting polytope, unlike Algorithm 4.1 of Chapter 4.

Recall that Algorithms 4.1 and 5.1 are based on the iterative application of the concept of one-step set, where the complexity of the generated polytopes tends to increase at each new iteration. In order to circunvent this numerical problem, Chapter 6 adopts a different strategy, already used for instance in [BPC+18, FEC20, OJD20], where the complexity of the polytopes (given by the number of vertices) is fixed *a priori*. In this case, the resulting optimization problem has bilinear constraints. Even if in principle only a local optimum can be found, the numerical examples of Chapter 6, obtained using the KNITRO toolbox [BNW06], provided quite satisfactory results.

The method of Chapter 6 deals not only with the stability analysis problem as Chapters 4 and 5, but also with the control design problem as Chapter 3, where the goal is to indirectly maximize the RAO of the resulting closed-loop system. As shown by the simulation examples, the polyhedral estimates of the RAO obtained with the piecewise linear control law of Chapter 6 tend to be larger than the ellipsoidal ones related to the linear feedback control law of Chapter 3. This result is not surprising, since the piecewise linear control law is more general and since the use of polytopes leads to a reduction of conservatism, as previously remarked.

Chapters 3-6 considered all a non-stochastic framework, where lower and upper bounds are imposed for the unknown, time-varying sampling interval of the system. As a common feature, the methods are based on difference inclusions that model the behavior of the system state at the sampling instants. This idea relies on the fact that the stability of the discrete-time model guarantees the one of the corresponding continuous-time system, as explained in Chapter 2. However, in the stochastic framework of Chapter 7, this property is not valid in general (cf. [TCL18, Pg. 222] and [AHS12, Pg. 610]) and the strategy mentioned above no longer works. That is why the theoretical developments of Chapter 7 were considerably different, being based on the framework of Piecewise Deterministic Markov Processes [Dav93].

The aim of Chapter 7 was to propose a control design method which guarantees the global stabilization in the mean square sense of the sampled-data system, where the control input is subject to sector bounded nonlinearities and the random sampling intervals have the Erlang distribution. The possibility of packet dropouts is explicitly taken into account through the Bernoulli distribution. Moreover, as shown in that chapter, the proposed approach leads to non-conservative stabilization conditions in the linear case.

8.1 Future works and perspectives

Regarding the method of Chapter 7, it would be interesting to consider, as already mentioned in Section 7.4, other (and more general) distribution functions for the sampling interval of the system. Another interesting idea is to consider, as in Chapters 3-6, the problem of local stability/stabilization of the origin. In this case, it would be necessary to adapt the definition of region of attraction of the origin to the stochastic case, using, for instance, the notion of *risk margin* adopted in [BDS03, GH18]. The idea is to define the RAO as the set of initial conditions such that the corresponding system trajectory converges to the origin with a probability of at least $1-\alpha$, where $\alpha \in (0,1)$ represents the risk margin. It is worth saying that it is not possible to define the RAO without this risk

margin, i.e. with $\alpha = 0$, in the general case.

A possibility of future work that is valid for both the stochastic and the non-stochastic cases consists in considering measurement noise in the control loop. In the stochastic case, a distribution function could be used to model the noise effects. In the non-stochastic case, on the other hand, lower and upper bounds could be imposed for the noise signal.

It would also be interesting to consider the problem of designing a state observer for the system, where the measurements are sporadically/randomly distributed in time. The stability of the resulting closed loop with a control law based on this observer could be investigated too.

Moreover, it would be interesting to deal with nonlinear system dynamics, since this thesis only focused on the simplest case where $\dot{x}_p = A_p x_p + B_p u$. Other types of sampling and other classes of control law besides the linear and the PWL feedbacks could be exploited too, in principle.

Regarding the method of Chapter 3, we highlight that it can be easily extended to cope with other sector-bounded input nonlinearities, as explained in Section 3.5. Moreover, it is possible to adapt the control design approach of Chapter 6, which considers a PWL state feedback, to the simpler case of a linear feedback.

Another idea of future work is to consider uncertainties in matrices A_p and B_p of the plant model. Note, in particular, that the discrete-time model derived in Section 2.1.2 to represent the sampled-data system depends on the exponential of A_p. To circumvent the difficulty of dealing with the exponential of an uncertain matrix, the systematic procedure based on Taylor series expansion proposed in [BMT+15] could, in principle, be exploited. The techniques of [CHV+10] and [JCMM13] are worth investigation too.

BIBLIOGRAPHY

[ACLC06] T. Alamo, A. Cepeda, D. Limon, and E. F. Camacho. A new concept of invariance for saturated systems. *Automatica*, 42(9):1515 – 1521, 2006.

[AF92] D. Avis and K. Fukuda. A pivoting algorithm for convex hulls and vertex enumeration of arrangements and polyhedra. *Discrete & Computational Geometry*, 8(3):295–313, 1992.

[AF09] J.-P. Aubin and H. Frankowska. *Set-valued analysis*. Springer Science & Business Media, 2009.

[AHS12] D. J. Antunes, J. P. Hespanha, and C. J. Silvestre. Volterra integral approach to impulsive renewal systems: application to networked control. *IEEE Transactions on Automatic Control*, 57(3):607–619, 2012.

[AHS13] D. J. Antunes, J. P. Hespanha, and C. J. Silvestre. Stability of networked control systems with asynchronous renewal links: an impulsive systems approach. *Automatica*, 49(2):402–413, 2013.

[AT19] T. Anevlavis and P. Tabuada. Computing controlled invariant sets in two moves. In *58th IEEE Conference on Decision and Control (CDC)*, pages 6248–6254, 2019.

[AW84] K. J. Aström and B. Wittenmark. *Computer Controlled Systems. Theory and Design*. Information and System Sciences Series. Prentice-Hall, 1984.

[BCM10] T. B. Blanco, M. Cannon, and B. D. Moor. On efficient computation of low-complexity controlled invariant sets for uncertain linear systems. *International Journal of Control*, 83(7):1339–1346, 2010.

[BDS03] S. Battilotti and A. De Santis. Stabilization in probability of nonlinear stochastic systems with guaranteed region of attraction and target set. *IEEE Transactions on Automatic Control*, 48(9):1585–1599, 2003.

[BEFB94] S. Boyd, L. El Ghaoui, E. Feron, and V. Balakrishnan. *Linear Matrix Inequalities in System and Control Theory*. SIAM Studies in Applied Mathematics, 1994.

[Bil95] P. Billingsley. *Probability and Measure*. John Wiley & Sons, 3rd edition, 1995.

[Bit91] G. Bitsoris. Existence of positively invariant polyhedral sets for continuous-time linear systems. *Control-Theory and Advanced Technology*, 7:407–427, 1991.

[Bla94] F. Blanchini. Ultimate boundedness control for uncertain discrete-time systems via set-induced Lyapunov functions. *IEEE Transactions on Automatic Control*, 39(2):428–433, 1994.

[BM15] F. Blanchini and S. Miani. *Set-Theoretic Methods in Control*. Birkhäuser, 2015.

[BMT+15] M. F. Braga, C. F. Morais, E. S. Tognetti, R. C. Oliveira, and P. L. Peres. Discretization and event triggered digital output feedback control of lpv systems. *Systems & Control Letters*, 86:54–65, 2015.

[BNW06] R. H. Byrd, J. Nocedal, and R. A. Waltz. Knitro: An integrated package for nonlinear optimization. *Large-Scale Nonlinear Optimization. Nonconvex Optimization and Its Applications*, 83:35–59, 2006.

[BPC+18] S. L. Brião, M. V. A. Pedrosa, E. B. Castelan, E. Camponogara, and L. S. de Assis. Explicit computation of stabilizing feedback control gains using polyhedral Lyapunov functions. In *IEEE International Conference on Automation/XXIII Congress of the Chilean Association of Automatic Control (ICA-ACCA)*, pages 1–6. IEEE, 2018.

[Bri13] C. Briat. Convex conditions for robust stability analysis and stabilization of linear aperiodic impulsive and sampled-data systems under dwell-time constraints. *Automatica*, 49(11):3449–3457, 2013.

[Bri18] C. Briat. Stability analysis and stabilization of lpv systems with jumps and (piecewise) differentiable parameters using continuous and sampled-data controllers. *arXiv:1705.00056*, 2018.

[CF95] T. Chen and B. A. Francis. *Optimal sampled-data control systems*. Springer, 1995.

[CH93] E. B. Castelan and J.-C. Hennet. On invariant polyhedra of continuous-time linear systems. *IEEE Transactions on Automatic control*, 38(11):1680–1685, 1993.

[CHV+10] M. B. G. Cloosterman, L. Hetel, N. Van de Wouw, W. P. M. H. Heemels, J. Daafouz, and H. Nijmeijer. Controller synthesis for networked control systems. *Automatica*, 46(10):1584–1594, 2010.

[CVHN09] M. B. G. Cloosterman, N. Van de Wouw, W. P. M. H. Heemels, and H. Nijmeijer. Stability of networked control systems with uncertain time-varying delays. *IEEE Transactions on Automatic Control*, 54(7):1575–1580, 2009.

[Dav93] M. H. A. Davis. *Markov Models & Optimization*, volume 49. Chapman & Hall/CRC Monographs on Statistics and Applied Probability, London, UK, 1993.

[DH99] C. E. T. Dórea and J.-C. Hennet. (a, b)-invariant polyhedral sets of linear discrete-time systems. *Journal of optimization theory and applications*, 103(3):521–542, 1999.

[DHTZ10] D. Dai, T. Hu, A. R. Teel, and L. Zaccarian. Output feedback synthesis for sampled-data system with input saturation. In *American Control Conference (ACC 2010)*, pages 1797–1802, Baltimore, USA, 2010.

[FA18] M. Fiacchini and M. Alamir. Computing control invariant sets in high dimension is easy. *arXiv:1810.10372*, 2018.

[FEC20] G. A. França dos Santos, J. G. Ernesto, and E. B. Castelan. Controle sob restrições de sistemas lineares – projeto de realimentação de saídas via programação bilinear (in portuguese). In *Anais do Congresso Brasileiro de Automática*, volume 2, 2020.

[FG18] M. Fiacchini and J. M. Gomes da Silva Jr. Stability of sampled-data control systems under aperiodic sampling and input saturation. In *57th IEEE Conference on Decision and Control (CDC)*, pages 6644–6649, 2018.

[FM16] M. Fiacchini and I.-C. Morărescu. Constructive necessary and sufficient condition for the stability of quasi-periodic linear impulsive systems. *IEEE Transactions on Automatic Control*, 61(9):2512–2517, 2016.

[FO11] H. Fujioka and Y. Oishi. A switched Lyapunov function approach to stability analysis of non-uniformly sampled-data systems with robust LMI techniques. In *8th Asian Control Conference (ASCC)*, pages 1487–1491, 2011.

[Fri10] E. Fridman. A refined input delay approach to sampled-data control. *Automatica*, 46(2):421–427, 2010.

[FSR04] E. Fridman, A. Seuret, and J.-P. Richard. Robust sampled-data stabilization of linear systems: An input delay approach. *Automatica*, 40(8):1141–1446, 2004.

[Fuj09] H. Fujioka. A discrete-time approach to stability analysis of systems with aperiodic sample-and-hold devices. *IEEE Transactions on Automatic Control*, 54(10):2440–2445, 2009.

[GH18] S. Gudmundsson and S. Hafstein. Probabilistic basin of attraction and its estimation using two Lyapunov functions. *Complexity*, 2018:1–9, 2018.

[GHP+03] G. Grimm, J. Hatfield, I. Postlethwaite, A. R. Teel, M. C. Turner, and L. Zaccarian. Antiwindup for stable linear systems with input saturation: an LMI-based synthesis. *IEEE Transactions on Automatic Control*, 48(9):1509–1525, 2003.

[GQST16] J. M. Gomes da Silva Jr., I. Queinnec, A. Seuret, and S. Tarbouriech. Regional stability analysis of discrete-time dynamic output feedback under aperiodic sampling and input saturation. *IEEE Transactions on Automatic Control*, 61(12):4176–4182, 2016.

[GT99] J. M. Gomes da Silva Jr. and S. Tarbouriech. Polyhedral regions of local stability for linear discrete-time systems with saturating controls. *IEEE Transactions on Automatic Control*, 44(11):2081–2085, 1999.

[GT01] J. M. Gomes da Silva Jr. and S. Tarbouriech. Local stabilization of discrete-time linear systems with saturating controls: an LMI-based approach. *IEEE Transactions on Automatic Control*, 46(1):119–125, 2001.

[GT05] J. M. Gomes da Silva Jr. and S. Tarbouriech. Anti-windup design with guaranteed region of stability: an LMI-based approach. *IEEE Transactions on Automatic Control*, 50(1):106–111, 2005.

[HDRJ11] L. Hetel, J. Daafouz, J.-P. Richard, and M. Jungers. Delay-dependent sampled-data control based on delay estimates. *Systems & Control Letters*, 60(2):146 – 150, 2011.

[HDTP13] L. Hetel, J. Daafouz, S. Tarbouriech, and C. Prieur. Stabilization of linear impulsive systems through a nearly-periodic reset. *Nonlinear Analysis: Hybrid Systems*, 7(1):4 – 15, 2013.

[Hes14] J. P. Hespanha. Modeling and analysis of networked control systems using stochastic hybrid systems. *Annual Reviews in Control*, 38(2):155–170, 2014.

[HFG21] D. D. Huff, M. Fiacchini, and J. M. Gomes da Silva Jr. Stabilization of aperiodic sampled-data linear systems with input constraints: a low complexity polyhedral approach. In *60th IEEE Conference on Decision and Control (CDC)*, 2021. https://doi.org/10.1109/CDC45484.2021.9683136.

[HFG22a] D. D. Huff, M. Fiacchini, and J. M. Gomes da Silva Jr. Mean square exponential stabilization of sampled-data systems subject to actuator nonlinearities, random sampling and packet dropouts. *Under review on IEEE Transactions on Automatic Control*, 2022.

[HFG22b] D. D. Huff, M. Fiacchini, and J. M. Gomes da Silva Jr. Necessary and sufficient convex condition for the stabilization of linear sampled-data systems under poisson sampling process. *IEEE Control Systems Letters*, 6:3403–3408, 2022. https://doi.org/10.1109/LCSYS.2022.3184902.

[HFG22c] D. D. Huff, M. Fiacchini, and J. M. Gomes da Silva Jr. Polyhedral estimates of the region of attraction of the origin of linear systems under aperiodic sampling and input saturation. *Automatica*, 144:110490, 2022. https://doi.org/10.1016/j.automatica.2022.110490.

[HFG22d] D. D. Huff, M. Fiacchini, and J. M. Gomes da Silva Jr. Polyhedral regions of stability for aperiodic sampled-data linear control systems with saturating inputs. *IEEE Control Systems Letters*, 6:241–246, 2022. https://doi.org/10.1109/LCSYS.2021.3066132.

[HFG22e] D. D. Huff, M. Fiacchini, and J. M. Gomes da Silva Jr. Stability and stabilization of aperiodic sampled-data systems subject to control input saturation: a set invariant approach. *IEEE Transactions on Automatic Control*, 67(3):1423–1429, 2022. https://doi.org/10.1109/TAC.2021.3064988.

[HFO+17] L. Hetel, C. Fiter, H. Omran, A. Seuret, E. Fridman, J.-P. Richard, and S.-I. Niculescu. Recent developments on the stability of systems with aperiodic sampling: An overview. *Automatica*, 76:309 – 335, 2017.

[HKJM13] M. Herceg, M. Kvasnica, C. N. Jones, and M. Morari. Multi-Parametric Toolbox 3.0. In *Proc. of the European Control Conference*, pages 502–510, 2013.

[HNX07] J. P. Hespanha, P. Naghshtabrizi, and Y. Xu. A survey of recent results in networked control systems. *Proceedings of the IEEE*, 95(1):138–162, 2007.

[HRDL22] Z. Hu, H. Ren, F. Deng, and H. Li. Stabilization of sampled-data systems with noisy sampling intervals and packet dropouts via a discrete-time approach. *IEEE Transactions on Automatic Control*, 67(6):3204–3211, 2022.

[JCMM13] M. Jungers, E. B. Castelan, V. M. Moraes, and U. F. Moreno. A dynamic output feedback controller for ncs based on delay estimates. *Automatica*, 49(3):788–792, 2013.

[KF13] C.-Y. Kao and H. Fujioka. On stability of systems with aperiodic sampling devices. *IEEE Transactions on Automatic Control*, 28(3):2085–2090, 2013.

[Kha02] H. Khalil. *Nonlinear Systems*. Prentice-Hall, 3rd edition, 2002.

[LF12] K. Liu and E. Fridman. Wirtinger's inequality and Lyapunov-based sampled-data stabilization. *Automatica*, 48(1):102 – 108, 2012.

[LL69] V. Lakshmikantham and S. Leela. *Differential and Integral Inequalities*, volume 1. Academic Press, 1969.

[LONH12] W. Lombardi, S. Olaru, S.-I. Niculescu, and L. Hetel. A predictive control scheme for systems with variable time-delay. *International Journal of Control*, 85(7):915–932, 2012.

[Lue97] D. G. Luenberger. *Optimization by vector space methods*. John Wiley & Sons, 1997.

[Ma91] C. C. H. Ma. Unstabilizability of linear unstable systems with input limits. *Journal of Dynamic Systems, Measurement, and Control*, 113(4):742–744, 1991.

[MNC01] S. Monaco and D. Normand-Cyrot. Issues on nonlinear digital control. *European Journal of Control*, 7(2):160–177, 2001.

[NHT08] P. Naghshtabrizi, J. P. Hespanha, and A. R. Teel. Exponential stability of impulsive systems with application to uncertain sampled-data systems. *Systems & Control Letters*, 57(5):378–385, 2008.

[NT01] D. Nesic and A. R. Teel. Sampled-data control of nonlinear systems: An overview of recent results. In *Perspectives in robust control. Lecture Notes in Control and Information Sciences*, volume 268, 2001.

[OJD20] A. C. C. Oliveira, F. L. Júnior, and C. E. T. Dórea. Cálculo de conjuntos invariantes controlados robustos com complexidade fixa usando otimização bilinear (in portuguese). In *Anais do Congresso Brasileiro de Automática*, volume 2, 2020.

[PP02] A. Papoulis and S. U. Pillai. *Probability, Random Variables and Stochastic Processes (International Edition)*. McGraw-Hill Education, 4th edition, 2002.

[Res92] S. I. Resnick. *Adventures in stochastic processes*. Birkhäuser Boston, 1992.

[RF10] H. Royden and P. Fitzpatrick. *Real Analysis*. Pearson, 4th edition, 2010.

[RHL77] N. Rouche, P. Habets, and M. Laloy. *Stability Theory by Liapunov's Direct Method*. Springer-Verlag, 1977.

[Sch93] R. Schneider. *Convex Bodies: The Brunn–Minkowski Theory*. Cambridge University Press, 1993.

[Seu12] A. Seuret. A novel stability analysis of linear systems under asynchronous samplings. *Automatica*, 48(1):177–182, 2012.

[SG12] A. Seuret and J. M. Gomes da Silva Jr. Taking into account period variations and actuator saturation in sampled-data systems. *Systems & Control Letters*, 61:1286–1293, 2012.

[SSC21] H. Sun, J. Sun, and J. Chen. Analysis and synthesis of networked control systems with random network-induced delays and sampling intervals. *Automatica*, 125:109385, 2021.

[SSY94] H. J. Sussmann, S. D. Sontag, and Y. Yang. A general result on the stabilization of linear systems using bounded controls. *IEEE Transactions on Automatic Control*, 39(12):2411–2425, 1994.

[STWH17] B. Shen, H. Tan, Z. Wang, and T. Huang. Quantized/saturated control for sampled-data systems under noisy sampling intervals: A confluent Vandermonde matrix approach. *IEEE Transactions on Automatic Control*, 62(9):4753–4759, 2017.

[SWH16] B. Shen, Z. Wang, and T. Huang. Stabilization for sampled-data systems under noisy sampling interval. *Automatica*, 63:162–166, 2016.

[TCL18] A. Tanwani, D. Chatterjee, and D. Liberzon. Stabilization of deterministic control systems under random sampling: Overview and recent developments. *Uncertainty in Complex Networked Systems*, pages 209–246, 2018.

[TGGQ11] S. Tarbouriech, G. Garcia, J. M. Gomes da Silva Jr., and I. Queinnec. *Stability and Stabilization of Linear Systems with Saturating Actuators*. Springer, 2011.

[TJ15] F. Tahir and I. M. Jaimoukha. Low-complexity polytopic invariant sets for linear systems subject to norm-bounded uncertainty. *IEEE Transactions on Automatic Control*, 60(5):1416–1421, 2015.

[TN08] M. Tabbara and D. Nesic. Input–output stability of networked control systems with stochastic protocols and channels. *IEEE Transactions on Automatic control*, 53(5):1160–1175, 2008.

[TSS14] A. R. Teel, A. Subbaraman, and A. Sferlazza. Stability analysis for stochastic hybrid systems: A survey. *Automatica*, 50(10):2435–2456, 2014.

[Van77] C. Van Loan. The sensitivity of the matrix exponential. *SIAM Journal on Numerical Analysis*, 14(6):971–981, 1977.

[ZBP01] W. Zhang, M. S. Branicky, and S. M. Phillips. Stability of networked control systems. *IEEE Control Systems Magazine*, 21(1):84–99, 2001.

[Zie95] G. M. Ziegler. *Lectures on Polytopes*. Springer-Verlag, 1995.

APPENDIX A PROOFS OF SOME RESULTS

A.1 Proof of Lemma 2.4

Since $\Psi_\Omega(x)$ is positively homogeneous of order 1 (see Lemma 2.2), it follows from the definition of the directional derivative $D^+\Psi_\Omega(x)$ that $D^+\Psi_\Omega(x)$ also is positively homogeneous of order 1, i.e.

$$D^+\Psi_\Omega(\lambda x) = \lambda D^+\Psi_\Omega(x) \quad \text{for } \lambda \geq 0.$$

Inequality (37) is only valid on the boundary of the set Ω (where $\Psi_\Omega(x) = 1$), but using the property above we can extend it to the whole space as described next. Given $x \in \mathbb{R}^n \setminus \{0\}$ (the case $x = 0$ is trivial), define $\bar{x} \triangleq x/\Psi_\Omega(x) \in \partial\Omega$. It follows that

$$D^+\Psi_\Omega(x) = D^+\Psi_\Omega\left(\Psi_\Omega(x)\bar{x}\right) = \Psi_\Omega(x) D^+\Psi_\Omega(\bar{x}) \leq \Psi_\Omega(x)\beta. \tag{174}$$

Combining now (36) and (174) we conclude that $\psi(t) = \Psi_\Omega(x(t))$ satisfies

$$\dot{\psi}(t) = D^+\Psi_\Omega(x(t)) \leq \beta\Psi_\Omega(x(t)) = \beta\,\psi(t) \quad \text{for almost all } t \tag{175}$$

along the trajectories of (31). Applying now Theorem 1.10.2 from [LL69] one has

$$\psi(t) \leq e^{\beta t}\psi(0), \quad \forall t \geq 0,$$

which is equivalent to (38).

A.2 Proof of Lemma 2.6

First let us show that a C-set Ω is always γ-invariant for the dynamics $\dot{x}(t) = A_c x(t)$ with $\gamma = \Psi_\Omega(A_c\Omega)$. Notice that for $x \in \partial\Omega$:

$$\begin{aligned} D^+\Psi_\Omega(x) &= \limsup_{h\to 0^+} \frac{\Psi_\Omega(x + hA_c x) - \Psi_\Omega(x)}{h} \\ &\leq \limsup_{h\to 0^+} \frac{\Psi_\Omega(x) + h\Psi_\Omega(A_c x) - \Psi_\Omega(x)}{h} = \Psi_\Omega(A_c x) \leq \Psi_\Omega(A_c\Omega) = \gamma \end{aligned}$$

where we used the fact that $\Psi_\Omega(x)$ is sub-additive and positively homogeneous of order 1 (see Lemma 2.2) and the last inequality follows from the relation $x \in \partial\Omega \subset \Omega$. From Definition 2.12, we conclude that the statement is indeed true.

The result of the lemma follows now directly from the fact that (41) implies, for $\beta \triangleq \dfrac{\|A_c\| r_2}{r_1}$, that

$$\Psi_{\Omega_i}(A_c\Omega_i) \leq \beta, \quad \forall i \in I, \tag{176}$$

which is equivalent to

$$A_c\Omega_i \subseteq \beta\Omega_i, \quad \forall i \in I. \tag{177}$$

To see that, consider $i \in I$ arbitrary. For all $x \in \Omega_i \subseteq \mathscr{B}_{r_2}$, one has:

$$\|A_c x\| \leq \|A_c\|\|x\| \leq \|A_c\| r_2.$$

Thus,

$$A_c x \in \|A_c\| r_2 \mathscr{B} = \frac{\|A_c\| r_2}{r_1}\mathscr{B}_{r_1} \subseteq \frac{\|A_c\| r_2}{r_1}\Omega_i = \beta\Omega_i,$$

and one concludes that (177) indeed holds.

A.3 Proof of Lemma 5.2

We will show the result only for $Q_J(\Omega)$, $\forall J \geq J^\star$. The proof for $Q(\Omega)$ is analogous (it suffices to replace Δ_J by Δ).

From (108) it follows that $Q_J(\Omega)$ is an intersection of closed and convex sets. Hence it is also closed and convex. Let us show that the origin is in the interior of $Q_J(\Omega)$. Notice that the set-valued map $\mathbb{R}^n \ni x \mapsto \mathscr{F}_{SNS}(x, \Delta_J, \mathscr{S}) \subset \mathbb{R}^n$ is continuous (according to Definition 1.4.3 of [AF09]). In particular, it is upper semicontinuous [AF09, Def. 1.4.1] at the origin. Thus, since Ω is a neighborhood of $\mathscr{F}_{SNS}(0, \Delta_J, \mathscr{S}) = \{0\}$ (recall that $0 \in \Omega^\circ$), there exists, by definition of upper semicontinuity, $c > 0$ such that $\mathscr{F}_{SNS}(x, \Delta_J, \mathscr{S}) \subseteq \Omega$ for all $x \in \mathscr{B}_c$. That is, $\mathscr{B}_c \subseteq Q_J(\Omega)$ and the conclusion follows.

To guarantee that $Q_J(\Omega)$ is a C-set, we still have to show that it is bounded. So let us prove the existence of $r = r(\gamma) > 0$ satisfying the statement of the lemma. Using the definitions of $A_x(\delta)$ and $K_x(\delta)$, we deduce from (103) after some algebraic manipulations that

$$\mathscr{F}_{SNS}(x_k, \delta_k, S_k) = x_{k+1}(x_k, \delta_k, S_k) = \begin{bmatrix} x_{p,k+1}(x_k, \delta_k) \\ u_{k+1}(x_k, \delta_k, S_k) \end{bmatrix} = \begin{bmatrix} x_{p,k+1}(x_k, \delta_k) \\ \mathrm{sat}_{S_k}\left(K_p x_{p,k+1}(x_k, \delta_k)\right) \end{bmatrix},$$
$$x_{p,k+1}(x_k, \delta_k) = \begin{bmatrix} e^{A_p\delta_k} & \int_0^{\delta_k} e^{A_p s}\mathrm{d}sB_p \end{bmatrix} x_k.$$

Given $\delta_A, \delta_B \in \Delta_J$, notice that

$$\begin{bmatrix} x_{p,k+1}(x_k, \delta_A) \\ x_{p,k+1}(x_k, \delta_B) \end{bmatrix} = \begin{bmatrix} e^{A_p\delta_A} & \int_0^{\delta_A} e^{A_p s}\mathrm{d}sB_p \\ e^{A_p\delta_B} & \int_0^{\delta_B} e^{A_p s}\mathrm{d}sB_p \end{bmatrix} x_k \triangleq \Lambda(\delta_A, \delta_B)x_k.$$

Then

$$\max\left\{ \begin{matrix} \|x_{p,k+1}(x_k, \delta_A)\|, \\ \|x_{p,k+1}(x_k, \delta_B)\| \end{matrix} \right\} \geq \frac{1}{\sqrt{2}}\|\Lambda(\delta_A, \delta_B)x_k\| \geq \frac{1}{\sqrt{2}}\sigma_{min}\left(\Lambda(\delta_A, \delta_B)\right)\|x_k\|. \tag{178}$$

Claim I. *$\sigma_{min}\left(\Lambda(\tau_m, \delta)\right) > 0$ if $\delta \in \Delta \setminus \Delta^\star$*

Proof: This is equivalent to the full column rank property of $\Lambda(\tau_m, \delta)$ because $n_p \geq m$. Since (recall that $\int_0^\delta Ae^{As}\mathrm{d}s = \int_0^\delta \frac{\mathrm{d}}{\mathrm{d}s}[e^{As}]\mathrm{d}s = [e^{As}]|_0^\delta$ for a matrix A)

$$\Lambda(\tau_m, \delta) = \underbrace{\begin{bmatrix} I_{n_p} & \int_0^{\tau_m} e^{A_p s}\mathrm{d}s \\ I_{n_p} & \int_0^{\delta} e^{A_p s}\mathrm{d}s \end{bmatrix}}_{\triangleq \Lambda_0(\tau_m, \delta)} \begin{bmatrix} I_{n_p} & 0 \\ A_p & I_{n_p} \end{bmatrix} \begin{bmatrix} I_{n_p} & 0 \\ 0 & B_p \end{bmatrix}$$

and B_p has full column rank by assumption, it suffices to prove that $\Lambda_0(\tau_m,\delta)$ is nonsingular. Assume by contradiction that $v=[v_1^T\ v_2^T]^T, v\neq 0$, with $v_1,v_2\in\mathbb{R}^{n_p}$, satisfies

$$\Lambda_0(\tau_m,\delta)v=0.$$

Then $v_2\neq 0$ and $\int_{\tau_m}^{\delta} e^{A_p s}\mathrm{d}s v_2=0$, i.e. $\int_{\tau_m}^{\delta} e^{A_p s}\mathrm{d}s$ is singular. But the eigenvalues of this matrix are given by $\bar{\lambda}=\int_{\tau_m}^{\delta} e^{\lambda s}\mathrm{d}s$, where λ is the corresponding eigenvalue of A_p, and $\delta\in\Delta\setminus\Delta^\star$, i.e. we are excluding the case $\delta=\tau_m+2\pi z/\omega_l, z\in\mathbb{Z}$, which would lead to $\bar{\lambda}=0$. ■

Consider now an ordering of the elements of $\Delta^\star$, i.e. $\tau_m=p_1<p_2<\ldots<p_{J^\star-1}<p_{J^\star}=\tau_M$, and take $i^\star\in\underset{i\in\mathbb{N}_{J^\star-1}}{\arg\max}\,(p_{i+1}-p_i)$. Notice in particular that

$$p_{i^\star+1}-p_{i^\star}\geq\frac{\tau_M-\tau_m}{J^\star-1}>\frac{\tau_M-\tau_m}{J^\star}=\tau_{J^\star}. \tag{179}$$

From (179) it follows that

$$\bar{\Delta}\triangleq[\frac{p_{i^\star+1}+p_{i^\star}-\tau_{J^\star}}{2},\frac{p_{i^\star+1}+p_{i^\star}+\tau_{J^\star}}{2}]\subset(p_{i^\star},p_{i^\star+1})\subseteq\Delta\setminus\Delta^\star \tag{180}$$

Moreover, since the length of $\bar{\Delta}$ is equal to $\tau_{J^\star}$ and the elements of Δ_J are equally spaced by the distance $\tau_J\leq\tau_{J^\star},\forall J\geq J^\star$, one has

$$\Delta_J\cap\bar{\Delta}\neq\emptyset,\ \forall J\geq J^\star. \tag{181}$$

Define $\bar{\sigma}\triangleq\inf\limits_{\delta\in\bar{\Delta}}\sigma_{min}\left(\Lambda(\tau_m,\delta)\right)$. It follows from the continuous dependence of $\delta\mapsto\sigma_{min}\left(\Lambda(\tau_m,\delta)\right)$, the compactness of $\bar{\Delta}$ and Claim I (which can indeed be applied since (180) holds) that $\bar{\sigma}>0$. Define now $r=r(\gamma)\triangleq\frac{\sqrt{2}}{\bar{\sigma}}\gamma$. Given arbitrary $J\geq J^\star$ and $x_k\notin\mathscr{B}_r$, let us show that $x_k\notin Q_J(\Omega)$, that is, $Q_J(\Omega)\subseteq\mathscr{B}_r,\forall J\geq J^\star$, as stated by the lemma.

In (178) choose $\delta_A=\tau_m\in\Delta_J$ and $\delta_B=\bar{\delta}$ for some $\bar{\delta}\in\Delta_J\cap\bar{\Delta}$ ($\Delta_J\cap\bar{\Delta}\neq\emptyset$ from (181)). Then, since $\|x_{k+1}\|\geq\|x_{p,k+1}\|$ and $x_k\notin\mathscr{B}_r$, it follows that

$$\max\left\{\begin{array}{l}\|x_{k+1}(x_k,\tau_m,S_k)\|,\\ \|x_{k+1}(x_k,\bar{\delta},S_k)\|\end{array}\right\}\geq\frac{1}{\sqrt{2}}\sigma_{min}\left(\Lambda(\tau_m,\bar{\delta})\right)\|x_k\|\geq\frac{1}{\sqrt{2}}\bar{\sigma}\|x_k\|>\frac{1}{\sqrt{2}}\bar{\sigma}r=\gamma.$$

Recalling that $\Omega\subseteq\mathscr{B}_\gamma$, this inequality means that $\mathscr{F}_{SNS}(x_k,\delta_k,S_k)=x_{k+1}(x_k,\delta_k,S_k)\notin\Omega$ at least for $\delta_k=\tau_m$ or $\delta_k=\bar{\delta}$ (independently of S_k). Since $\tau_m,\bar{\delta}\in\Delta_J$, it follows from Definition 5.5 that $x_k\notin Q_J(\Omega)$, as we wanted to show.

A.4 Proof of Lemma 5.3

Since the set-valued map $\mathbb{R}^n\ni x\mapsto\mathscr{F}_{SNS}(x,\Delta,\mathscr{S})\subset\mathbb{R}^n$ is continuous, it follows that the one-step set $Q(\Omega)$ of any open set $\Omega\subseteq\mathbb{R}^n$ is also open [AF09, Proposition 1.4.4][1]. In particular, $Q(\Theta_2^\circ)=Q(\Theta_2^\circ)^\circ$ and we conclude that

$$Q(\Theta_1)\underbrace{\subset}_{\Theta_1\subset\Theta_2^\circ}Q(\Theta_2^\circ)=Q(\Theta_2^\circ)^\circ\subseteq Q(\Theta_2)^\circ$$

where the first inclusion is strict being $Q(\Theta_1)$ a C-set (Lemma 5.2).

[1] $Q(\Omega)$ is called the core of Ω by $\mathscr{F}_{SNS}(\cdot,\Delta,\mathscr{S})$ in [AF09].

A.5 Proof of Lemma 5.5

Let us consider the nontrivial case $c \neq 0$. Since by definition $Q_J(\Omega) \supseteq Q(\Omega), \forall J \in \mathbb{N}_+$, and $0 \in Q(\Omega)^\circ$, there exists $r_1 > 0$ such that

$$\mathscr{B}_{r_1} \subseteq Q_J(\Omega), \quad \forall J \in \mathbb{N}_+. \tag{182}$$

Moreover, from Lemma 5.2, there exists $r_2 > 0$ such that

$$Q_J(\Omega) \subseteq \mathscr{B}_{r_2}, \quad \forall J \geq J^\star. \tag{183}$$

Combining (182) and (183), Lemma 2.6 guarantees the existence of $\beta \in \mathbb{R}$ such that $Q_J(\Omega)$ is β-invariant for $\dot{x}(t) = A_c x(t)$ for all $J \geq J^\star$. It then follows from Remark 5.1 that $\beta^J(\Omega) \leq \beta, \forall J \geq J^\star$. Thus:

$$1 \leq \alpha^J(\Omega) = \max\{1, e^{\beta^J(\Omega)\tau_J}\} \leq \max\{1, e^{\beta\tau_J}\} \overset{J\to\infty}{\to} 1 \tag{184}$$

since $\tau_J \to 0$ as $J \to \infty$. That is, given $c \in (0,1)$, there exists $\bar{J} \geq J^\star$ such that $\alpha^J(\Omega) < 1/c$, $\forall J \geq \bar{J}$. Therefore:

$$cQ(\Omega) \subset Q(\Omega)^\circ/\alpha^J(\Omega) \subseteq Q_J(\Omega)^\circ/\alpha^J(\Omega) = \hat{Q}_J(\Omega)^\circ, \quad \forall J \geq \bar{J},$$

where the first set inclusion holds since $Q(\Omega)$ is a C-set (Lemma 5.2) and the equality follows from the definition of $\hat{Q}_J(\Omega)$.

A.6 Proof of Lemma 5.6

Consider first the claim below.

Claim II.

$$\{\alpha^J(\Omega_i)\}_{J=J^\star}^{\infty} \to 1 \textit{ uniformly in } i \in \mathbb{N} \tag{185}$$

Proof: The proof follows the same reasoning of Appendix A.5:

- Since $Q(\Omega_0) \subseteq Q_J(\Omega_0) \subseteq Q_J(\Omega_i), \forall J \in \mathbb{N}_+, \forall i \in \mathbb{N}$, there exists $r_1 > 0$ such that

  $$\mathscr{B}_{r_1} \subseteq Q_J(\Omega_i), \quad \forall J \in \mathbb{N}_+, \forall i \in \mathbb{N}.$$

  Moreover, from Assumption 5.1, $\Omega_i \subseteq \Gamma_{SNS} \subseteq \mathscr{B}_\gamma, \forall i \in \mathbb{N}$. Thus, using Lemma 5.2, it follows that there exists $r_2 = r_2(\gamma) > 0$ such that

  $$Q_J(\Omega_i) \subseteq \mathscr{B}_{r_2}, \quad \forall J \geq J^\star, \forall i \in \mathbb{N}.$$

  Then, from Lemma 2.6, there exists $\beta \in \mathbb{R}$ such that $Q_J(\Omega_i)$ is β-invariant for $\dot{x}(t) = A_c x(t)$, $\forall J \geq J^\star, \forall i \in \mathbb{N}$.

- It follows that $\beta^J(\Omega_i) \leq \beta, \forall J \geq J^\star, \forall i \in \mathbb{N}$ (see Remark 5.1).

- As shown in (184), the sequence $\{\alpha^J(\Omega_i)\}_{J \geq J^\star}$ is lower and upper bounded for all $i \in \mathbb{N}$ by sequences that do not depend on i and converge to 1.

■

Since, from (119b), $\Omega_{i_1} \subset \Omega^\circ_{i_1+1}$, it follows that $Q(\Omega_{i_1}) \subset Q(\Omega_{i_1+1})^\circ$ (Lemma 5.3). Thus, recalling that $Q(\Omega_{i_1})$ and $Q(\Omega_{i_1+1})$ are C-sets (Lemma 5.2), there exists $c_1 \in (0,1)$ such that

$$Q(\Omega_{i_1}) \subseteq c_1 Q(\Omega_{i_1+1}). \tag{186}$$

Consider now $c_2 \in (c_1,1)$. Applying Lemma 5.5, there exists $\bar{J} \geq J^\star$ such that

$$c_2 Q(\Omega_{i_1+1}) \subseteq \hat{Q}_J(\Omega_{i_1+1}), \quad \forall J \geq \bar{J}. \tag{187}$$

We can split the rest of the proof into two cases depending on the value J_{i_1+2} of J used by the algorithm to generate the set Ω_{i_1+2}, according to (119e).

a) $J_{i_1+2} \geq \bar{J}$: the proof ends here with $i_2 = i_1 + 2$ because

$$Q(\Omega_{i_1}) \underbrace{\subset}_{(186),c_2>c_1} c_2 Q(\Omega_{i_1+1}) \underbrace{\subseteq}_{(187)} \hat{Q}_{J_{i_1+2}}(\Omega_{i_1+1}) \underbrace{=}_{(119e)} \Omega_{i_1+2} = \Omega_{i_2}.$$

b) $J_{i_1+2} < \bar{J}$: from (185), there exists $\hat{J} \geq J^\star$ such that

$$\alpha^J(\Omega_i) < c_2/c_1, \quad \forall i \in \mathbb{N}, \forall J \geq \hat{J}. \tag{188}$$

Notice now that the sequence $\{J_i\}_{i\in\mathbb{N}_+}$ generated by the algorithm is strictly increasing (see Remark 5.2), so sooner or later the value of J_i will reach $\max\{\bar{J},\hat{J}\}$, i.e. there exists $i_2 > i_1 + 2$ such that $J_{i_2} \geq \max\{\bar{J},\hat{J}\}$. Then

$$c_2 Q(\Omega_{i_1+1}) \underbrace{\subseteq}_{(187)} \hat{Q}_{J_{i_2}}(\Omega_{i_1+1}) \underbrace{\subseteq}_{\alpha^{J_{i_2}}(\Omega_{i_1+1})\geq 1} Q_{J_{i_2}}(\Omega_{i_1+1}) \underbrace{\subseteq}_{\substack{\Omega_{i_1+1}\subseteq\Omega_{i_2-1} \text{ since} \\ i_1+1<i_2-1}} Q_{J_{i_2}}(\Omega_{i_2-1}). \tag{189}$$

Multiplying (189) by c_1/c_2 and combining it to (186) we conclude that

$$Q(\Omega_{i_1}) \underbrace{\subseteq}_{(186)} c_1 Q(\Omega_{i_1+1}) \underbrace{\subseteq}_{(189)} \frac{c_1}{c_2} Q_{J_{i_2}}(\Omega_{i_2-1}) \underbrace{\subset}_{J_{i_2}\geq\hat{J},(188)} Q_{J_{i_2}}(\Omega_{i_2-1})/\alpha^{J_{i_2}}(\Omega_{i_2-1})$$
$$= \hat{Q}_{J_{i_2}}(\Omega_{i_2-1}) \underbrace{=}_{(119e)} \Omega_{i_2}.$$

A.7 Proof of Theorem 7.2

We will show that $(q(t),x(t))$ given by (149) with $K = YW_v^{-1}$ satisfies (147) for all initial conditions (q_0,x_0), where $c > 0$ will be appropriately chosen and $\gamma > 0$ is given by the statement of the theorem. Then property (147) will also hold for system (146), according to the reasoning in Section 7.1.1, implying that (146) is MES. A time-varying function $W(q,x,t)$ will be considered, where, since $(q(t),x(t))$ is a PDMP, $(q(t),x(t),t)$ is also a PDMP [Dav93, Pg. 84]. Thus, for a function of the form

$$W(q,x,t) = e^{\gamma t} V(q,x), \tag{190}$$

the Dynkin's formula analogous to (153) holds with (cf. [Dav93, Pg. 84])

$$\mathfrak{U}W(q,x,t) = e^{\gamma t}(\gamma V(q,x) + \mathfrak{U}V(q,x)) \tag{191}$$

as long as (152) is satisfied (with $V(\cdot)$ replaced by $W(\cdot)$). Let us now show that (152) indeed holds for $W(q,x,t)$ given by (190) with

$$V(q,x) \triangleq x^T P_q x, \tag{192}$$

where $P_q \triangleq W_q^{-1} \succ 0, \forall q \in \mathbb{N}_\nu$. Define $\mathrm{Proj}_x \Psi$ as the projection of the $(\mathbb{N}_\nu \times \mathbb{R}^n)$-valued function Ψ onto $\mathbb{R}^n$ and denote by $\Psi^k(\cdot)$ the map $x \mapsto \mathrm{Proj}_x \Psi((q(r_k^-),x),\theta_k), \forall k \geq 1$. Note that $x(t)$ in (149) can be expressed by[2]:

$$x(t) = e^{A_c(t-r_{N_t})} \circ \Psi^{N_t} \circ e^{A_c(r_{N_t}-r_{N_t-1})} \circ \cdots\cdots \circ \Psi^2 \circ e^{A_c(r_2-r_1)} \circ \Psi^1 \circ e^{A_c r_1} x_0 \tag{193}$$

where N_t, defined in (150), counts the number of resets until time t and $\circ$ denotes the composition of functions. Let $c_1 \triangleq \|A_c\|$, $c_2 \triangleq \max\{1, \|A_d\| + \|B_r\|\|D\|\|K\|\}$ and $\bar{c} \triangleq \max_{q\in\mathbb{N}_\nu} \|P_q\|$ and note from (149c) that

$$\|\mathrm{Proj}_x \Psi(q,x,\theta)\| \leq c_2\|x\|, \ \forall (q,x,\theta) \in E \times \{0,1\}.$$

Then, from (193), one concludes that $\|x(t)\| \leq c_2^{N_t} e^{c_1 t}\|x_0\|$. Moreover, for $k \geq 1$,

$$\begin{aligned} \|x(r_k)\| &\leq c_2^k e^{c_1 r_k}\|x_0\|, \\ \|x(r_k^-)\| &\leq c_2^{k-1} e^{c_1 r_k}\|x_0\| \leq c_2^k e^{c_1 r_k}\|x_0\|. \end{aligned} \tag{194}$$

Thus, given $T \in \mathbb{R}_+$ and $(q_0,x_0) \in E$, one has

$$\begin{aligned} &\mathbb{E}\left[\sum_{r_k \leq T} |W(q(r_k),x(r_k),r_k) - W(q(r_k^-),x(r_k^-),r_k)|\right] \\ &\leq \mathbb{E}\left[\sum_{r_k \leq T} e^{\gamma r_k}\left(x^T(r_k)P_{q(r_k)}x(r_k) + x^T(r_k^-)P_{q(r_k^-)}x(r_k^-)\right)\right] \\ &\underbrace{\leq}_{(194)} \mathbb{E}\left[\sum_{r_k \leq T} e^{\gamma r_k} 2\bar{c}(c_2^k e^{c_1 r_k}\|x_0\|)^2\right] \leq \mathbb{E}\left[\sum_{r_k \leq T} e^{\gamma T} 2\bar{c}(c_2^k e^{c_1 T}\|x_0\|)^2\right] \\ &= e^{T(\gamma+2c_1)} 2\bar{c}\|x_0\|^2 \mathbb{E}\left[\sum_{k=0}^{N_T} c_2^{2k}\right] \triangleq C\mathbb{E}\left[\sum_{k=0}^{N_T} c_2^{2k}\right] \\ &= C\sum_{j=0}^{\infty}\left(P[N_T = j]\sum_{k=0}^{j} c_2^{2k}\right) = C\sum_{k=0}^{\infty}\left(c_2^{2k}\sum_{j=k}^{\infty} P[N_T = j]\right) \\ &= C\sum_{k=0}^{\infty}\left(c_2^{2k} P[N_T \geq k]\right) = C\sum_{k=0}^{\infty}\left(c_2^{2k} P[r_k \leq T]\right) < \infty \end{aligned}$$

where the order of summation was changed in the third-to-last equality, and the last inequality follows from [Res92, Theorem 3.3.1]. Consequently, (152) holds, as we wanted to show, and Theorem 7.1 can indeed be applied to $W(q,x,t)$ defined by (190) and (192), in which case

$$\mathfrak{L}V(q,x) = 2x^T P_q A_c x + \lambda\left(x^T P_{q+1} x - x^T P_q x\right), \qquad \text{if } q < \nu, \tag{195a}$$

$$\mathfrak{L}V(q,x) = 2x^T P_\nu A_c x + \lambda\left(\mu_1 g^T(x) P_1 g(x) + \mu_0 x^T P_1 x - x^T P_\nu x\right), \qquad \text{if } q = \nu. \tag{195b}$$

[2]Sometimes, as in (193), we identify a matrix $M \in \mathbb{R}^{m\times n}$ with the corresponding linear operator $M : \mathbb{R}^n \to \mathbb{R}^m$, i.e. $M(x) = Mx$.

Next, inequalities (156) will be used to show that

$$\mathfrak{U}W(q,x,t) \leq 0,\ \forall (q,x,t) \in \mathbb{N}_\nu \times \mathbb{R}^n \times \mathbb{R}_{\geq 0}. \tag{196}$$

Left and right multiplying (156b) by $\mathrm{Diag}(P_\nu, T, I_n, I_n)$ (where $T \triangleq S^{-1}$) and then applying the Schur's complement, one gets:

$$\begin{bmatrix} P_\nu A_c + A_c^T P_\nu + (\gamma - \lambda) P_\nu & \star \\ TDK & -2T \end{bmatrix} + \begin{bmatrix} A_d & B_r \\ I_n & 0 \end{bmatrix}^T \begin{bmatrix} \lambda \mu_1 P_1 & 0 \\ 0 & \lambda \mu_0 P_1 \end{bmatrix} \begin{bmatrix} A_d & B_r \\ I_n & 0 \end{bmatrix} \preceq 0.$$

Then, left and right multiplying the relation above by $[x^T \ \ \bar{\phi}^T(Kx)]$ and its transpose, respectively, applying Lemma 7.1 and combining the resulting inequality to (146c), (191) and (195b), one concludes that (196) holds for all $(q,x,t) \in \{\nu\} \times \mathbb{R}^n \times \mathbb{R}_{\geq 0}$. In a similar manner, it is possible to left and right multiply LMI (156a) by $\mathrm{Diag}(P_q, I_n)$ and, then, to apply the Schur's complement. Using (195a), it follows that (196) holds for all $(q,x,t) \in \mathbb{N}_{\nu-1} \times \mathbb{R}^n \times \mathbb{R}_{\geq 0}$.

Thus, applying Theorem 7.1 and relation (196), one has, for $t \geq 0$:

$$\begin{aligned} \mathbb{E}[W(q(t),x(t),t)] &= W(q_0,x_0,0) + \mathbb{E}\left[\int_0^t \mathfrak{U}W(q(s),x(s),s)\mathrm{d}s\right] \\ &\leq W(q_0,x_0,0),\ \forall (q_0,x_0) \in E. \end{aligned} \tag{197}$$

Substituting (190) and (192) in (197), one then gets, for $t \geq 0$:

$$e^{\gamma t}\mathbb{E}[x^T(t)P_{q(t)}x(t)] \leq x_0^T P_{q_0} x_0,\ \forall (q_0,x_0) \in E.$$

At last, defining $\underline{c} \triangleq \min_{q \in \mathbb{N}_\nu} \lambda_{min}(P_q) > 0$ and $c \triangleq \bar{c}/\underline{c}$, we conclude after some algebraic manipulations that $\mathbb{E}[\|x(t)\|^2] \leq ce^{-\gamma t}\|x_0\|^2$ for all initial conditions, i.e. (147) holds, as we wanted to show.

A.8 Proof of Theorem 7.3

The proof of the sufficiency part of the result is analogous to the one of Theorem 7.2 *mutatis mutandis* and will be omitted. Next, we prove the necessity part. In view of the arguments in Section 7.1.1, we consider system (149) in the proof, i.e. we show that constraints (159) can be satisfied for appropriately chosen matrices Y and $W_q^L, q \in \mathbb{N}_\nu$, if system (149) satisfies (147) for some feedback gain $K \in \mathbb{R}^{m \times n}$ and for all initial conditions.

Consider a function $V : E \to \mathbb{R}_{\geq 0}$ defined by

$$V(q_0,x_0) \triangleq \mathbb{E}_{(q_0,x_0)}\left[\int_0^\infty \|x(s)\|^2 \mathrm{d}s\right] \tag{198}$$

where $\mathbb{E}_{(q_0,x_0)}$ emphasizes that the initial condition considered is $(q(0),x(0)) = (q_0,x_0)$ with probability one (the subscript will be omitted from now on). From (147), $V(q_0,x_0)$ is indeed well defined (i.e. it is finite). More precisely, interchanging expectation with integral operations, one has

$$V(q_0,x_0) = \int_0^\infty \mathbb{E}\left[\|x(s)\|^2\right] \mathrm{d}s \leq \int_0^\infty ce^{-\gamma s}\|x_0\|^2 \mathrm{d}s = c\|x_0\|^2/\gamma < \infty.$$

Let us show that $V(q_0,x_0) = x_0^T P_{q_0} x_0$ for appropriately chosen matrices $P_q, q \in \mathbb{N}_\nu$. Note that in the linear case the solution $x(t)$ of (149) depends linearly on x_0. In other words, (193) reduces to an expression of the form

$$x(t) = \Phi(t,q_0)x_0,$$

where the (random) transition matrix of the system $\Phi(t,q_0)$ depends on the initial condition q_0, as explicitly shown in the notation. Thus, substituting the relation above in (198), one gets

$$V(q_0,x_0) = x_0^T \left(\int_0^\infty \mathbb{E}[\Phi^T(s,q_0)\Phi(s,q_0)]\mathrm{d}s \right) x_0 \triangleq x_0^T P_{q_0} x_0. \tag{199}$$

Let us prove that $P_q = P_q^T$ is positive definite for all $q \in \mathbb{N}_\nu$. Consider again (198) and note that

$$\begin{aligned} V(q_0,x_0) &= \mathbb{E}\left[\int_0^\infty \|x(s)\|^2 \mathrm{d}s \right] \geq \mathbb{E}\left[\int_0^{r_1} \|x(s)\|^2 \mathrm{d}s \right] \\ &= \mathbb{E}\left[\int_0^{r_1} \|e^{A_c s}x_0\|^2 \mathrm{d}s \right] \geq \|x_0\|^2 \mathbb{E}\left[\int_0^{r_1} e^{-2\|A_c\|s} \mathrm{d}s \right] \end{aligned}$$

where we used the fact that $x(t) = e^{A_c t}x_0$ before the first reset time r_1 of (149), and the lower bound for $\|x(t)\|$ comes from [Kha02, Exercise 3.17]. Fix now a constant (deterministic) value $\bar{r} > 0$ and observe that

$$\begin{aligned} V(q_0,x_0) &\geq \|x_0\|^2 \mathbb{E}\left[\int_0^{r_1} e^{-2\|A_c\|s} \mathrm{d}s \right] \\ &= \|x_0\|^2 \left(\mathbb{E}\left[\int_0^{r_1} e^{-2\|A_c\|s} \mathrm{d}s \middle| r_1 > \bar{r} \right] P[r_1 > \bar{r}] + \mathbb{E}\left[\int_0^{r_1} e^{-2\|A_c\|s} \mathrm{d}s \middle| r_1 \leq \bar{r} \right] P[r_1 \leq \bar{r}] \right) \\ &\geq \|x_0\|^2 \mathbb{E}\left[\int_0^{r_1} e^{-2\|A_c\|s} \mathrm{d}s \middle| r_1 > \bar{r} \right] P[r_1 > \bar{r}] \geq \|x_0\|^2 \mathbb{E}\left[\int_0^{\bar{r}} e^{-2\|A_c\|s} \mathrm{d}s \middle| r_1 > \bar{r} \right] P[r_1 > \bar{r}]. \end{aligned}$$

As $r_1 = \rho_0$ by definition, from (151) it follows that $P[r_1 > \bar{r}] = P[\rho_0 > \bar{r}] = e^{-\lambda \bar{r}}$. Then:

$$V(q_0,x_0) \geq \|x_0\|^2 \int_0^{\bar{r}} e^{-2\|A_c\|s} \mathrm{d}s e^{-\lambda \bar{r}} = L\|x_0\|^2 \tag{200}$$

with $L \triangleq e^{-\lambda \bar{r}} \int_0^{\bar{r}} e^{-2\|A_c\|s} \mathrm{d}s > 0$. Comparing (200) and (199), it follows that $P_q \succ 0, \forall q \in \mathbb{N}_\nu$, as claimed.

Note now from (199), (158) and definitions (154) and (155) that

$$\mathfrak{U}V(q,x) = x^T M_q x, \ \forall (q,x) \in E, \tag{201}$$

where we replaced (q_0,x_0) by (q,x) and

$$M_q \triangleq \begin{cases} 2P_q A_c + \lambda(P_{q+1} - P_q), & \text{if } q < \nu, \\ 2P_\nu A_c + \lambda(\mu_1 A_d^T P_1 A_d + \mu_0 P_1 - P_\nu), & \text{if } q = \nu. \end{cases} \tag{202}$$

Applying Theorem 32.2 of [Dav93] to (198), we also know that

$$\mathfrak{U}V(q,x) = -\|x\|^2, \ \forall (q,x) \in E. \tag{203}$$

Combining (201), (202) and (203), one has:

$$\begin{aligned} P_q A_c + A_c^T P_q + \lambda(P_{q+1} - P_q) &= -I_n \prec 0, \ \forall q < \nu \\ P_\nu A_c + A_c^T P_\nu + \lambda(\mu_1 A_d^T P_1 A_d + \mu_0 P_1 - P_\nu) &= -I_n \prec 0. \end{aligned}$$

From (158) and the Schur's complement, the inequalities above are equivalent to (159) with $W_q^L \triangleq P_q^{-1}, \forall q \in \mathbb{N}_\nu$, and $Y \triangleq K W_\nu^L$, which ends the proof.